CABLE-OPERATED ZERO-IMPEDANCE DECOUPLER (COZID)

Michael A. Bowes, et al

Kaman Aerospace Corporation

Prepared for:

Army Air Mobility Research and Development Laboratory

April 1974

EUSTIS DIRECTORATE POSITION STATEMENT

The work reported herein showed that the COZID concept is a possible approach to eliminating helicopter/external load resonance with 1/rev vibratory forces, providing the aircraft can accept the associated weight and logistic penalties.

The conclusions contained herein are concurred in by this Directorate.

The technical monitor for this contract was Mr. Richard E. Lane, Military Operations Technology Division.

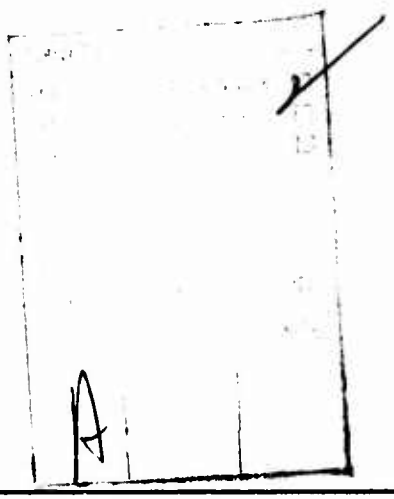

Unclassified

SECURITY CLASSIFICATION OF THIS PAGE (When Data Entered)

AD780 822

REPORT DOCUMENTATION PAGE

READ INSTRUCTIONS BEFORE COMPLETING FORM

1. REPORT NUMBER: USAAMRDL-TR-74-4	2. GOVT ACCESSION NO.
3. RECIPIENT'S CATALOG NUMBER	
4. TITLE (and Subtitle): CABLE-OPERATED ZERO-IMPEDANCE DECOUPLER (COZID)	5. TYPE OF REPORT & PERIOD COVERED: Final report
6. PERFORMING ORG. REPORT NUMBER: Kaman report R-1190	
7. AUTHOR(s): Michael A. Bowes, Ross F. Metzger	8. CONTRACT OR GRANT NUMBER(s): Contract DAAJ02-73-C-0027
9. PERFORMING ORGANIZATION NAME AND ADDRESS: Kaman Aerospace Corporation, Old Windsor Road, Bloomfield, Connecticut 06002	10. PROGRAM ELEMENT, PROJECT, TASK AREA & WORK UNIT NUMBERS: Task 1F162202AA3303
11. CONTROLLING OFFICE NAME AND ADDRESS: Eustis Directorate, U. S. Army Air Mobility R&D Laboratory, Fort Eustis, Virginia 23604	12. REPORT DATE: April 1974
	13. NUMBER OF PAGES: ~~136~~ 147
14. MONITORING AGENCY NAME & ADDRESS (if different from Controlling Office)	15. SECURITY CLASS. (of this report): Unclassified
	15a. DECLASSIFICATION/DOWNGRADING SCHEDULE

16. DISTRIBUTION STATEMENT (of this Report)

Approved for public release; distribution unlimited.

17. DISTRIBUTION STATEMENT (of the abstract entered in Block 20, if different from Report)

18. SUPPLEMENTARY NOTES

19. KEY WORDS (Continue on reverse side if necessary and identify by block number)

Vibration isolators
Cargo
Model tests
Hooks
Trade-off analyses

20. ABSTRACT (Continue on reverse side if necessary and identify by block number)

An analytical and experimental program has been conducted applying the Cable-Operated Zero-Impedance Decoupler (COZID) to helicopter external cargo vertical bounce. The COZID is a passive, antiresonant device which, when properly tuned to the helicopter 1-P frequency, provides dynamic decoupling of

DD FORM 1 JAN 73 1473 EDITION OF 1 NOV 65 IS OBSOLETE

Unclassified

SECURITY CLASSIFICATION OF THIS PAGE (When Data Entered)

the helicopter and slung load. Analytically derived COZID features include:

- High static stiffness.
- Independence of tuned antiresonant frequency with helicopter weight, slung load and sling stiffness.

Parametric studies have been performed applying the COZID to the UH-1, YUH-60, YUH-61, CH-47, CH-46 and CH-53 helicopters. Additionally, parameters of a laboratory test model COZID have been derived. Results of these studies are given in terms of design charts, relating COZID geometry, size, weight and static rotation. In all cases it is shown that a reasonably sized COZID configuration may be defined, having a parametric weight of less than 2 percent of the maximum aircraft external cargo weight.

A laboratory model COZID has been designed, fabricated and tested. Transmissibility testing has been performed with this model as part of a dynamic system incorporating simulated helicopter mass, sling spring rate and slung load mass. The impact of variable sling system dynamics on COZID performance has been investigated, with the COZID model tuned to antiresonance at 3 Hz, 4.8 Hz, and 7.8 Hz. In all cases, the model test results correlate well with analytical predictions.

A preliminary design for a full-scale COZID has been prepared. The subject of this design is the CH-47B/C helicopter, having an external load capacity of 20,000 pounds. This design is compatible with the CH-47B/C airframe as well as with the proposed universal sling system. Weight of the COZID design is estimated to be 367 pounds, representing an aircraft weight penalty of less than 1.5 percent of the maximum external load.

It is recommended that COZID development be continued through an experimental program involving flight testing of full-scale hardware. Design, fabrication and testing of a folded COZID for the UH-1 application is suggested, with full-scale testing preceded by laboratory evaluation of the folded configuration COZID.

PREFACE

The program was conducted by Kaman Aerospace Corporation, Division of Kaman Corporation, Bloomfield, Connecticut, under Contract DAAJ02-73-C-0027, with the Eustis Directorate, U. S. Army Air Mobility Research and Development Laboratory (USAAMRDL), Fort Eustis, Virginia. USAAMRDL technical monitor for this effort was Mr. R. E. Lane, Maintenance and Analysis, Military Operations Technology Division.

The authors acknowledge the contributions made by Mr. H. A. Cooke, Mr. W. G. Flannelly and Mr. R. Jones, as well as other members of the Kaman Aerospace Corporation staff.

TABLE OF CONTENTS

	PAGE
PREFACE	v
LIST OF ILLUSTRATIONS	ix
LIST OF TABLES	xii
INTRODUCTION	1
THE OCCURRENCE OF VERTICAL BOUNCE AND ITS EFFECTS	1
ALLEVIATION	4
DYNAMIC DECOUPLING	13
ANALYSIS	15
SIMPLE COZID ANALYSIS	15
COZID/EXTERNAL LOAD SYSTEM ANALYSIS	25
ALTERNATE COZID CONFIGURATIONS	36
PARAMETRIC STUDY	39
HELICOPTER APPLICATIONS	39
MODEL STUDY	66
EXPERIMENTAL EVALUATION	69
COZID MODEL AND TEST STAND	69
TEST OBJECTIVES AND METHODS	69
TEST RESULTS	77
CH-47B/C COZID PRELIMINARY DESIGN	101
DESIGN CRITERIA	101
COZID DESIGN	106

TABLE OF CONTENTS (Continued)

	PAGE
CONCLUSIONS AND RECOMMENDATIONS.	114
REFERENCES	116
APPENDIXES	
I. TORSIONAL SPRING (FOLDED) COZID ANALYSES.	118
II. TORSIONAL ELASTOMERIC SPRING DESIGN.	124
III. STRESS ANALYSES	129
LIST OF SYMBOLS	133

LIST OF ILLUSTRATIONS

FIGURE		PAGE
1	Susceptibility of Humans to Whole-Body Vertical Vibration.	3
2	Application of Damping to the External Cargo System.	5
3	Comparison of Vertical Bounce and Dangerous Hook Release (DHR) Criteria for Army Cargo Helicopters.	11
4	COZID Schematic	14
5	Simplified COZID Model.	16
6	Static Forces Acting on COZID Inertia Wheel	18
7	Impact of COZID Geometry on Effective Stiffness	20
8	Simple COZID Dynamic Model.	22
9	Effect of Changing Load Mass on Simple COZID Transmissibility.	26
10	Helicopter/External Load Dynamic System Model With Dual-Cylinder COZID.	27
11	Static Forces Acting on Dual-Cylinder COZID and Sling	29
12	Typical Helicopter/COZID/Sling/External Load Transmissibility Curves.	37
13	Alternate COZID Configurations.	38
14	Antiresonant Bandwidth.	44
15	UH-1D COZID Parameters.	48
16	YUH-60 COZID Parameters	51
17	YUH-61 COZID Parameters	54
18	CH-47B/C COZID Parameters	57

LIST OF ILLUSTRATIONS (Continued)

FIGURE		PAGE
19	CH-46D COZID Parameters.	60
20	CH-53D COZID Parameters.	63
21	COZID Model Design Chart	68
22	COZID Model and Test Stand	70
23	COZID Model.	71
24	Inertia Wheel and Inertia Discs.	72
25	Instrumentation Arrangement.	75
26	Effect of Isolated Weight on Soft Sling Dynamic System Transmissibility - No COZID.	80
27	Effect of Isolated Weight on Moderate Stiffness Sling Dynamic System Transmissibility - No COZID	81
28	Effect of Isolated Weight on Stiff Sling Dynamic System Transmissibility - No COZID.	82
29	Transmissibilities of COZID Configurations 1, 2 and 3 With No Sling ($k_s \rightarrow \infty$) - 20-Pound Isolated Weight.	84
30	Transmissibilities of COZID Configurations 1, 2 and 3 With No Sling ($k_s \rightarrow \infty$) - 40-Pound Isolated Weight.	85
31	Comparison of Theoretical Transmissibility With Test Data - Configuration 2 COZID With 40-Pound Isolated Weight	86
32	Effect of Sling Stiffness and Isolated Weight on Configuration 1 COZID Transmissibility	88
33	Effect of COZID Use on Dynamic System Transmissibility - k_s = 203 Lb/In., W_{SL} = 30 Pounds.	91

LIST OF ILLUSTRATIONS (Continued)

FIGURE		PAGE
34	Effect of Sling Stiffness and Isolated Weight on Configuration 2 COZID Transmissibility.	93
35	Effect of Sling Stiffness and Isolated Weight on Configuration 3 COZID Transmissibility.	97
36	CH-47B/C External Cargo System Arrangement	102
37	Standard CH-47B/C External Cargo Hook in Stowed Position.	103
38	Universal Sling System Pendant - 20,000-Pound Capacity	105
39	CH-47B/C COZID Installation	107
40	CH-47B/C COZID in Closed, Extended and Full-Load Conditions.	108
41	CH-47B/C COZID Storage.	109
42	Folded Dual-Cylinder COZID.	119
43	Static Forces and Moments Acting on One Inertia Wheel of Folded, Dual-Cylinder COZID	120
44	Torsional Elastomeric Spring.	125
45	Strain Relationship for Torsional Elastomeric Spring.	127
46	Spring Rate Relationship for Torsional Elastomeric Spring with σ_{max} = 50%, G = 50 psi.	128

LIST OF TABLES

TABLE		PAGE
I	Sling Spring Rates Which Will Preclude Vertical Bounce - for Soft and Stiff Sling Systems.	8
II	Input Data for Parametric Studies.	40
III	Test Equipment	74
IV	Model Helicopter/Sling/Load Dynamic System Parameters.	79
V	Model Helicopter/Sling/Load Dynamic System Measured and Predicted Resonance Frequencies.	79
VI	COZID Model Parameters	83
VII	Design Parameters for CH-47B/C COZID	110
VIII	Maximum Bending Stress Vs Cable Diameter . . .	130
IX	Ultimate Strength Required Vs Number of Cables Used	131

INTRODUCTION

The ability of the helicopter to carry heavy, oversized cargo external to the airframe is a major contributor to the vehicle's operational flexibility. This capability permits the rapid transfer of an almost unlimited variety of materiel without the imposition of severe restrictions on materiel size, shape or weight distribution. One factor which imposes a potential limitation on this flexibility is the generation of high airframe/external load vibration levels caused by resonance or near resonance of the helicopter/sling/external cargo dynamic system with rotor induced forces. Alleviation of this condition, which is generally referred to as vertical bounce, is the ultimate objective of the Cable-Operated Zero-Impedance Decoupler (COZID) development effort described in this report.

THE OCCURRENCE OF VERTICAL BOUNCE AND ITS EFFECTS

Within this report, the term vertical bounce refers to any excessive once-per-revolution (1-P) helicopter and/or external load vibration resulting from amplification of rotor-induced forces* due to airframe/external cargo dynamic response characteristics. This condition is associated with resonance or near resonance of the helicopter-sling-load dynamic system with rotor 1-P forces. Depending on a number of factors, including magnitude of 1-P forces, degree of resonant amplification, fuselage bending response, and weight of the external load, vertical bounce may evidence itself as extremely severe vibration, perhaps resulting in failure to complete the mission, as moderately severe vibration, or as only mild vibration of little or no consequence.

A number of helicopters are known to have experienced vertical bounce, either in their development period or in service. Appendix II of USAAMRDL 71-61 (Reference 1), for example, refers to vertical bounce problems encountered during CH-54A development. Gabel and Wilson (Reference 2) discuss vertical bounce problems in connection with the CH-47 and describe a soft sling system designed to preclude vertical bounce in service. Similarly, certain UH-1 helicopters are required to utilize a soft pendant (flexible loop) on all external cargo-carrying missions.

*1-P rotor forces are due primarily to rotor blade out of track.

The presence of excessive 1-P vibration levels may have adverse effects on the helicopter vehicle, its crew and their mission effectiveness. As has been shown, for example in Reference 3, high vehicle vibration levels can result directly in decreased aircraft reliability and maintainability. In this study, reduction of rotor-induced vibration levels resulted in comparable reductions in component failure rates and maintenance requirements. While this study specifically referred to the reduction of N-per-rev (N-P)* vibration, similar conclusions may be drawn with respect to the effects of 1-P vibration on aircraft R&M.

The effects of low-level vibration on crew performance are well known. Vibration-related fatigue results in reduced crew proficiency, with the degree of reduced proficiency related to vibration level, frequency and crew exposure time. With regard to Army cargo helicopters, 1-P frequencies are all within the range of maximum human susceptibility to whole body vertical vibration. This is shown in Figure 1, which was excerpted from Figure 36 of Reference 4.

The high 1-P vibration levels associated with vertical bounce may have a serious impact on mission effectiveness, beyond the general effects of reduced vehicle R&M and crew performance. Vibration may become severe enough to cause termination of the mission either at the inception of the mission or at some later time when termination may result in loss of the load. Short of failure to complete the mission, vertical bounce may cause the pilot to reduce speed, and thereby lessen 1-P rotor forces, at a time when reduced aircraft speed compromises safety, for example, during retrieval of cargo from a hostile area.

In addition to the above deleterious effects of vertical bounce, resonance or near resonance of the helicopter/sling load dynamic system is a necessary, though not sufficient, condition to the occurrence of pilot induced oscillation (PIO), described in Reference 2. PIO refers to a specific, potentially catastrophic dynamic condition wherein the presence of the pilot and rotor thrust control system contributes to the basic 1-P vibration. In this case, the pilot experiences body motion in response to 1-P vertical aircraft vibration (vertical bounce). The pilot, in turn, exerts an involuntary 1-P control force on the rotor thrust control lever (which in most cases is aligned vertically), causing a

*Vibration frequency equal to the product of rotor rpm and number of blades.

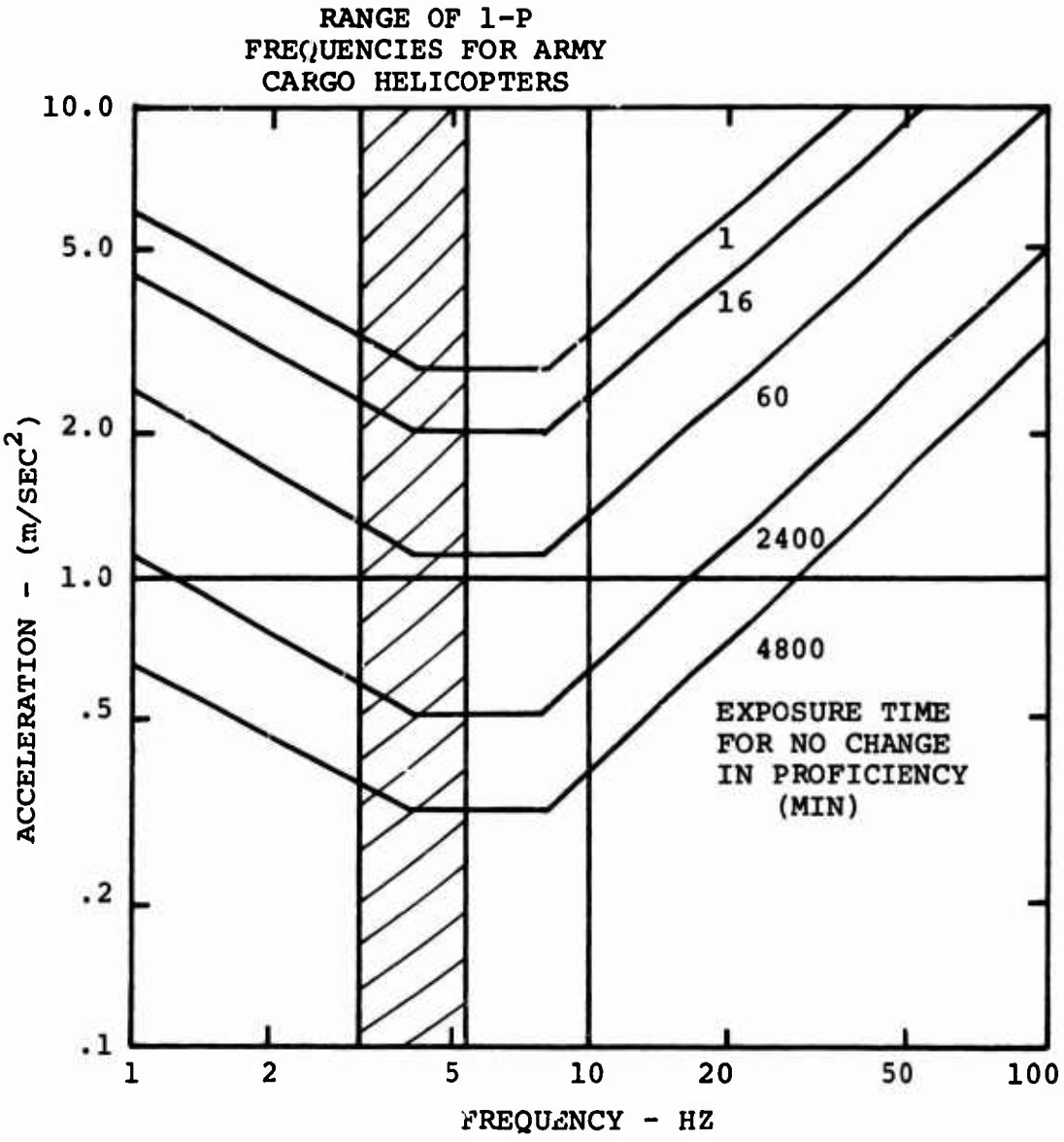

Figure 1. Susceptibility of Humans to Whole-Body Vertical Vibration.

1-P rotor thrust oscillation. Depending upon the dynamics of the particular situation, the feedback loop thus formed may result in the divergent oscillation known as PIO.

ALLEVIATION

Vertical bounce may occur whenever the aircraft/sling/slung load dynamic system has its natural frequency at or near 1-P of the main rotor. The severity of vibration due to this condition will depend on a number of factors, including weight of the load, nearness of the aircraft vertical bending frequency to 1-P, and magnitude of 1-P rotor forces. Methods which have been suggested for use in alleviating or preventing vertical bounce include:

- Damping, added to the aircraft/sling/slung load dynamic system, to limit the buildup of vibration amplitude.
- Detuning of the sling system to insure that the system resonant frequency will be either above or below a critical range around 1-P.
- Use of a dynamic device to dynamically decouple the load at 1-P, without excessive static deflection of the load.

In addition to these, modification of the thrust control system has been suggested (Reference 2) as a means of preventing PIO, a special case of vertical bounce. Each of the above approaches is discussed below.

Sling System Damping

Theoretically, either series or parallel damping may be used to alleviate vertical bounce. These alternate approaches are illustrated in Figure 2. While each is capable of limiting resonant amplification of helicopter/load vibration, only the series damped approach is practical, due to the physical size of the damping element which must be used to provide parallel damping. As shown in Figure 2, a damping element arranged in parallel with the cargo sling system must be connected between the helicopter and load.

Series damping, though physically practical, is difficult to apply because of the wide range of sling configurations which might be utilized in service. Since with a series damped system, damping capacity is related to the spring rate of the series element to which the damper is attached (in this case, the spring rate of the sling), specification

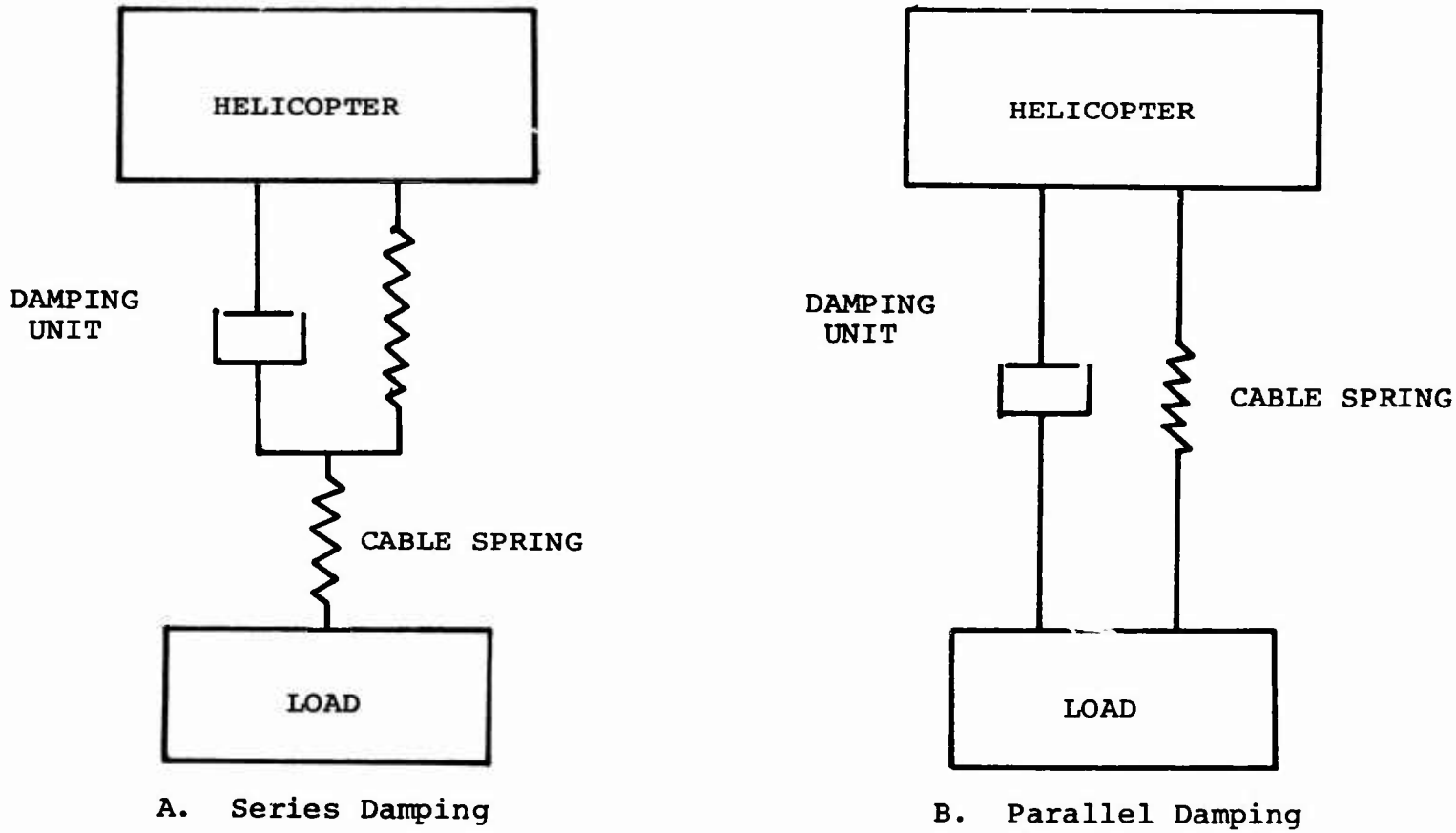

Figure 2. Application of Damping to the External Cargo System.

of damper characteristics is difficult. A damper optimized for a given sling spring rate may fail to provide the necessary damping when a different sling arrangement, having a different spring rate, is used. The problem of specifying a damping element compatible with all sling configurations is aggravated by the fact that most, if not all, available applicable dampers suffer from environmental effects, which impact their basic damping characteristics. Additionally, series damping requires the use of a spring in parallel with the damper, as shown in Figure 2. This additional spring reduces the effective spring rate of the sling, increasing static deflection of the load, a highly undesirable effect*.

Sling System Detuning

Vertical bounce may also be prevented by detuning the aircraft/sling/slung load dynamic system. This is accomplished by providing a sling system satisfying either of the following conditions:

- Soft Sling - The sling system spring rate is kept low enough to limit the system natural frequency to the region below a critical frequency band about f_{1-P}.
- Stiff Sling - The sling system spring rate is kept high enough to limit the system natural frequency to the region above a critical frequency band about f_{1-P}.

Choice of appropriate sling system parameters for detuning the dynamic system is influenced by the magnitude of the allowable dynamic system amplification, the range of helicopter vehicle weights, and the range of external cargo weights.

Studies reported in Reference 2 suggest that a dynamic system amplification of approximately 1.5 may be tolerated with no sustained vertical bounce. Use of this criterion results in the definition of allowable helicopter/sling/slung load resonance frequency ranges which are given by the following:

- The resonance must lie below .76 times the 1-P frequency with the minimum vehicle and external cargo weights expected in use (soft sling).

*The impact of load static deflection on system stored energy is discussed in the section on Sling System Detuning.

- The resonance must lie above 1.79 times the 1-P frequency with the minimum vehicle weight and maximum external cargo weight expected in use (stiff sling).

The maximum soft sling spring rate (k_{max}) and minimum stiff sling spring rate (k_{min}) are given as:

$$k_{max} = \frac{1}{g}\left[2\pi \cdot .76 \cdot f_{1-P}\right]^2 \left[\frac{(W_{a/c})_{min} \cdot (W_{sl})_{min}}{(W_{ac})_{min} + (W_{sl})_{min}}\right] \quad (1)$$

$$k_{min} = \frac{1}{g}\left[2\pi \cdot 1.79 \cdot f_{1-P}\right]^2 \left[\frac{(W_{a/c})_{min} \cdot (W_{sl})_{max}}{(W_{a/c})_{min} + (W_{sl})_{max}}\right] \quad (2)$$

Values for maximum soft sling spring rate and minimum stiff sling spring rate for Army cargo helicopters are given in Table I. These values take into account an assumed ±2 percent variation in f_{1-P}.

While the use of soft or stiff sling systems will prevent vertical bounce, certain practical considerations limit their universal application. With regard to stiff sling systems, it is practically impossible to insure that the sling system, consisting of pendant and bridle, will have a spring rate in excess of those required in Table I. In most cases the spring rate of the bridle alone will be sufficiently low to put the sling system into the vertical bounce range, even considering an infinite pendant stiffness. For example, using four-legged bridles made up of leg components from the proposed universal sling system* results in bridle spring rates ranging from 16,000 lb/in. to 29,000 lb/in. for a 6000-pound-capacity bridle, and 32,000 to 65,000 lb/in. for the 25,000-pound-capacity bridle, when 0-degree to 45-degree rigging is considered. For all the helicopter applications of Table I, the lower limits of bridle spring rate are lower than the stiff sling system spring rate required to preclude vertical bounce. The use of a stiff sling system to prevent vertical bounce is therefore not feasible.

*Details of the universal sling system were obtained from the Army.

TABLE I. SLING SPRING RATES WHICH WILL PRECLUDE VERTICAL BOUNCE - FOR SOFT AND STIFF SLING SYSTEMS*

A/C	1-P Frequency (Hz)	A/C Weight (lb)	Slung Load Weight (lb)		Maximum Soft Sling Spring Rate (lb/in.)	Minimum Stiff Sling Spring Rate (lb/in.)
			Minimum**	Maximum		
UH-1D	5.40	5400	1350	4000	1738	21,955
YUH-60	4.38	13,481	3370	13,481	3055	42,373
YUH-61	4.92	12,686	3171	12,686	3627	50,313
CH-47C	4.08	20,000	5000	20,000	3972	57,804
CH-46D	4.40	13,000	3250	10,000	2805	35,865
CH-53D	3.17	23,000	5750	19,000	2505	35,790

* Data for existing A/C were obtained from various flight manuals; YUH-60 and YUH-61 data were provided by the Army.

**Based on minimum significant slung load equal to 25% of A/C weight.

The use of a soft (low spring rate) element in the sling system (soft sling) is an effective means for preventing vertical bounce. In fact, this method is presently in use, on UH-1D and CH-47 aircraft, and is slated for use in the universal sling system presently under development. The use of a soft pendant does, however, introduce the possibility of dangerous hook release (DHR) resulting from the high strain energy stored in heavily loaded, low-stiffness pendants, since under heavy load it is possible to have sufficient energy stored in a soft pendant to launch the hook as high as the aircraft fuselage or rotor, should the load be released suddenly*.

If it is assumed that the pendant behaves as a linear spring, with no internal damping, then, under load the stored energy, E_s, is

$$E_s = 1/2\ k_p \delta_{ST}^2 \tag{3}$$

where

k_p = pendant spring rate - lb/in.

δ_{ST} = static deflection - in.

Under normal load release conditions, this energy is gradually reduced to zero as the sling system tension is removed, and no energy imbalance results. If, however, the load is released at the hook suddenly, prior to complete energy dissipation, an energy imbalance results which tends to launch the hook upward toward the helicopter. Assuming no vertical helicopter motion (rebound)**, with the vehicle initially directly above the suspended load, the energy required to launch the hook to the height of the fuselage is equal to the change in hook potential energy over a height differential equal to the pendant length. This is

$$E_p = \ell \cdot W_H \tag{4}$$

---

* The equations governing DHR are derived in an alternate manner in Appendix II of Reference 8.

**While the helicopter will rebound after sudden load release, the force acting to cause this motion is the same as the force acting on the pendant hook. Because of the large differential between helicopter and hook masses, the hook will accelerate much faster than the helicopter, reaching its maximum travel before any appreciable helicopter motion can take place.

where

E_p = potential energy - in.-lb

ℓ = pendant length - in.

W_H = hook weight - lb

Combining Equations (3) and (4) and making a substitution for δ_{ST} in terms of W_{SL} and k_p, with

$$\delta_{ST} = \frac{W_{SL}}{k_p} \tag{5}$$

results in the equation for minimum pendant spring rate needed to preclude DHR, K_{DHR}. This is given by

$$K_{DHR} = \frac{(W_{SL})^2}{2W_H \ell} \tag{6}$$

Using Equation (6), curves of K_{DHR} vs slung load have been generated for both 6000-pound and 25,000-pound-capacity pendants. These curves are shown in Figure 3. Also plotted in Figure 3 are maximum spring rates which will preclude vertical bounce for each of the aircraft under study. For all but the UH-1D, the use of a sling system soft enough to prevent vertical bounce results in a situation where DHR is possible.

Prevention of Pilot-Induced Oscillation

As discussed previously, a potentially divergent aircraft oscillation may result due to dynamic coupling between the aircraft/external load dynamic system and the pilot/thrust control dynamic system. This phenomenon, known as pilot-induced oscillation (PIO), is a special, severe case of vertical bounce. Solutions for this problem, suggested and evaluated in Reference 2, are based on modification of the control system response. Both frictional damping and viscous

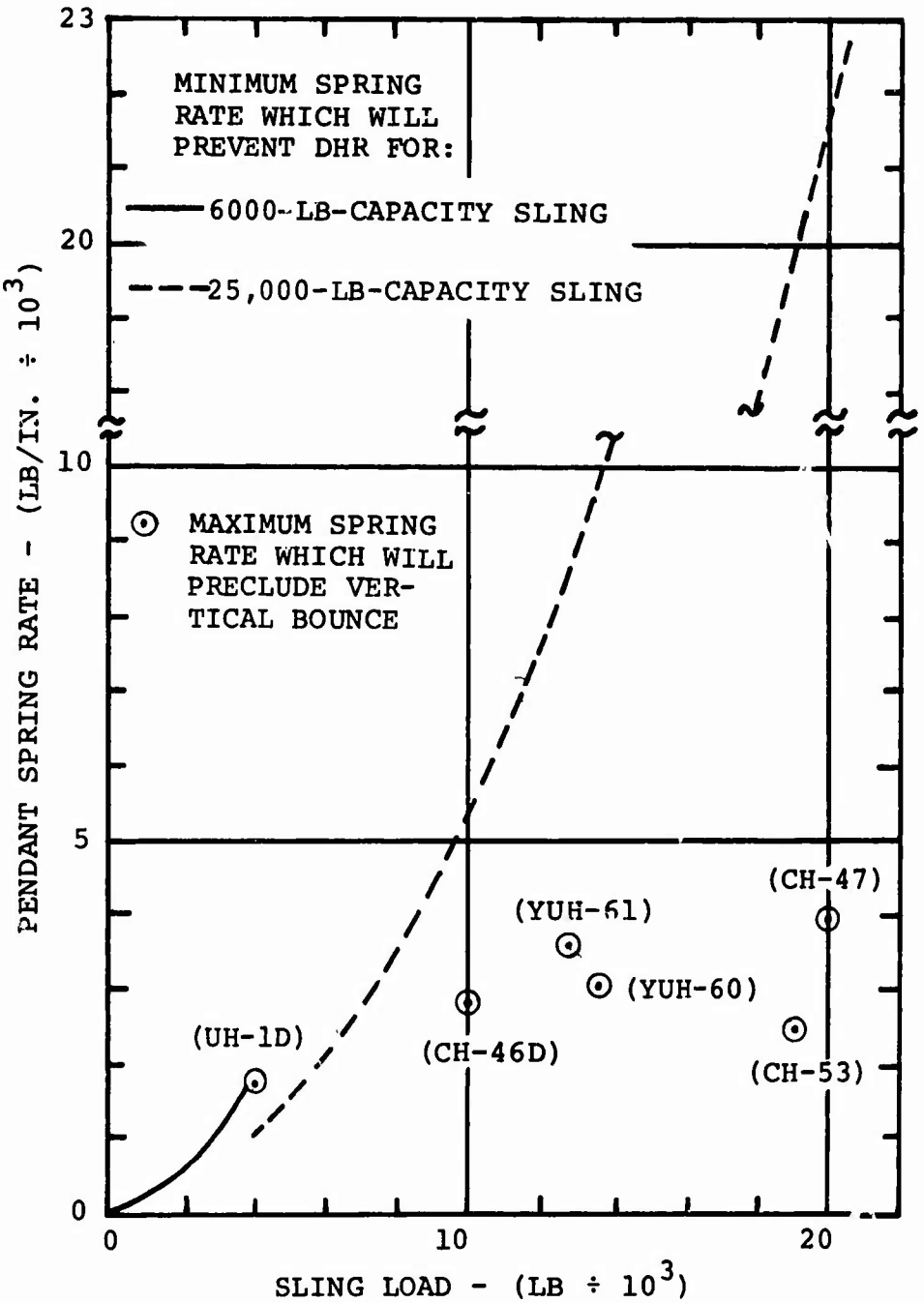

Figure 3. Comparison of Vertical Bounce and Dangerous Hook Release (DHR) Criteria for Army Cargo Helicopters.

damping were evaluated*, on an experimental basis, as well as direct modification of the response of the boost system.

Results of the Reference 2 testing indicate that while increased damping of the control system will alleviate PIO, a great deal of added damping is required. The required damping may be easily obtained with a frictional damper, which may be adjusted to provide the required damping force irrespective of the magnitude of the 1-P excitation. Viscous damping was found to be impractical since the required damping force could not be obtained with a viscous damper having a reasonable damping capacity. Failure of viscous damping is attributed to the low magnitude of vibratory velocity generated at the 1-P frequency.

The Reference 2 study also explored the use of a modified thrust control system boost actuator which directly modified control system response to dynamic inputs at the thrust lever. This modification consisted of replacement of the original high-gain actuator with an actuator providing high output for normal control inputs, but low output for small-amplitude inputs such as those expected from 1-P vibration of the thrust lever. This system prevented PIO and was considered the optimum solution, of those investigated in Reference 2.

While the above thrust control system modifications were found to be capable of preventing vertical-bounce-connected PIO, several drawbacks must be considered. The use of constant-force frictional damping increases the control load felt by the pilot and limits his ability to provide rapid control inputs; therefore, pilot acceptance is highly questionable. Additionally, as pointed out in Reference 2, frictional dampers have been historically unreliable and prone to erratic operation. Incorporation of a pilot adjustment capability opens the door for misadjustment (or deliberate disabling of the damper), in which case PIO would again be possible.

Prevention of PIO through adjustment of the thrust control boost system adds to the complexity of the system, thereby reducing system reliability. Additionally, keying PIO prevention to boost system performance results in a situation where boost system failure may lead to PIO, thereby removing the option of flying the aircraft with no boost, if such an option is available.

---

*Reference 2

The major drawback to the use of the above PIO preventing methods is, however, the fact that they do not eliminate vertical bounce, but only mitigate one of its effects. High 1-P vehicle vibration levels due to resonance or near resonance of the helicopter/external load may still occur, and their direct effects on vehicle R&M, crew performance and mission performance may still be felt.

DYNAMIC DECOUPLING

Vertical bounce may be prevented by providing dynamic decoupling between the helicopter and external cargo, such that the dynamic system resonance may not occur at the 1-P frequency. This effect is achieved by the Cable-Operated Zero-Impedance Decoupler (COZID) shown schematically in Figure 4.

With the COZID installed, as shown in Figure 4, application of helicopter vibratory excitation forces to the COZID results in the creation of both elastic and inertial forces within the device. The elastic forces result from stretching of the internal springs, while the inertial forces are generated due to translational and rotational motion of the inertia cylinders. At a single predetermined frequency, in this case 1/rev of the rotor, inertia and elastic forces cancel, and forces at that frequency are not transmitted through the COZID. The frequency at which this force cancellation takes place is known as the antiresonance frequency, and at this frequency the device is said to have a zero transfer impedance. At its tuned frequency, the COZID has a theoretical transmissibility, i.e., load response divided by helicopter response, of zero. Zero transmissibility is maintained irrespective of helicopter weight, external cargo weight and sling spring rate.

The fundamental characteristics of the COZID have been determined and demonstrated through a series of Kaman-sponsored internal research and development efforts conducted previous to the contract effort discussed in this report. Initial COZID investigations described in Reference 5 were primarily analytical, with concentration on development and use of the basic equations of motion. Subsequent to this, preliminary vibration testing of a simple COZID model was performed, as described in Reference 6. Preliminary testing was followed by a more extensive test program involving the design, fabrication and use of a sling load decoupler test stand. This effort is described in Reference 7. Pre-contract COZID development culminated with the fabrication of a small, dual-cylinder COZID demonstration model.

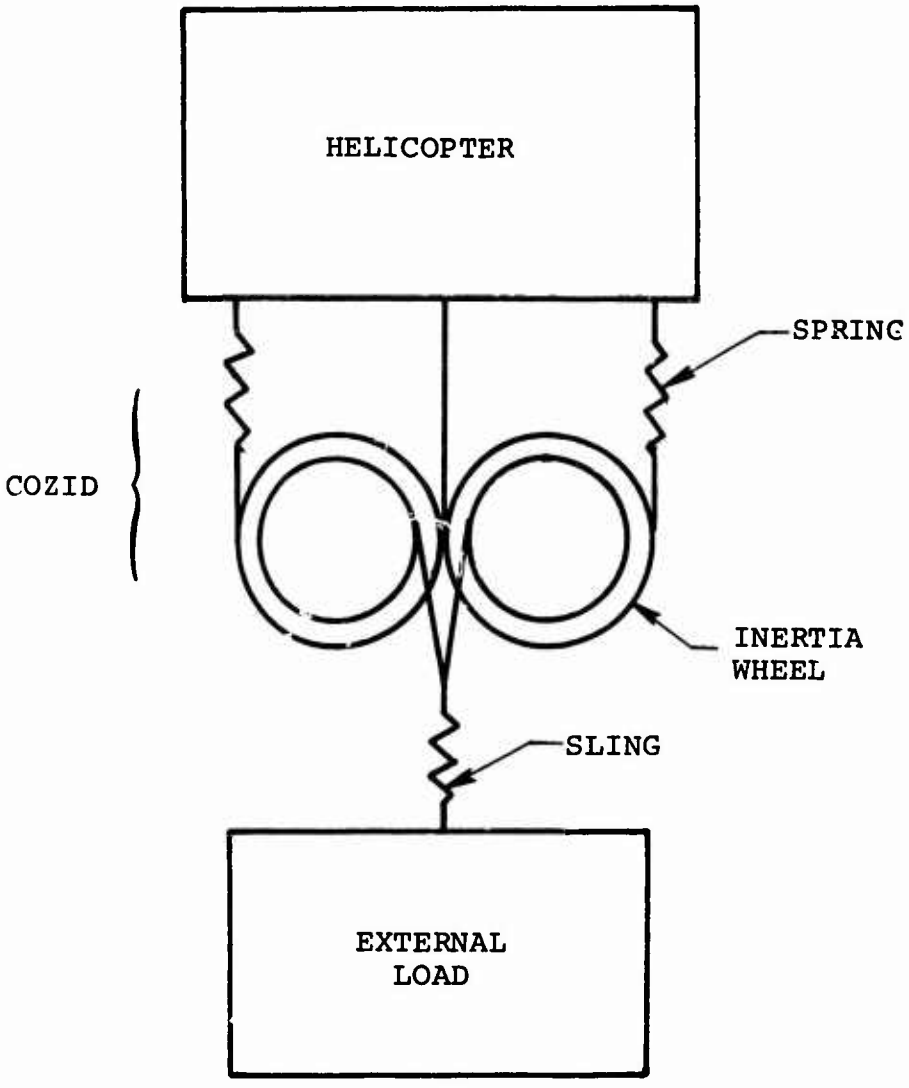

Figure 4. COZID Schematic.

ANALYSIS

SIMPLE COZID ANALYSIS

Operation of the COZID is most readily explained by considering the equations governing operation of a simplified model, such as that shown in Figure 5. This model contains all elements essential to the operation of the device, including:

(1) One, or more, high-rotational-inertia compound pulleys (inertia wheels) having unequal support and load cable attachment radii.

(2) One, or more, elastic elements (springs) arranged in such a way as to resist rotation and translation of the inertia wheels.

The inertia wheel and load are supported by the support spring and load cables, which are attached in such a manner as to allow translation and rotation of the inertia wheel. This is accomplished by allowing sufficient free cable to enable each cable to wrap and unwrap from the circumference of the wheel in response to inertia wheel motion. Translation of the wheel in a negative direction, with the helicopter held fixed, for example, results in a negative wheel rotation, which is accommodated by unwrapping of the support cable, wrapping up of the spring and load cables, and stretching of the spring. This type of motion is identical to that which the device undergoes in response to static loading. Release of a static load results in positive translation and rotation of the inertia wheel, wrapping up of the support cable, unwrapping of spring and load cables, and release of spring tension.

Response of the COZID to dynamic loading, such as would be applied due to vibration of the helicopter, is similar to the static response. The COZID experiences rotational and translational motion, which is accompanied by cable wrapping and unwrapping. In the dynamic case, however, helicopter, COZID and load motions result in the generation of inertial forces, which are applied to the support, spring and load cables. These forces add, vectorially, with the dynamic restoring force due to relative motion across the COZID spring.

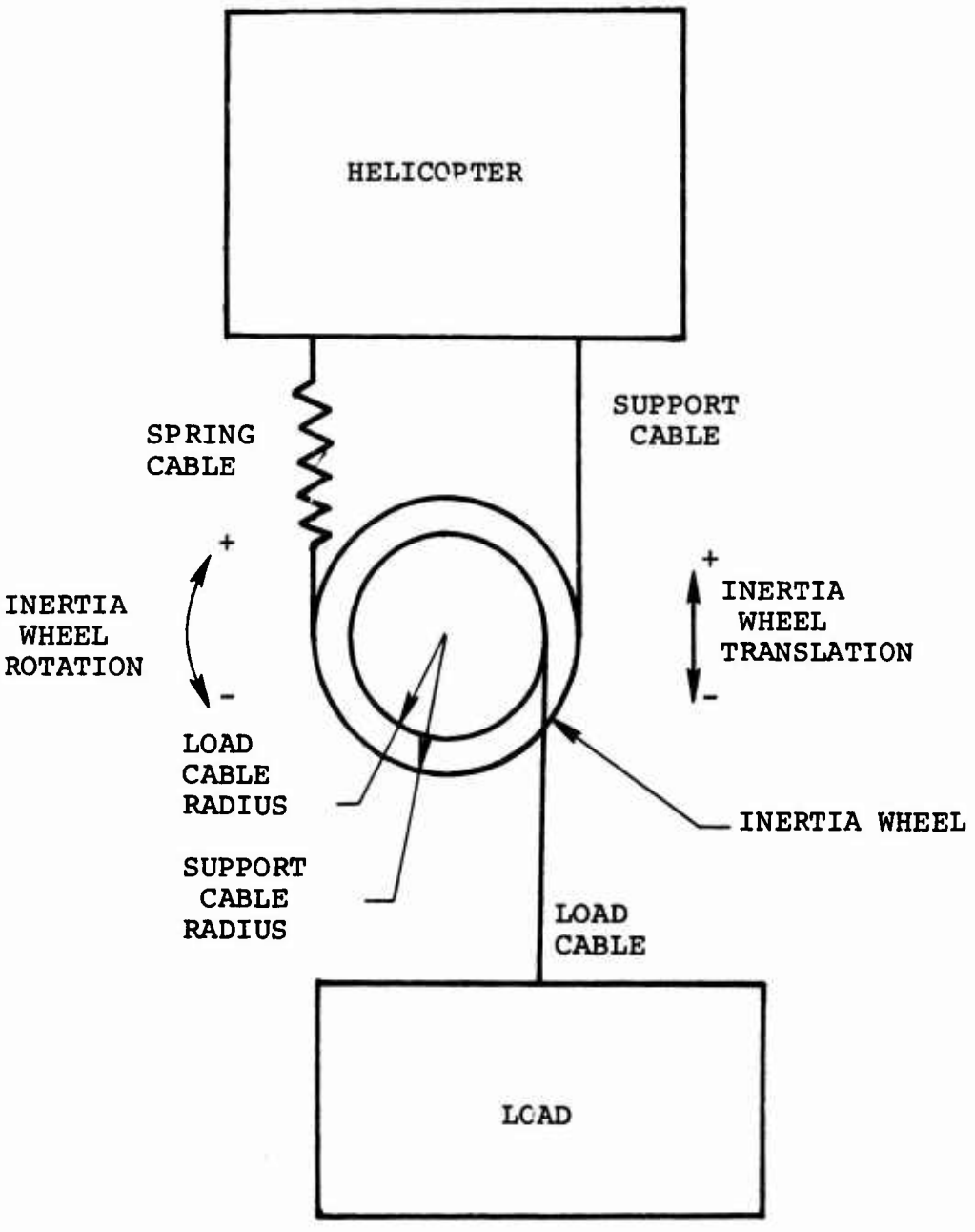

Figure 5. Simplified COZID Model.

The resultant cable forces, and their relative phasing, vary with frequency in such a way that at a specific frequency the support and spring cable dynamic forces cancel, resulting in zero dynamic force applied to the load cable. At this frequency the ratio of helicopter applied dynamic force to load response, known as the helicopter/load transfer impedance, goes to zero, and no load motion results, regardless of the magnitude of excitation applied at the helicopter. In effect, the COZID decouples the load from the helicopter at this frequency, known as the antiresonant frequency.

COZID response to static and dynamic loads is determined by a number of factors, both internal and external to the device itself. Equations governing COZID response are derived and discussed in the following sections.

Static Response

The static forces acting on the simplified COZID model of Figure 5 are the spring force (F_k), the support force (F_s) and the load weight (L)*. These forces act as shown in Figure 6 and result in the COZID and load motions shown. Balancing forces and moments results in relationships for spring and support forces, in terms of load weight and COZID geometry. These relationships are

$$F_k = \frac{L(R - r)}{2R} \tag{7}$$

$$F_s = \frac{L(R + r)}{2R} \tag{8}$$

If the COZID internal spring rate is assumed to have the value k_c, Equation (7) may be rewritten in terms of k_c and the deflection at point k on the COZID, z_k, which is due to relative motion across the internal spring. This is

$$z_k = \frac{L(R - r)}{2k_c R} \tag{9}$$

*COZID weight is ignored.

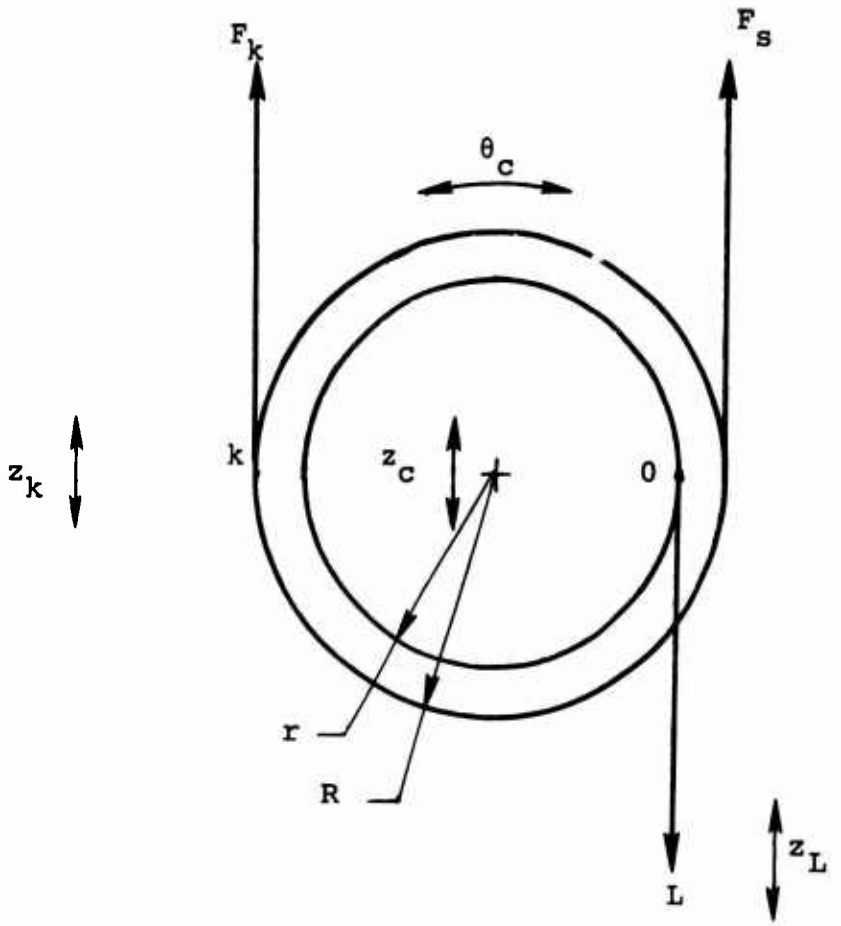

Figure 6. Static Forces Acting on COZID Inertia Wheel.

Since the COZID is restrained to roll without sliding on the support cable, rotation of the COZID (θ_c) is simply related to deflection at point k, with

$$\theta_c = \frac{z_k}{2R} = \frac{L(R - r)}{4k_c R^2} \tag{10}$$

Translation of the load, z_L, is then given by the vector sum of translation of the COZID cg, z_c, given by

$$z_c = \frac{z_k}{2} = \frac{L(R - r)}{4k_c R} \tag{11}$$

and translation of point 0, z_o, due to rotation of the COZID, given by

$$z_o = \theta_c(-r) = \frac{-L(R - r)r}{4k_c R^2} \tag{12}$$

Load translation, z_L, is then

$$z_L = \frac{L(1 - r/R)^2}{4k_c} \tag{13}$$

Rearrangement of Equation (13) provides a relationship for the effective COZID spring rate (K_c), given by

$$K_c = \frac{L}{z_L} = \frac{4k_c}{(1 - r/R)^2} \tag{14}$$

Static deflection under a load, L, may then be calculated using

$$\delta_{ST} = L/K_c \tag{15}$$

The impact of COZID geometry on effective stiffness, given by Equation (14), is illustrated in Figure 7, which shows the ratio of effective spring rate to COZID spring stiffness, K_c/k_c, as a function of the ratio r/R. The ability to achieve a high effective stiffness while maintaining a low internal spring rate is one of the most significant features

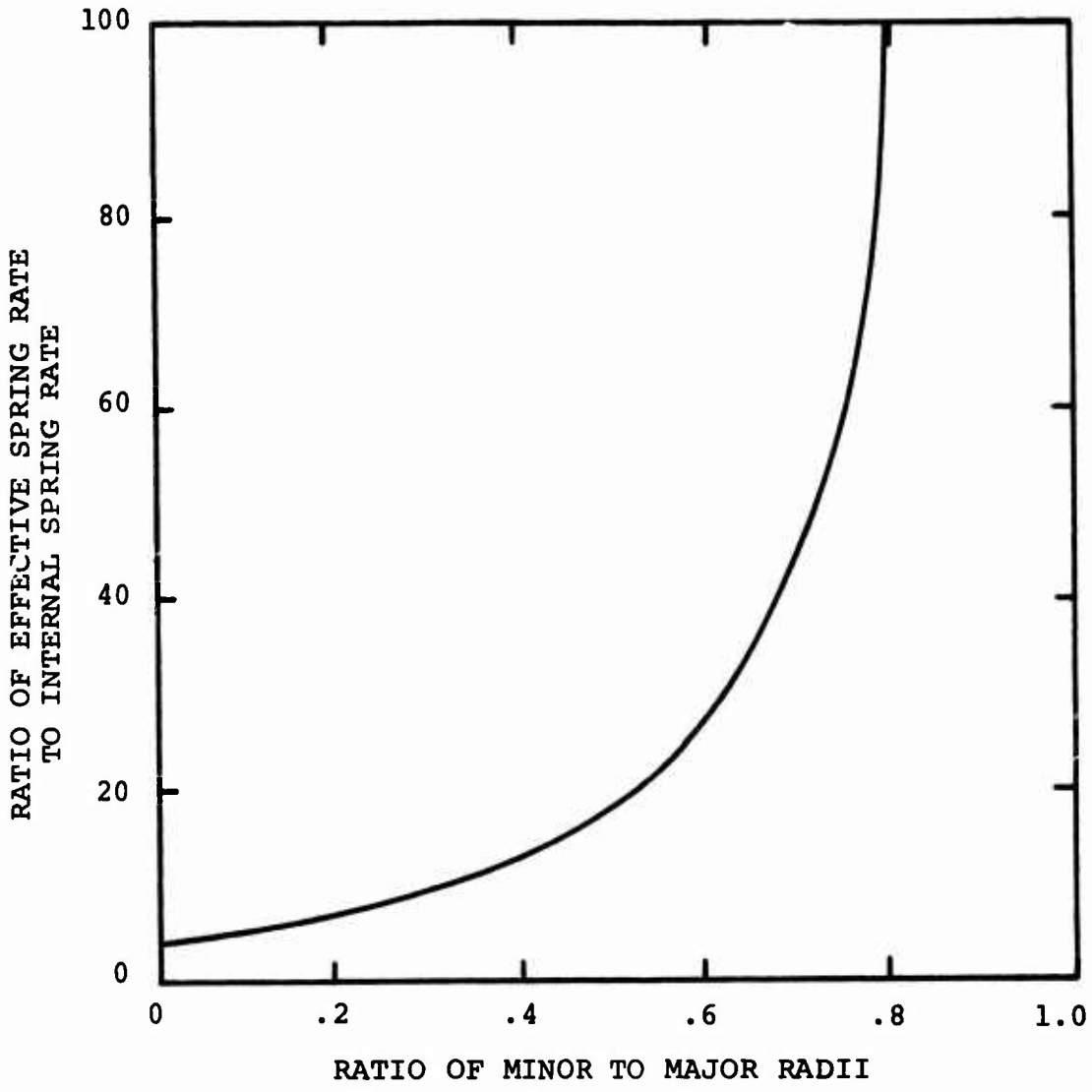

Figure 7. Impact of COZID Geometry on Effective Stiffness.

of the COZID. This feature permits the design of a low-weight COZID while maintaining a low load deflection.

Dynamic Response

Referring to the COZID dynamic model of Figure 8, potential energy (V) and kinetic energy (T) equations are

$$T = 1/2\ M_L \dot{z}_L^2 + 1/2\ M_c \dot{z}_c^2 + 1/2\ I_c \dot{\theta}_c^2 \tag{16}$$

$$V = 1/2\ k_c (z_H - z_k)^2 \tag{17}$$

Consideration of the geometry yields

$$\dot{\theta}_c = \frac{1/R(\dot{z}_L - \dot{z}_H)}{1 - r/R} \tag{18}$$

$$\dot{z}_c = \frac{\dot{z}_L - (r/R\dot{z}_H)}{(1 - r/R)} \tag{19}$$

$$z_H - z_k = \frac{2(z_L - z_H)}{(1 - r/R)} \tag{20}$$

Substitution of Equations (18), (19) and (20) into Equations (16) and (17) results in energy relationships in terms of helicopter and load motions only, with

$$T = 1/2\ M_L \dot{z}_L^2 + \frac{1/2}{(1 - r/R)^2}\left(M_c(\dot{z}_L - (r/R)\dot{z}_H)^2 + \frac{I_c}{R^2}(\dot{z}_L - \dot{z}_H)^2 \right) \tag{21}$$

$$V = 1/2\ \frac{4k_c}{(1 - r/R)^2}\ [z_L - z_H]^2 \tag{22}$$

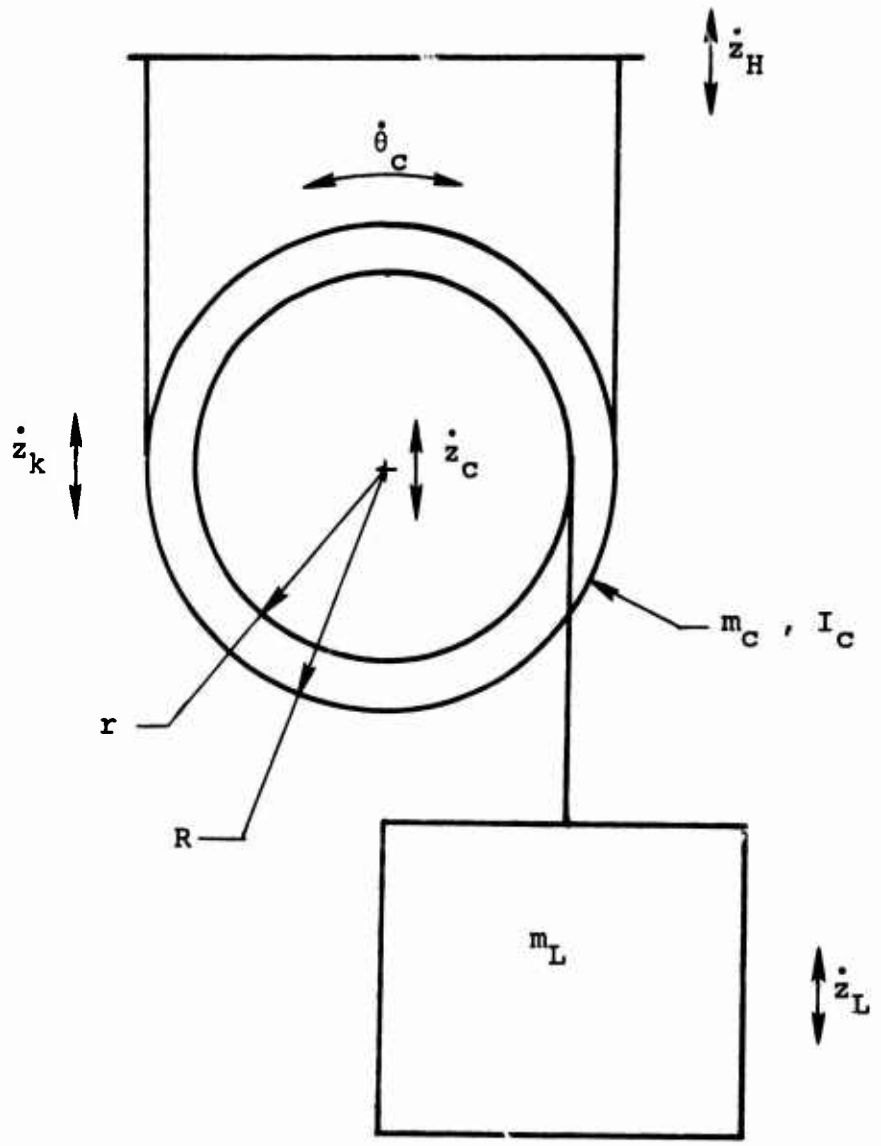

Figure 8. Simple COZID Dynamic Model.

Use of Lagrange's equation,

$$\frac{d}{dt}\left(\frac{\partial T}{\partial \dot{z}}\right) - \frac{\partial T}{\partial z} + \frac{\partial V}{\partial z} = F_z \tag{23}$$

for motion of the supported mass, M_L, yields the differential equation of motion:

$$\left[M_L + \frac{M_c + I_c/R^2}{(1 - r/R)^2} \right] \ddot{z}_L + \frac{4k_c}{(1 - r/R)^2} z_L$$

$$- \left[\frac{(r/R)M_c + I_c/R^2}{(1 - r/R)^2} \right] \ddot{z}_H - \frac{4k_c}{(1 - r/R)^2} z_H = 0 \tag{24}$$

Assuming a solution of the form

$$z = \bar{z}\, e^{j\omega t} \tag{25}$$

results in the equation of motion:

$$\left\{ \frac{4k_c}{(1 - r/R)^2} - \omega^2 \left[M_L + \frac{M_c + I_c/R^2}{(1 - r/R)^2} \right] \right\} z_L$$

$$- \left\{ \frac{4k_c}{(1 - r/R)^2} - \omega^2 \left[\frac{(r/R)M_c + I_c/R^2}{(1 - r/R)^2} \right] \right\} z_H = 0 \tag{26}$$

COZID transmissibility (T), the ratio of load motion, z_L, to helicopter motion, z_H, is obtained directly from Equation (26), with

$$T = \frac{\dfrac{4k_c}{(1 - r/R)^2} - \omega^2\left[\dfrac{(r/R)M_c + I_c/R^2}{(1 - r/R)^2}\right]}{\dfrac{4k_c}{(1 - r/R)^2} - \omega^2\left[M_L + \dfrac{M_c + I_c/R^2}{(1 - r/R)^2}\right]} \qquad (27)$$

The transmissibility resonance ($T \to \infty$) frequency (ω_R) is calculated by setting the denominator of Equation (27) to zero and solving for ω_R, with

$$\omega_R = \sqrt{\frac{4k_c}{M_L(1 - r/R)^2 + M_c + I_c/R^2}} \qquad (28)$$

Antiresonance occurs when the transmissibility goes to zero ($T \to 0$). The antiresonant frequency (ω_{AR}) is calculated by setting the numerator of Equation (27) to zero, with

$$\omega_{AR} = \sqrt{\frac{4k_c}{(r/R)M_c + I_c/R^2}} \qquad (29)$$

Referring to Equation (28), it is seen that the Figure 8 dynamic system transmissibility resonance frequency (ω_R) is a function of external dynamics (M_L) as well as COZID parameters (k_c, R, r, M_c, I_c). Changing external dynamic parameters, for example, increasing or decreasing the isolated mass (M_L), results in a shift in resonance frequency. The change in this resonance frequency is, however, affected by COZID parameters; in fact, the presence of the COZID limits the range over which the resonance may be shifted. Thus, for the simple COZID/dynamic system of Figure 8*, the resonant frequency is bound to a range, below the antiresonant frequency, having a lower limit of zero for $M_c/M_L = 0$, and an upper limit for $M_c/M_L = \infty$ given by

*Assuming positive values of R and r with R > r.

$$\omega_{R_{(max)}} = \omega_{AR} \sqrt{\frac{r/R + \rho_c^2/R^2}{1 + \rho_c^2/R^2}} \qquad (30)$$

where $\rho_c^2 = I_c/M_c$. This relationship may be utilized to select COZID parameters which preclude high values of transmissibility (T) even for the case of off-antiresonance excitation. For the case of helicopter external load isolation, Equation (30) is used to account for normal variation in rotor rpm (excitation frequency).

The equation for antiresonant frequency (ω_{AR}), Equation (29), demonstrates the most significant dynamic characteristic of the COZID. In this equation, ω_{AR} is shown to be a function of internal COZID parameters only. Tuning is accomplished by selection of suitable values of k_c, R, r, M_c and I_c, and this tuning is not affected by external dynamic parameters. This characteristic is fundamental to the application of the COZID as a helicopter external load isolator, because of the wide range of external cargo which must be carried and the wide range of sling systems which may be used*.

Transmissibility of the simple COZID of Figure 8, given by Equation (27), is illustrated in Figure 9. Shown are transmissibility curves for a simple COZID for two isolated masses. Resonant and antiresonant frequencies, ω_R and ω_{AR}, are shown as points of infinite and zero transmissibility, respectively.

COZID/EXTERNAL LOAD SYSTEM ANALYSIS

Figure 10 illustrates the helicopter/external load dynamic system incorporating a dual-cylinder** COZID. The system shown is a free-free system with four inertial masses (M_H, M_L, M_{c1} and M_{c2}) and three elastic elements (k_s, k_{c1} and k_{c2}). Static and dynamic equations for this system are developed and discussed in the following paragraphs.

---

* The impact of sling dynamic properties on COZID performance is discussed in the section on COZID/External Load System Analysis.

**The dual-cylinder COZID is a derivative of the single-cylinder COZID discussed in the section on Simple COZID Analysis.

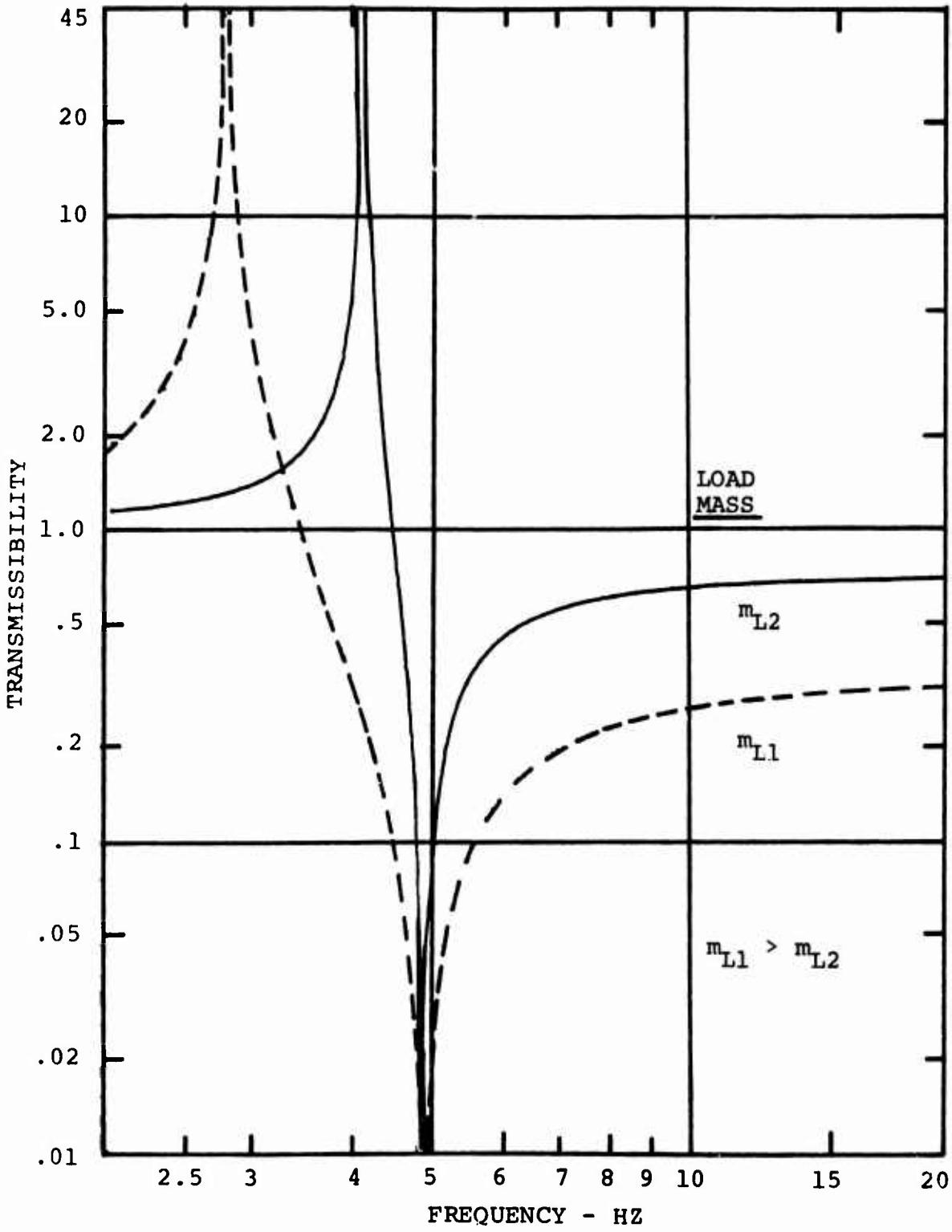

Figure 9. Effect of Changing Load Mass on Simple COZID Transmissibility.

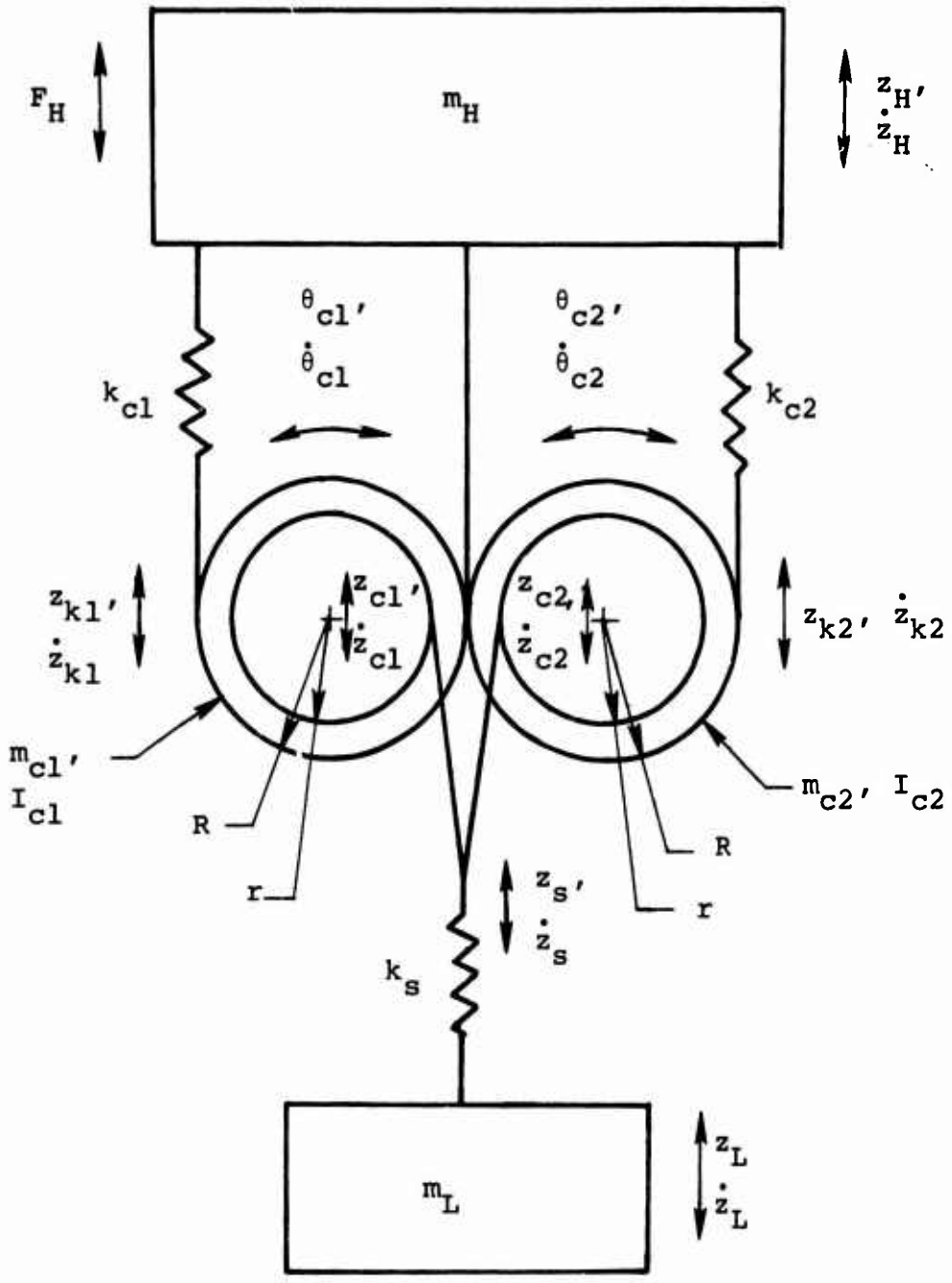

Figure 10. Helicopter/External Load Dynamic System Model With Dual-Cylinder COZID.

Static Analysis

Resolution of the static forces acting on the COZID, shown in Figure 11, results in the following equations for spring and support cable forces* (F_k and F_s):

$$F_{k_1} = F_{k_2} = \frac{L/2(R - r)}{2R} \tag{31}$$

$$F_{s_1} = F_{s_2} = \frac{L/2(R + r)}{2R} \tag{32}$$

Spring deflections are then

$$z_{k_1} = L/2(R - r)/2k_1R \tag{33}$$

$$z_{k_2} = L/2(R - r)/2k_2R \tag{34}$$

Inextensibility of the support cable results in pure rolling motion between the two inertia wheels, with

$$\theta_{c_1} = \frac{L/2(R - r)}{4k_1R^2} \tag{35}$$

$$\theta_{c_2} = \frac{- L/2(R - r)}{4k_2R^2} \tag{36}$$

Motion of the COZID/sling attachment point, z_s, is then given by

$$z_s = \frac{L/2(1 - r/R)^2}{4k_1} \tag{37}$$

---

* Assuming equal load sharing by the two inertia wheels and ignoring inertia wheel weight.

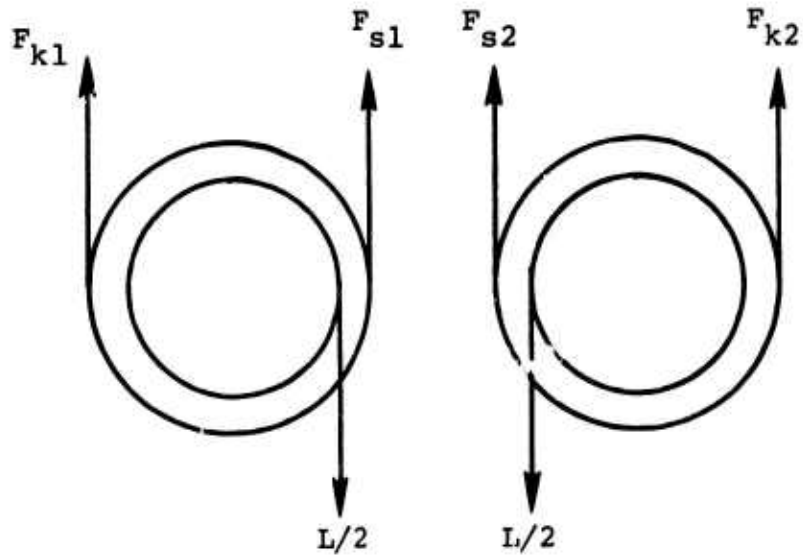

Figure 11. Static Forces Acting on Dual-Cylinder COZID and Sling.

or

$$z_s = \frac{L/2(1 - r/R)^2}{4k_2} \tag{38}$$

which requires that

$$k_{c_1} = k_{c_2}$$

If it is assumed that

$$k_{c_1} = k_{c_2} = kc/2 \tag{39}$$

where k_c is the total internal stiffness, the static deflection across the dual-cylinder COZID, equal to z_s, is given by

$$z_s = \frac{L(1 - r/R)^2}{4k_c} \tag{40}$$

The effective dual-cylinder COZID spring rate is then

$$K_c = \frac{4k_c}{(1 - r/R)^2} \tag{41}$$

and the static deflection of the load due to COZID stiffness is

$$\delta_{ST} = L/K_c \tag{42}$$

Comparison of Equations (41) and (42) with Equations (11) and (12) reveals that, for the same total internal spring rate the simple and dual-cylinder COZID configurations have identical statics.

Consideration of the force acting on the sling, with spring rate, k_s, results in an equation for load static deflection due to sling stiffness. This is

$$(\delta_{ST})_s = L/k_s \tag{43}$$

Since the COZID and sling are in parallel, the total effective spring rate of the Figure 10 system is

$$K_E = \frac{K_c k_s}{K_c + k_s} \tag{44}$$

and the total static deflection is

$$\delta_{ST}' = \frac{L(K_c + k_s)}{K_c k_s} \tag{45}$$

Dynamic Analysis

Potential and kinetic energy equations for the dynamic system of Figure 10 are

$$V = 1/2\ k_s(z_s - z_L)^2 + 1/2\ k_{c_1}(z_H - z_{k_1})^2 + 1/2\ k_{c_2}(z_H - z_{k_2})^2 \tag{46}$$

$$T = 1/2\ M_H\dot{z}_H^2 + 1/2\ M_L\dot{z}_L^2 + 1/2\ M_{c1}\dot{z}_{c1}^2 + 1/2\ M_{c2}\dot{z}_{c2}^2 + 1/2\ I_{c1}\dot{\theta}_{c1}^2 + 1/2\ I_{c2}\dot{\theta}_{c2}^2 \tag{47}$$

Consideration of Figure 10 geometry results in energy relationships involving helicopter, COZID/sling attachment point and load motions (z_H, z_s and z_L) only, with

$$\dot{\theta}_{c1} = -\dot{\theta}_{c2} = \frac{1/R(\dot{z}_s - \dot{z}_H)}{(1 - r/R)} \tag{48}$$

$$\dot{z}_{c1} = \dot{z}_{c2} = \frac{\dot{z}_s - (r/R)\dot{z}_H}{(1 - r/R)} \tag{49}$$

$$(z_H - z_{k_1}) = (z_H - z_{k_2}) = \frac{2(z_s - z_H)}{(1 - r/R)} \tag{50}$$

and

$$V = 1/2\ k_s(z_s - z_L)^2 + 1/2 \cdot \frac{4k_{c1}}{(1 - r/R)^2}(z_s - z_H)^2$$

$$+ 1/2\ \frac{4k_{c2}}{(1 - r/R)^2}(z_s - z_H)^2 \tag{51}$$

$$T = 1/2\ M_H\dot{z}_H^2 + 1/2\ M_L\dot{z}_L^2 + 1/2\ \frac{M_{c1}}{(1 - r/R)^2}(\dot{z}_s - (r/R)\dot{z}_H)^2$$

$$+ 1/2\ \frac{M_{c2}}{(1 - r/R)^2}(\dot{z}_s - (r/R)\dot{z}_H)^2 + 1/2\ \frac{I_{c1}}{R^2(1 - r/R)^2}(\dot{z}_s -$$

$$\dot{z}_H)^2 + 1/2\ \frac{I_{c2}}{R^2(1 - r/R)^2}(\dot{z}_H - \dot{z}_s)^2 \tag{52}$$

Imposition of the requirement for COZID symmetry permits simplifying assumptions with regard to inertia wheel and internal spring characteristics, with

$$M_{c1} = M_{c2} = 1/2\ M_c$$

$$I_{c1} = I_{c2} = 1/2\ I_c \tag{53}$$

$$k_{c1} = k_{c2} = 1/2\ k_c$$

where M_c, I_c and k_c are total COZID mass, inertia and internal spring rate, respectively. Substitution of these variables in Equations (51) and (52) yields

$$V = 1/2\ k_s(z_s - z_L)^2 + 1/2\ \frac{4k_c}{(1 - r/R)^2}(z_s - z_H)^2 \tag{54}$$

$$T = 1/2\, M_H \dot{z}_H^2 + 1/2\, M_L \dot{z}_L^2 + 1/2\, \frac{M_c}{(1 - r/R)^2} (\dot{z}_s - (r/R)\dot{z}_H)^2$$

$$+ 1/2\, \frac{I_c}{R^2(1 - r/R)^2} (\dot{z}_s - \dot{z}_H)^2 \quad (55)$$

Application of Lagrange's equation, Equation (23), for helicopter, COZID/sling attachment point, and load motions results in the three equations of motion for the dynamic system of Figure 10. Expressed in matrix form, these equations are shown in Equation (56).

Consideration of a finite sling spring rate (k_s) in the helicopter/external load system results in an additional degree of freedom, evident in the equations of motion. This added complexity makes quantitative interpretation of the equations, in terms of dynamic system physical responses, more difficult than interpretation of simple COZID responses. A qualitative interpretation of these equations is, however, presented in the following paragraphs.

As with all three-degree-of-freedom dynamic systems, the Figure 10 system is characterized by three resonance frequencies. For this system, which is statically unsupported (free-free), one of these resonances will always occur at zero frequency. The two remaining resonances will vary in frequency, dependent upon COZID, as well as external, dynamic parameters. In general, with the COZID geometry of Figure 10*, one resonance will always be at a frequency below the antiresonant frequency, (ω_{AR}), regardless of external dynamic parameters (M_H, M_L, k_s). The remaining resonance may occur above or below the antiresonance, but may not be coincident with the antiresonant frequency.

Antiresonance of the Figure 10 dynamic system occurs when the transmissibility, i.e., the ratio of load motion (z_L) to helicopter motion (z_H), goes to zero. With respect to the system equation of motion, decoupling takes place when the

*Specifically with R > r.

$$\begin{bmatrix} \begin{bmatrix} 4k_c \\ -\omega^2[(1-r/R)^2 M_H + (r/R)^2 M_c + I_c/R^2] \end{bmatrix} & -\begin{bmatrix} 4k_c \\ -\omega^2[(r/R)M_c + I_c/R^2] \end{bmatrix} & \begin{bmatrix} 0 \end{bmatrix} \\ -\begin{bmatrix} 4k_c \\ -\omega^2[M_c(r/R) + I_c/R^2] \end{bmatrix} & \begin{bmatrix} 4k_c + k_s \\ -\omega^2[M_c + I_c/R^2] \end{bmatrix} & -\begin{bmatrix} k_s \end{bmatrix} \\ \begin{bmatrix} 0 \end{bmatrix} & -\begin{bmatrix} k_s \end{bmatrix} & \begin{bmatrix} k_s \\ -\omega^2 M_L \end{bmatrix} \end{bmatrix} \begin{bmatrix} z_H \\ z_s \\ z_L \end{bmatrix} = \begin{bmatrix} F_H(1-r/R)^2 \\ 0 \\ 0 \end{bmatrix} \tag{56}$$

off-diagonal terms of the sub-matrix

$$\begin{bmatrix} 4k_c \\ -\omega^2[(1-r/R)^2 M_H + (r/R)^2 M_c + I_c/R^2] \end{bmatrix} - \begin{bmatrix} 4k_c \\ -\omega^2[(r/R)M_c + I_c/R^2] \end{bmatrix}$$

$$-\begin{bmatrix} 4k_c \\ -\omega^2[(r/R)M_c + I_c/R^2] \end{bmatrix} \qquad \begin{bmatrix} 4k_c + k_s \\ -\omega^2[M_c + I_c/R^2] \end{bmatrix}$$

go to zero. The antiresonant frequency ω_{AR} is then given by

$$\omega_{AR} = \sqrt{\frac{4k_c}{M_c(r/R) + I_c/R^2}} \tag{57}$$

Comparison of Equation (57) with Equation (29) shows the frequency of the antiresonance produced by the dual-cylinder COZID to be the same as that produced by the simple COZID discussed previously, assuming identical geometry (R and r), total COZID mass (M_c), inertia (I_c) and spring rate (k_c).

The number of inertia wheels used has no bearing on the dynamic performance of the COZID, provided total mass and inertia are maintained constant. It can be further stated that the general arrangement of the COZID, including number and location of elastic as well as inertial elements, has no bearing on its dynamic performance, provided appropriate geometrical, inertial and elastic parameters are selected.

Transmissibility (T) of the Figure 10 dynamic system will differ from that of the simple COZID in two significant ways. First, the transmissibility will display two resonant frequencies (ω_{R1} and ω_{R2}) rather than the single transmissibility resonance shown for the simple COZID. Secondly, the transmissibility above the antiresonance will reflect that of a simple spring mass system, with an exponentially decreasing transmissibility above resonance. This is in contrast to the simple COZID, which displays an increasing, but finite valued, transmissibility above the antiresonant frequency.

With regard to frequency placement of the Figure 10 transmissibility resonances, two alternative arrangements are possible. These are:

(1) Two resonances below the antiresonant frequency.

(2) One resonance below and one above the antiresonant frequency.

Typical system responses for both of these conditions are shown in Figure 12.

As mentioned previously, resonance frequencies of the Figure 10 helicopter/external load dynamic system are dependent on external dynamics as well as the parameters of the COZID itself. While some control of resonance frequencies is possible through COZID parameter selection, variation in resonance will occur with changing helicopter mass, sling spring rate and external load mass. Design of COZID systems to achieve appropriate antiresonance frequencies while maintaining acceptable resonance frequency ranges is discussed in the following section.

ALTERNATE COZID CONFIGURATIONS

The equations and theoretical performance characteristics derived in this section with reference to the single-cylinder and dual-cylinder COZID models of Figures 5 and 10 are equally applicable to all COZID configurations which incorporate the following essential features:

(1) One, or more, high-rotational-inertia compound pulleys.

(2) One, or more, elastic elements arranged to resist pulley rotation and translation.

A number of alternate COZID configurations, each satisfying the preceding requirements in a different manner, are shown in Figure 13.

All of the COZID configurations shown in Figure 13 have identical dynamic characteristics. Because of this, all of the parametric study data, as well as all of the model test results presented in the subsequent sections of this report, are equally relevant to each of the configurations shown. This interchangeability permits the selection of a specific COZID configuration solely on the basis of physical compatibility with a given application.

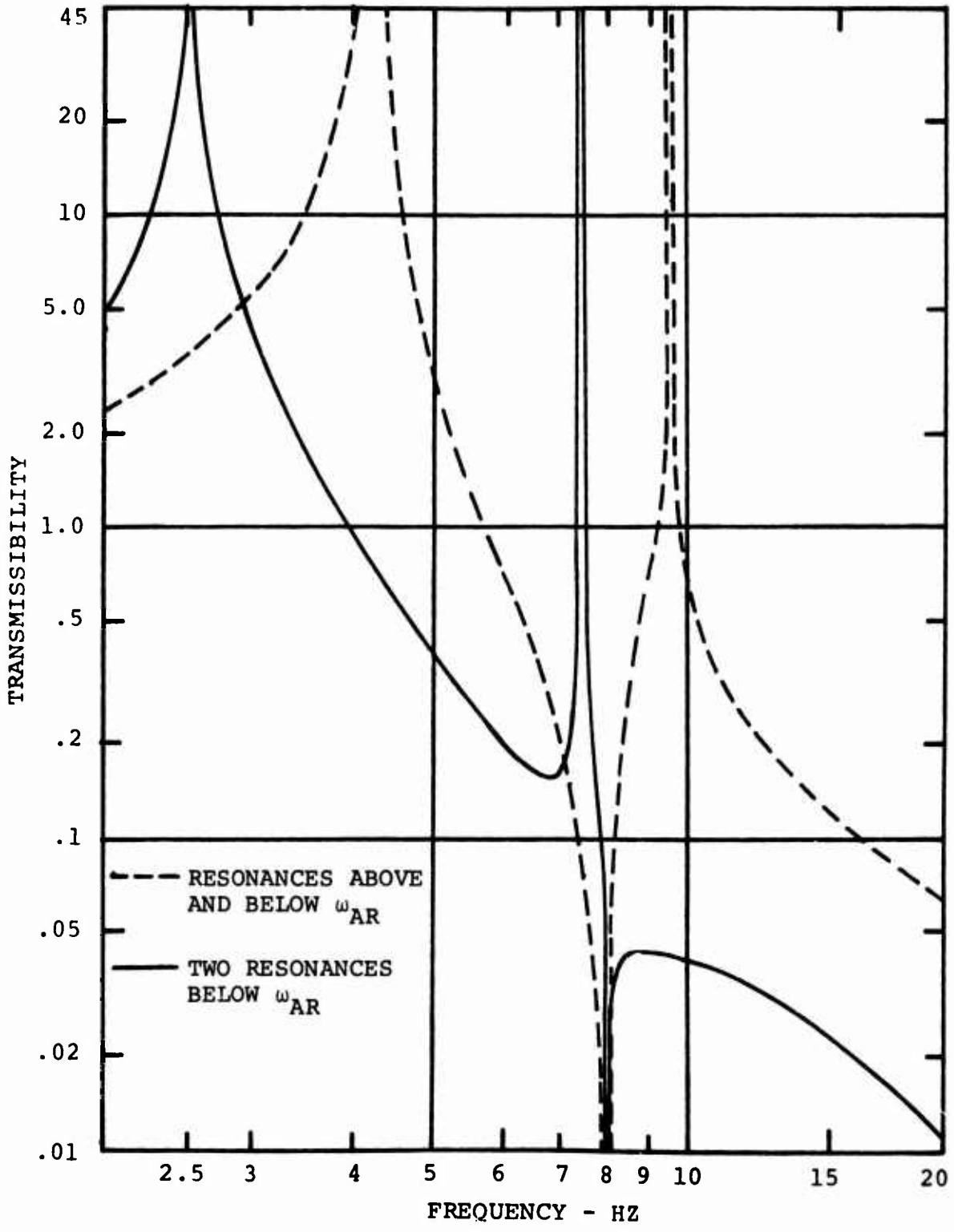

Figure 12. Typical Helicopter/COZID/Sling/External Load Transmissibility Curves.

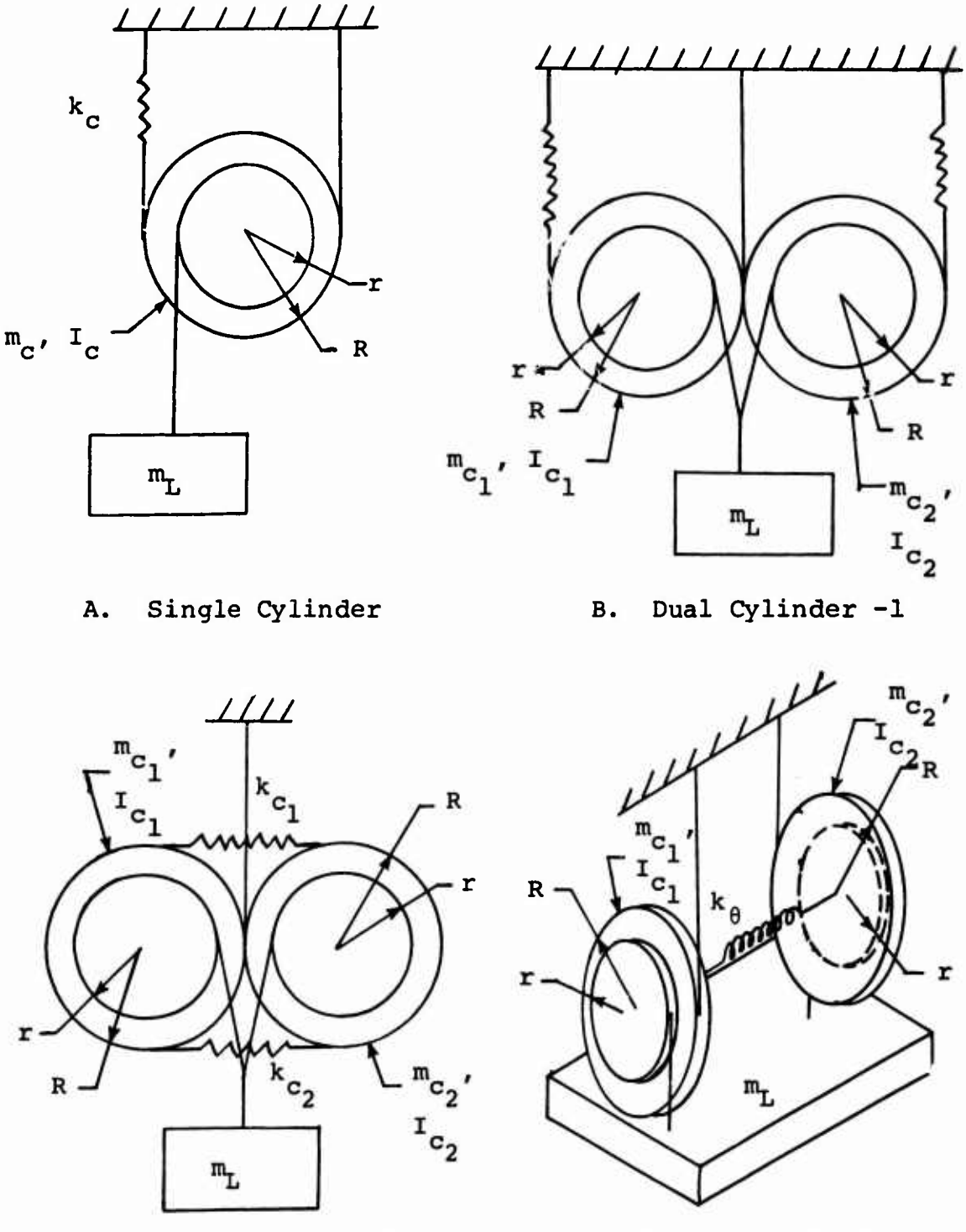

A. Single Cylinder

B. Dual Cylinder -1

C. Dual Cylinder -2

D. Folded Dual Cylinder

Figure 13. Alternate COZID Configurations.

PARAMETRIC STUDY

Parametric studies were performed applying the COZID to each of the Army cargo helicopters listed in Table I. In addition, a parametric study was undertaken to define the parameters of a model COZID, suitable for laboratory evaluation. These studies were conducted using computer programs based on COZID static and dynamic equations derived in the analysis section. As a result of these studies, design charts were prepared giving ranges of allowable COZID parameters for each full-scale and model application. These design charts are presented and discussed in the following paragraphs. The methods used to generate the charts are also discussed, and the limitations of their usage are defined.

HELICOPTER APPLICATIONS

Referring to Equation (56) of the previous section, it is seen that the dynamic response of the helicopter/COZID/sling load dynamic system is dependent on a large number of parameters. Included among these are parameters which relate to the specific helicopter application, including:

- M_H - the helicopter mass
- M_L - the external load mass
- k_s - the sling spring rate
- f_{1-P} - the main rotor once-per-revolution frequency

All of these parameters are essential as input to the parametric study. These data are given in Table II for helicopters of interest.

Helicopter weights shown in Table II are representative of the minimum vehicle weight for the external cargo-carrying mission. External load weights, shown for each helicopter, are the maximum external load capacity, based on gross weight minus vehicle weight*, and a minimum external cargo weight

*Maximum external cargo weights for the UTTAS A/C (YUH-60 and YUH-61) are based on growth of the design capacity to maximum external cargo equal to the vehicle weights.

TABLE II. INPUT DATA FOR PARAMETRIC STUDIES*

Helicopter	f_{1-P} (hz)	Helicopter Weight (lb)	External Cargo Weight - lb		Sling Spring Rate - lb/in.	
			Minimum	Maximum	Minimum	Maximum
UH-1D	5.4	5400	1350	4000	2000	29,000
YUH-60	4.38	13,481	3370	13,481	4000	65,000
YUH-61	4.92	12,686	3171	12,686	4000	65,000
CH-47B/C	4.0 to 4.16	20,000	5000	20,000	4000	65,000
CH-46D	4.4	13,000	3250	10,000	4000	65,000
CH-53D	3.1 to 3.24	23,000	5750	19,000	4000	65,000

* Data for existing A/C were taken from pilots' manuals. YUH-60 and YUH-61 data were provided by the Army.

equal to 25 percent of the aircraft weight*.

The values for sling system spring rates given in Table II are based on the use of elements (pendants and bridles) from the proposed universal sling system. Minimum sling spring rates result from the use of the prescribed soft pendants for 6000-pound- and 20,000-pound-capacity slings. Maximum sling spring rates are based on the use of a stiff pendant ($k \rightarrow \infty$) with a four-legged bridle rigged at zero degrees**. In actual practice the range of sling system spring rate would not be as great as that shown in Table II, since the requirement for a soft sling is related to vertical bounce prevention and, with the COZID, this requirement is negated.

Dynamic Performance Criterion

Helicopter/external load vertical bounce occurs as a result of resonant amplification of main rotor 1-P vibratory forces. The degree of amplification, and consequently the probability of vertical bounce, is governed by the helicopter/load dynamic coupling characteristics, which are determined by the parameters of the dynamic system.

For dynamic systems exhibiting good coupling, as evidenced by high helicopter to load transmissibility at f_{1-P}, the possibility of vertical bounce is great. This possibility decreases with decreasing 1-P transmissibility, until, at a given critical value of transmissibility, the helicopter and load are effectively decoupled. For transmissibilities at or below this critical value, vertical bounce will not occur.

Experimental work reported in Reference 2 and described in the Introduction suggests a critical transmissibility of 1.5. In the Reference 2 effort, numerous dynamic systems were subjected to testing, with no evidence of sustained vertical bounce found for systems having 1-P transmissibilities less than or equal to 1.5. In the absence of additional data either substantiating or refuting this result, this critical transmissibility has been adopted as the criterion for

---

* The assumption of a minimum significant cargo weight is based on Reference 1, which cites data showing no tendency to sustain vertical bounce for load/vehicle ratios of .5 or lower.

**Sling system spring rate equations are given in Appendix II of Reference 1.

determining the susceptibility of a given dynamic system to vertical bounce. Conversely, the ability of a given COZID to maintain dynamic system one-per-rev transmissibility less than 1.5 is taken to be the primary indicator of acceptable COZID dynamic performance.

Discussions of COZID properties, presented in the Analysis section, have described the capability of the COZID to attain a low transmissibility at a given, preselected frequency, and to maintain this low transmissibility regardless of changes in external parameters. For applications where the excitation frequency is constant, this characteristic is the only one of concern. For the typical helicopter application, however, the excitation frequency, f_{1-P}, is not constant, but will vary over a fixed, predetermined range depending upon pilot rpm selection. To provide the required dynamic decoupling in this application, the helicopter to load transmissibility must be kept below 1.5 over this entire range, for all possible dynamic system configurations. Consequently, selection of COZID parameters for a given helicopter application must be predicated on attainment of a predictable, low-transmissibility frequency band, encompassing the range of possible 1-P rotor frequencies. This low-transmissibility frequency band is referred to as the antiresonant bandwidth.

The antiresonant bandwidth is defined in terms of the maximum allowable transmissibility. For the present case, with a maximum allowable transmissibility of 1.5, the antiresonant bandwidth is defined as the absolute range of frequency, inclusive of the tuned frequency, over which the transmissibility does not exceed 1.5. The antiresonant bandwidth is determined entirely by the frequency placement of the dynamic system resonances and antiresonance. In contrast to the antiresonant frequency, which is constant for a given COZID configuration, the antiresonant bandwidth will vary with varying helicopter mass, load mass, and sling spring rate, and therefore it will be different for each sling configuration used.

While it is not possible to maintain a constant antiresonant bandwidth with changing system dynamic parameters, it is always possible to select COZID parameters which insure sufficient bandwidth to meet performance requirements.

This is accomplished by considering the extremes of dynamic system parameters* in conjunction with the known f_{1-P} limits. Given these data as inputs, the COZID is designed to minimum bandwidth requirements for the extreme cases. Bandwidths of all dynamic systems having parameters within these extremes will then, of necessity, exceed the minimum. The anti-resonant bandwidth of a typical COZID application is illustrated in Figure 14.

Attainment of an antiresonant bandwidth sufficient to encompass the entire 1-P frequency range is the only COZID dynamic performance requirement for the present application. Antiresonant tuning at a specific frequency, for example, the mean frequency of the 1-P frequency range, is not essential, nor is it necessary to achieve a very low anti-resonant transmissibility, provided this transmissibility is less than 1.5.

For the purposes of the parametric study, application of a COZID performance criterion based on achieving a minimum antiresonant bandwidth was found to be impractical. This was due primarily to the lengthy calculation procedure required, and the large number of aircraft applications requiring study. This criterion was, however, applied during the CH-47B/C preliminary design effort discussed in the Preliminary Design section.

The dynamic performance criterion developed for the parametric study utilizes resonance/antiresonance frequency separation and assumes an antiresonant frequency equal to the nominal 1-P frequency. Resonance/antiresonance frequency separation is readily calculated, and it provides a relative measure of the tolerance of a given COZID design to varying rotor speed.

---

* As pointed out in the Introduction, the extreme sling configurations are those which result in the highest and lowest resonant frequencies. These are, respectively:

- minimum significant external load and stiffest sling
- maximum external load and softest sling.

These data are given in Table II for each helicopter application of interest.

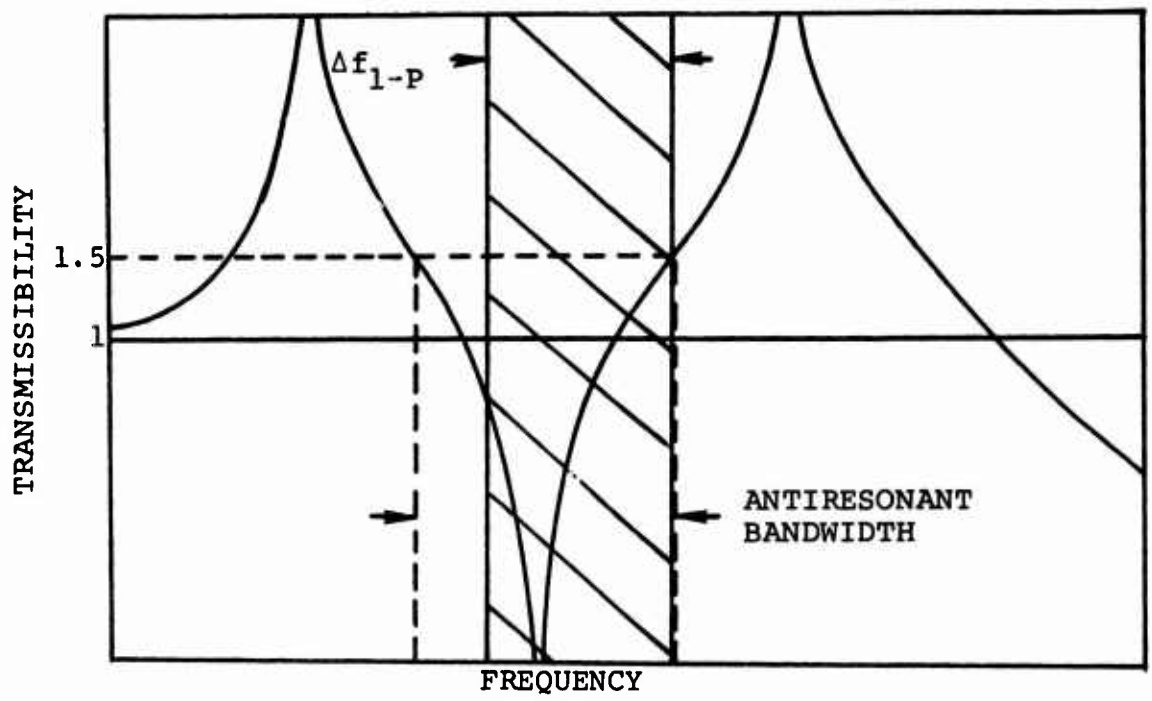

A. Antiresonant Bandwidth With $W_L = (W_L)_{max}$, $k_s = (k_s)_{min}$

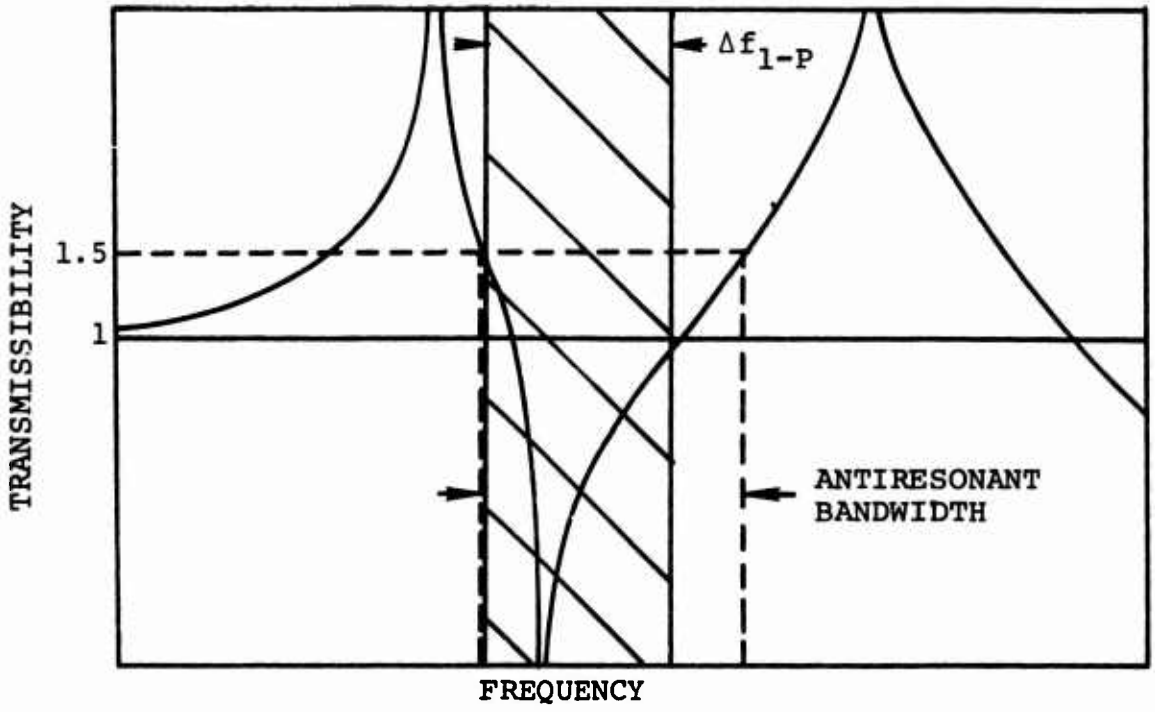

B. Antiresonant Bandwidth With $W_L = (W_L)_{min}$, $k_s = (k_s)_{max}$

Figure 14. Antiresonant Bandwidth.

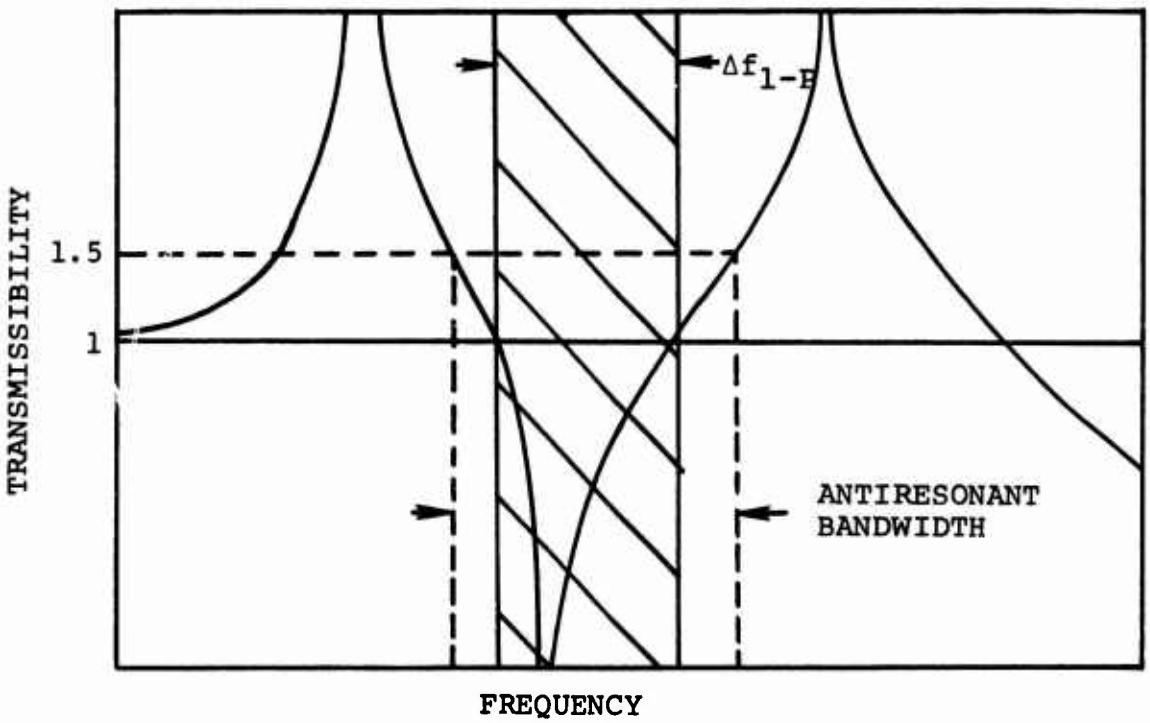

C. Antiresonant Bandwidth for $(W_L)_{min} < W_L < (W_L)_{max}$, $(k_s)_{min} < k_s < (k_s)_{max}$

Figure 14 - Concluded.

The antiresonant bandwidth varies approximately in direct proportion to the resonant/antiresonant separation, with a constant of proportionality nearly equal to one. Specifics of the performance criterion used are given in the following paragraphs.

Study Methods and Results

Definition of a COZID configuration requires the specification of a number of parameters reflecting mass, stiffness, inertia and geometrical properties.

The following COZID parameters, used in the present effort, completely define a given configuration:

- R - the outer (support cable) radius
- r/R - the ratio of inner (load cable) radius to outer radius
- $M_C/(M_L)_{max}$ - the ratio of COZID mass to maximum external load mass
- θ_{ST} - the static rotation of the COZID inertia wheel

The above independent variables have been chosen for a number of reasons. The outer radius, R, for example, is strongly related to both static and dynamic performance, and it also provides a measure of inertia wheel overall size. The radius ratio, r/R, is the primary variable affecting resonant/antiresonant frequency separation, one of the two key dynamic performance considerations. COZID to maximum load mass ratio provides a measure of the weight penalty imposed by the use of the COZID and gives the basis for weight versus size trade-off studies. Inertia wheel static rotation is significant since θ_{ST} is directly related to

internal COZID stiffness, with

$$k_c = \frac{(1 - r/R)W_{SL}}{4 \cdot \theta_{ST} \cdot R} \tag{58}$$

load static deflection, with

$$\delta_{ST} = \theta_{ST} \cdot R \cdot (1 - r/R) \tag{59}$$

and COZID cg static deflection, with

$$(z_c)_{ST} = \theta_{ST} \cdot R \qquad (60)$$

With respect to the remaining variables, only the COZID inertia, I_c, remains undefined. Within the parametric study, the value of I_c is calculated using a fixed relationship between inertia wheel mass, M_c, and outer radius, R. This relationship is based on a practically attainable value of inertia wheel radius of gyration, ρ_c.

The parametric study results are obtained in two steps. The first step involves selection of parameters satisfying the requirement for tuned antiresonance at the nominal 1-P frequency of the subject helicopter*. Results of this step are a series of curve families relating R and r/R. Within each family of curves, the static rotation θ_{ST} is kept constant and a number of plots of R vs r/R are generated corresponding to constant mass ratio, $M_c/(M_{SL})_{max}$. A series of such curve families is generated, each family corresponding to a different static rotation, θ_{ST}. In effect, each individual curve represents a line of constant tuning. Constant antiresonance curves for each helicopter application are shown as solid lines in the design charts, Figures 15 through 20.

The second step in the parametric study involves the calculation of a constant resonant/antiresonant frequency separation (F_R) curve for each helicopter application and static stiffness. These curves, shown as dashed lines in Figures 15 through 20, reflect a common, minimum resonance/antiresonance frequency separation of 5 percent. COZID configurations lying above and to the left of the curves shown will have greater than 5 percent separation, while those below and to the right will have less than 5 percent separation.

The curves of Figures 15 through 20 illustrate the range of COZID parameters which would result in COZID configurations suitable for each of the helicopter applications shown.

---

* Nominal 1-P frequencies used are given in Table II. For the CH-47 and CH-53 aircraft, the nominal 1-P frequency is taken as the upper limit of the range shown.

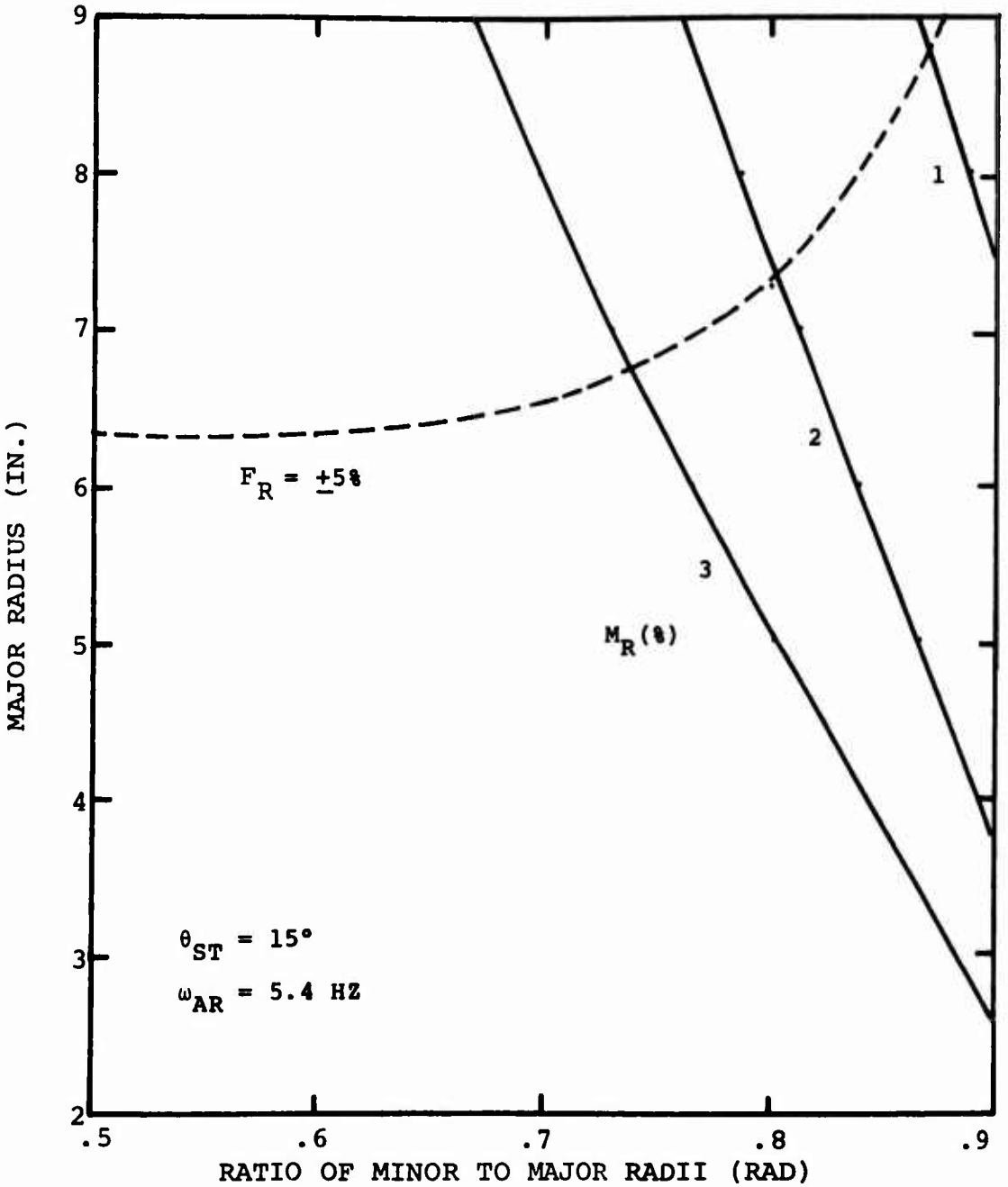

Figure 15. UH-1D COZID Parameters.

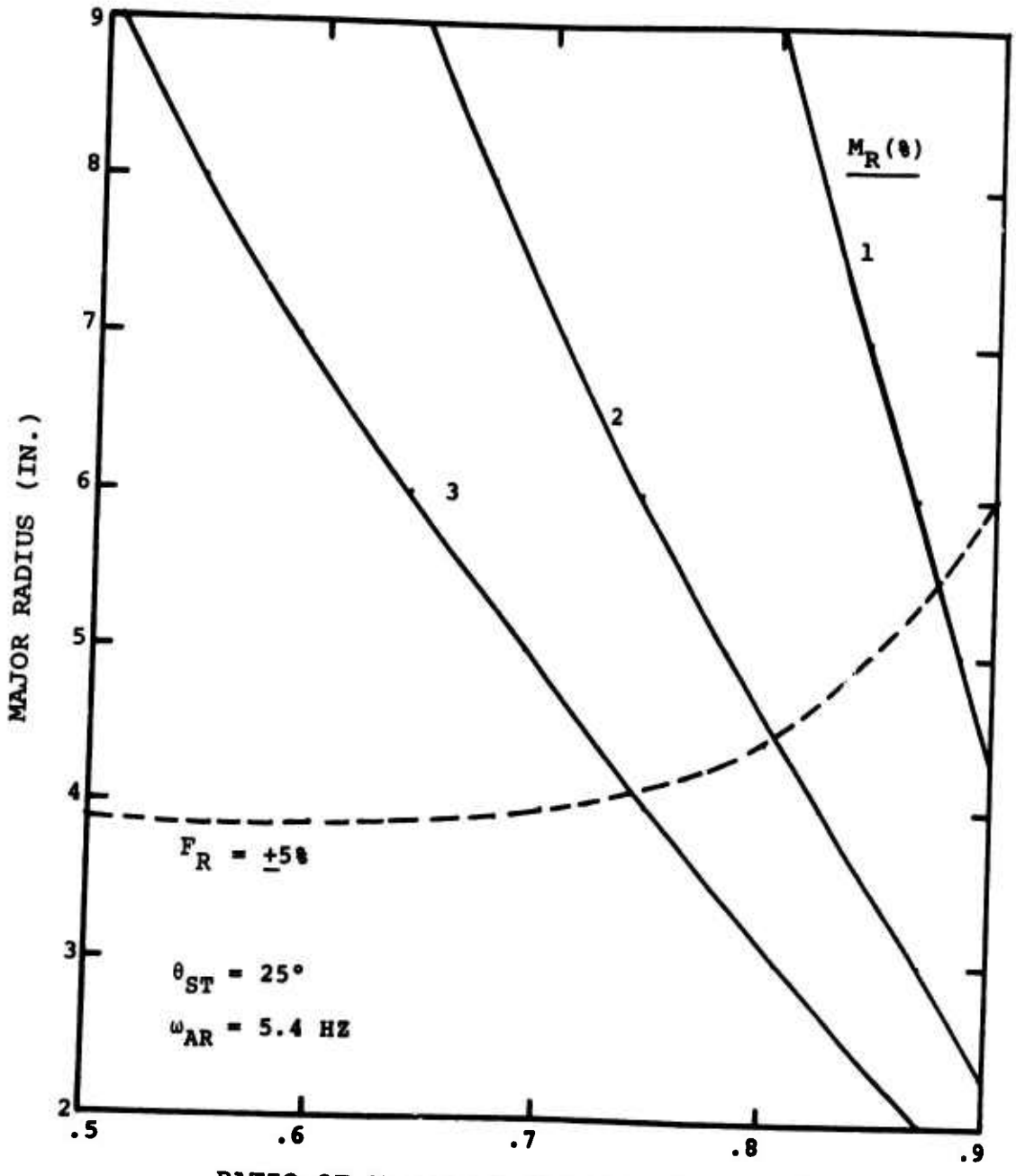

Figure 15 - Continued.

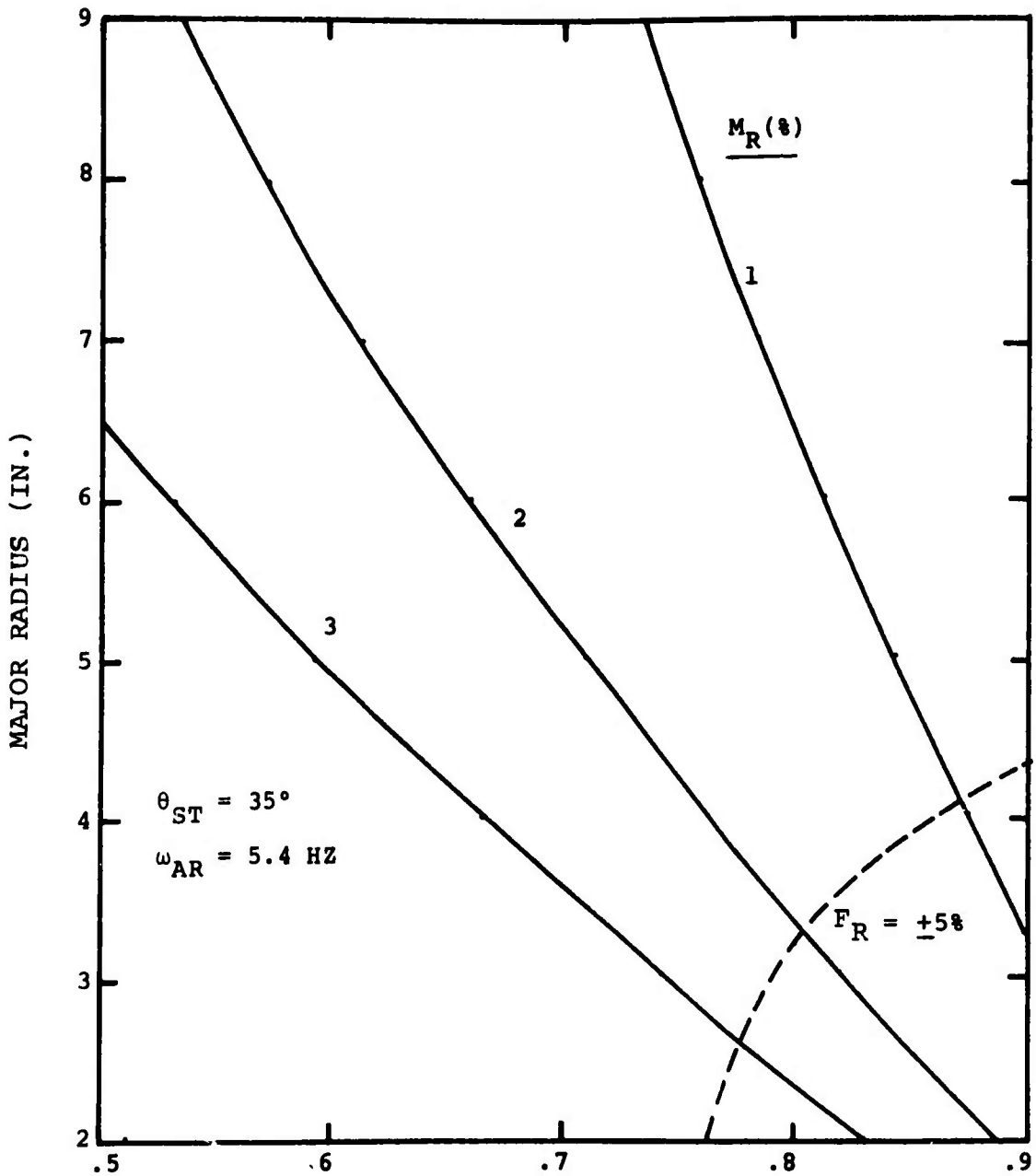

Figure 15 - Concluded.

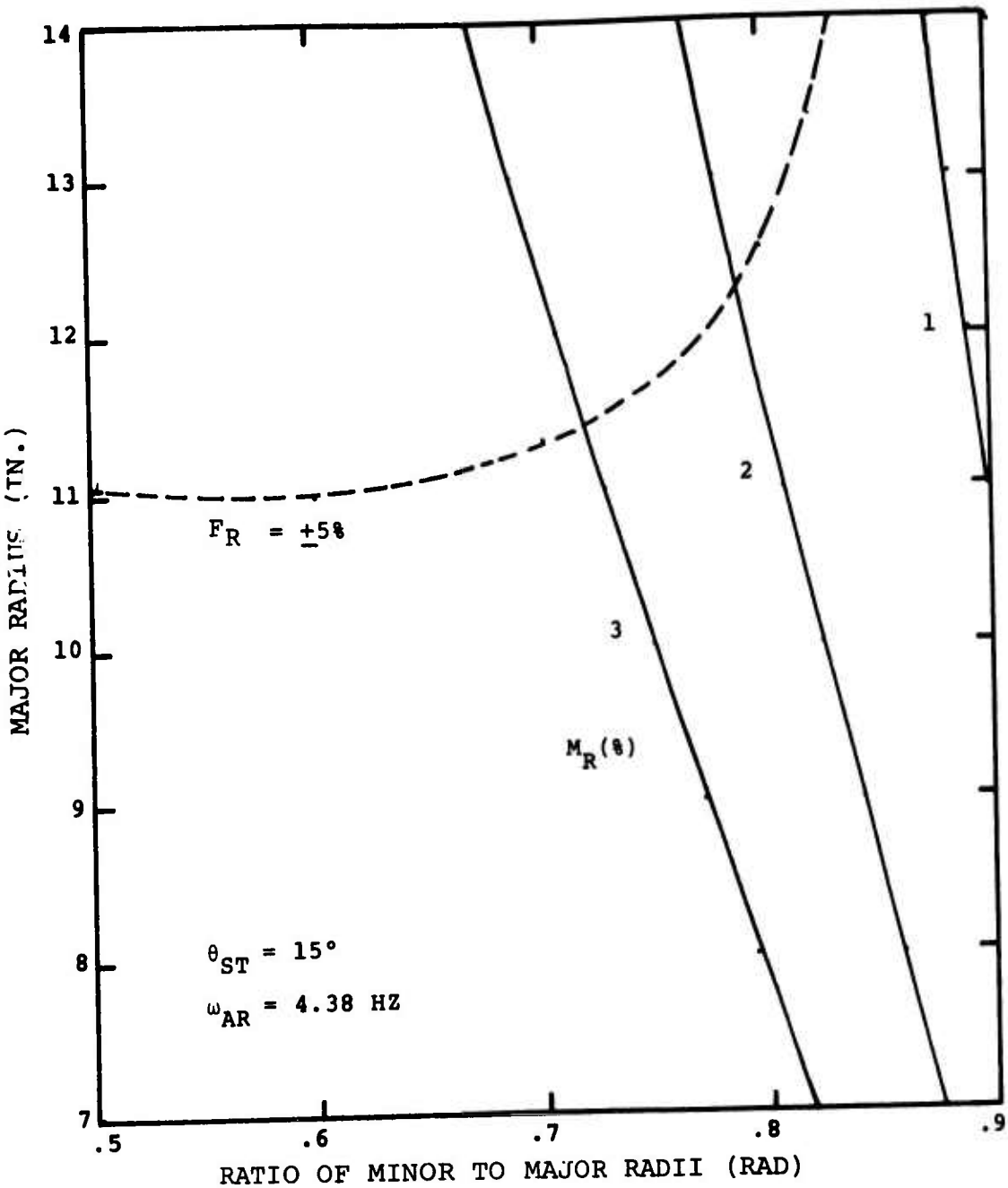

Figure 16. YUH-60 COZID Parameters.

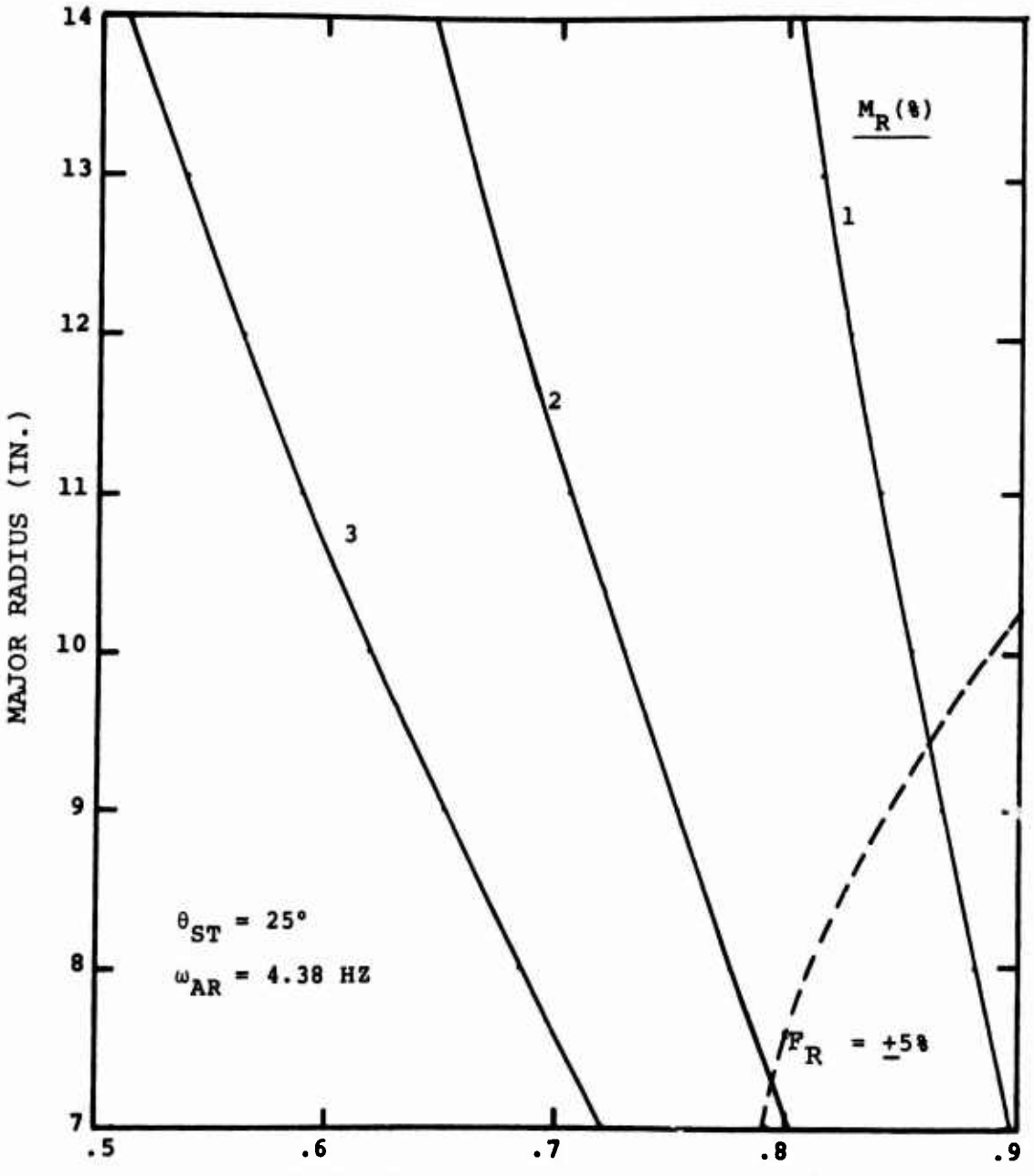

Figure 16 - Continued.

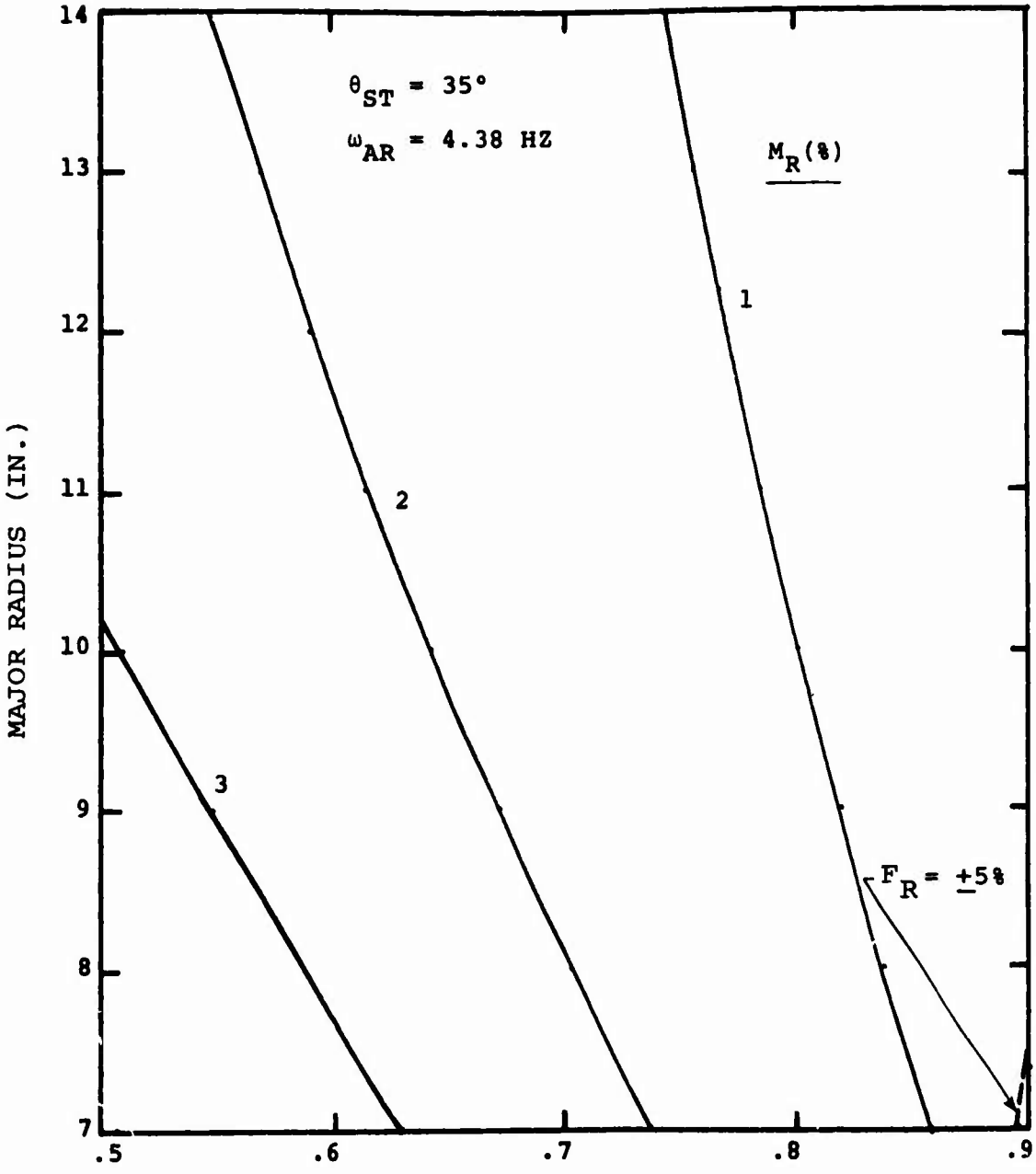

Figure 16 - Concluded.

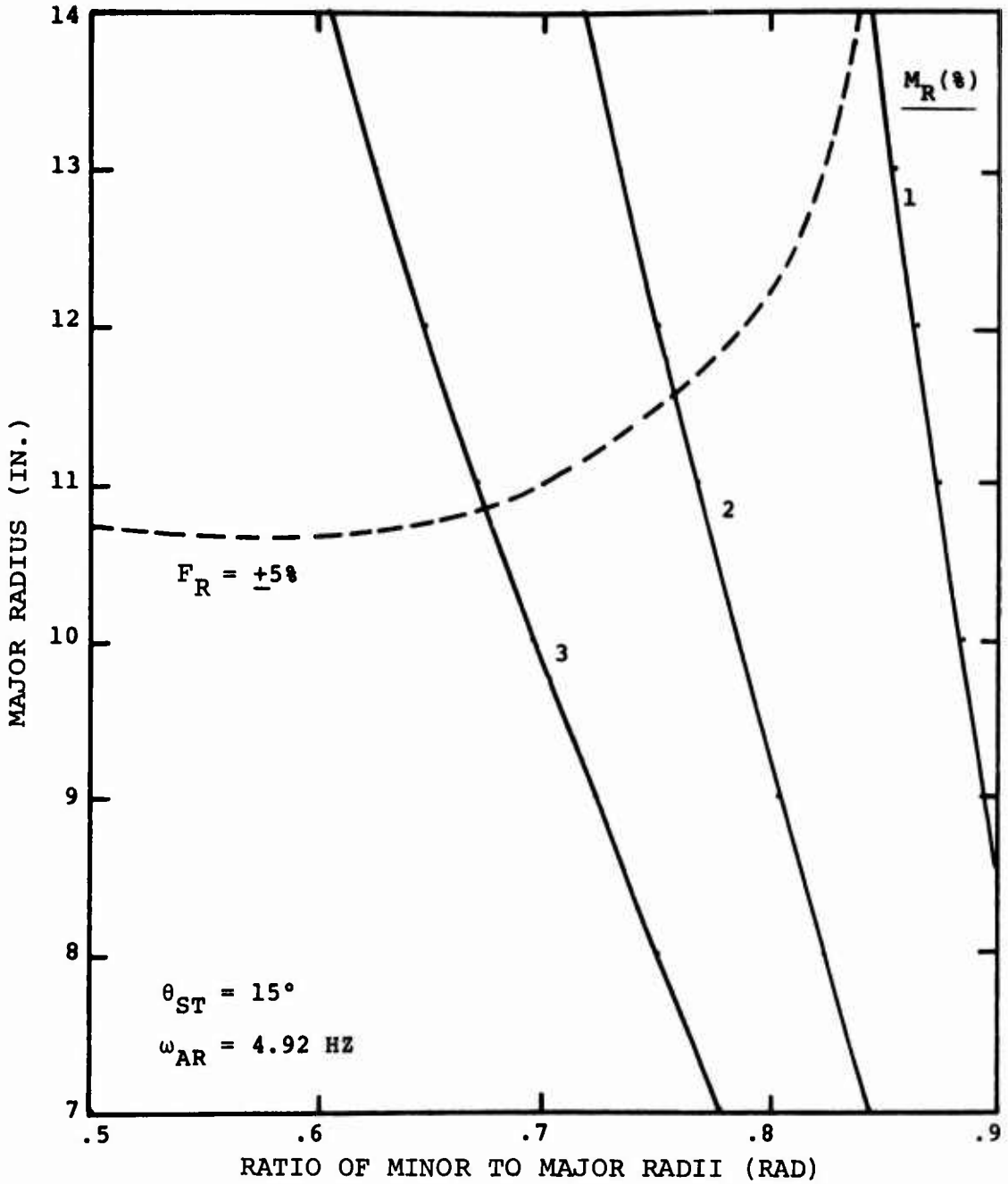

Figure 17. YUH-61 COZID Parameters.

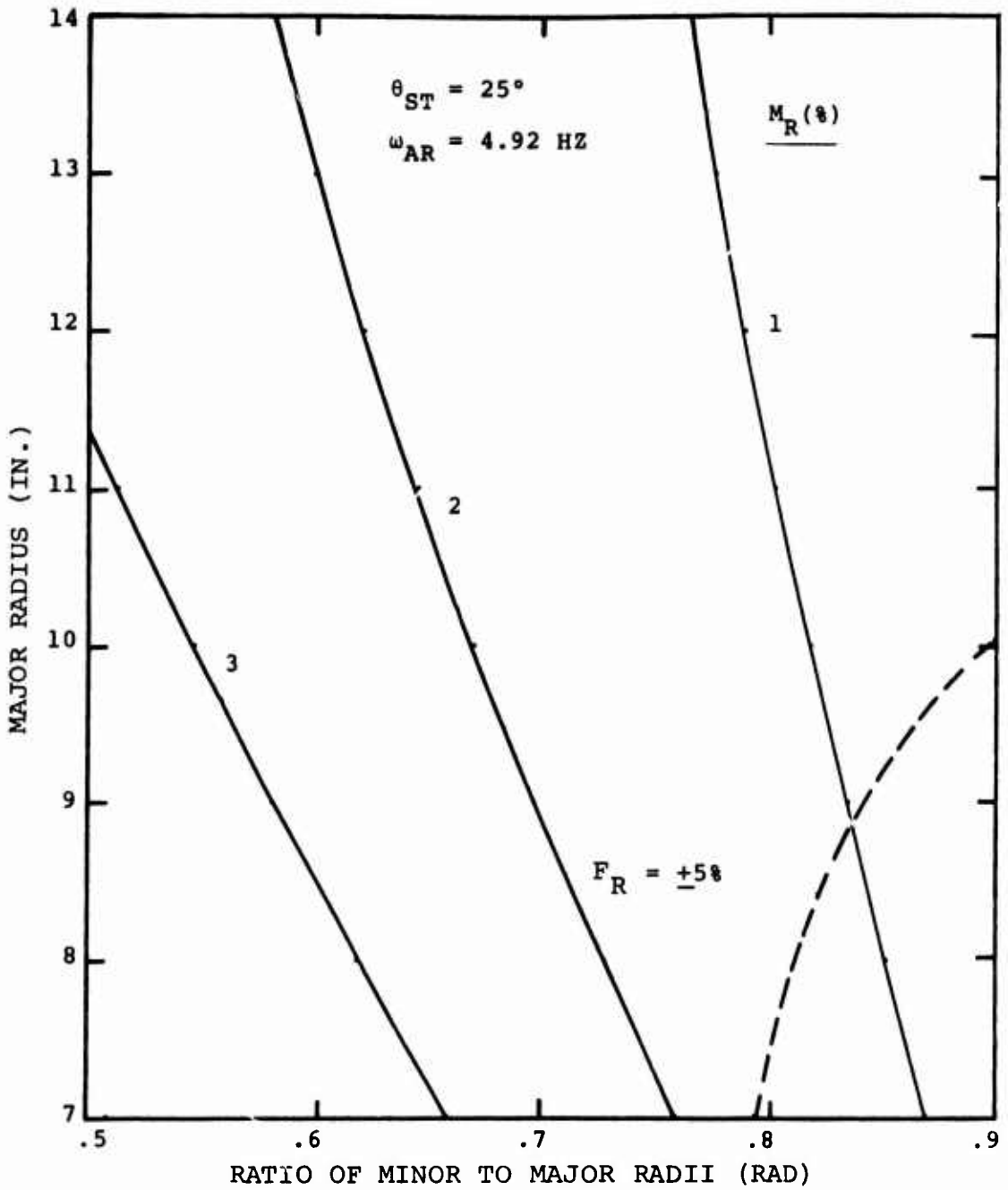

Figure 17 - Continued.

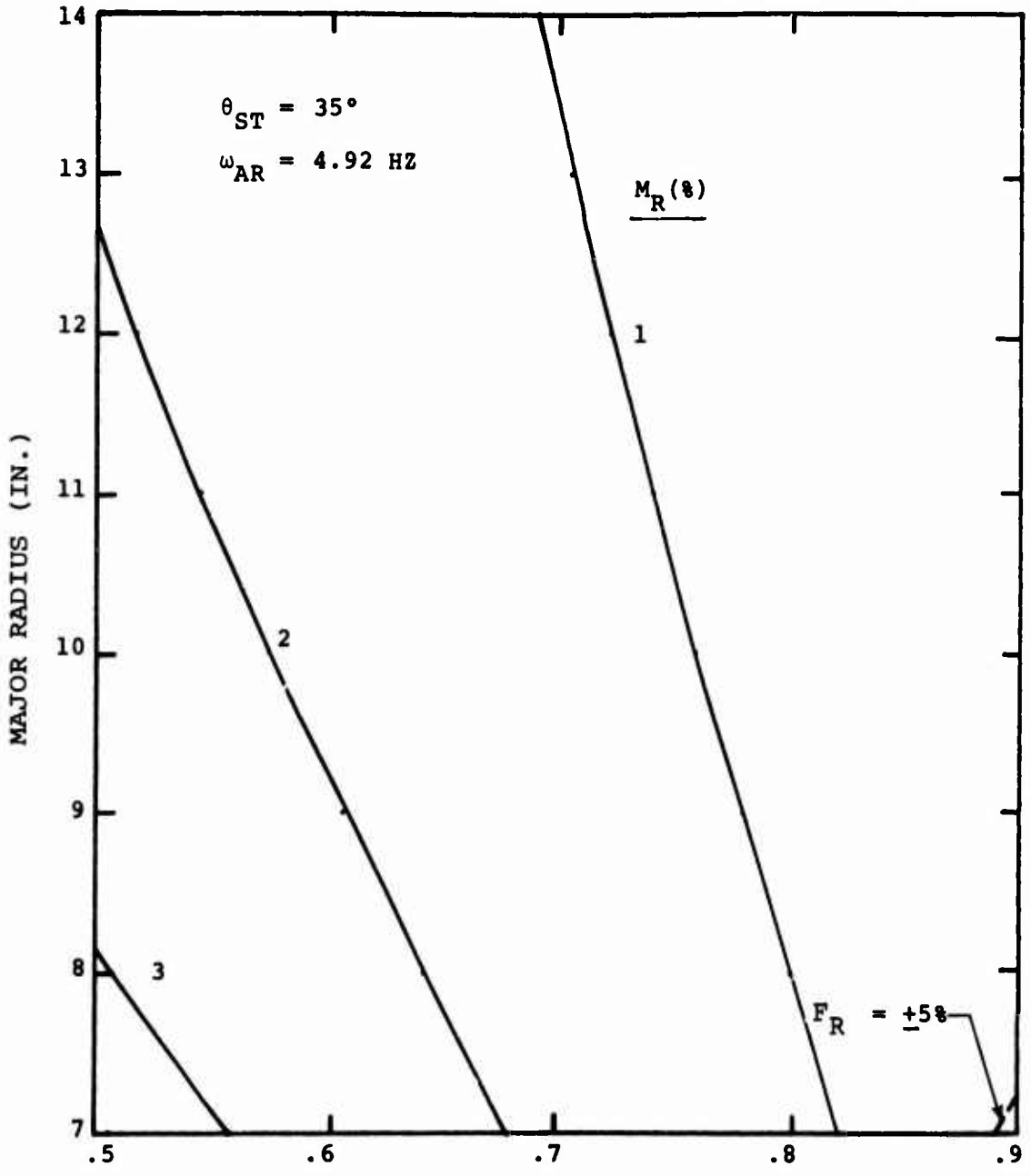

RATIO OF MINOR TO MAJOR RADII (RAD)

Figure 17 - Concluded.

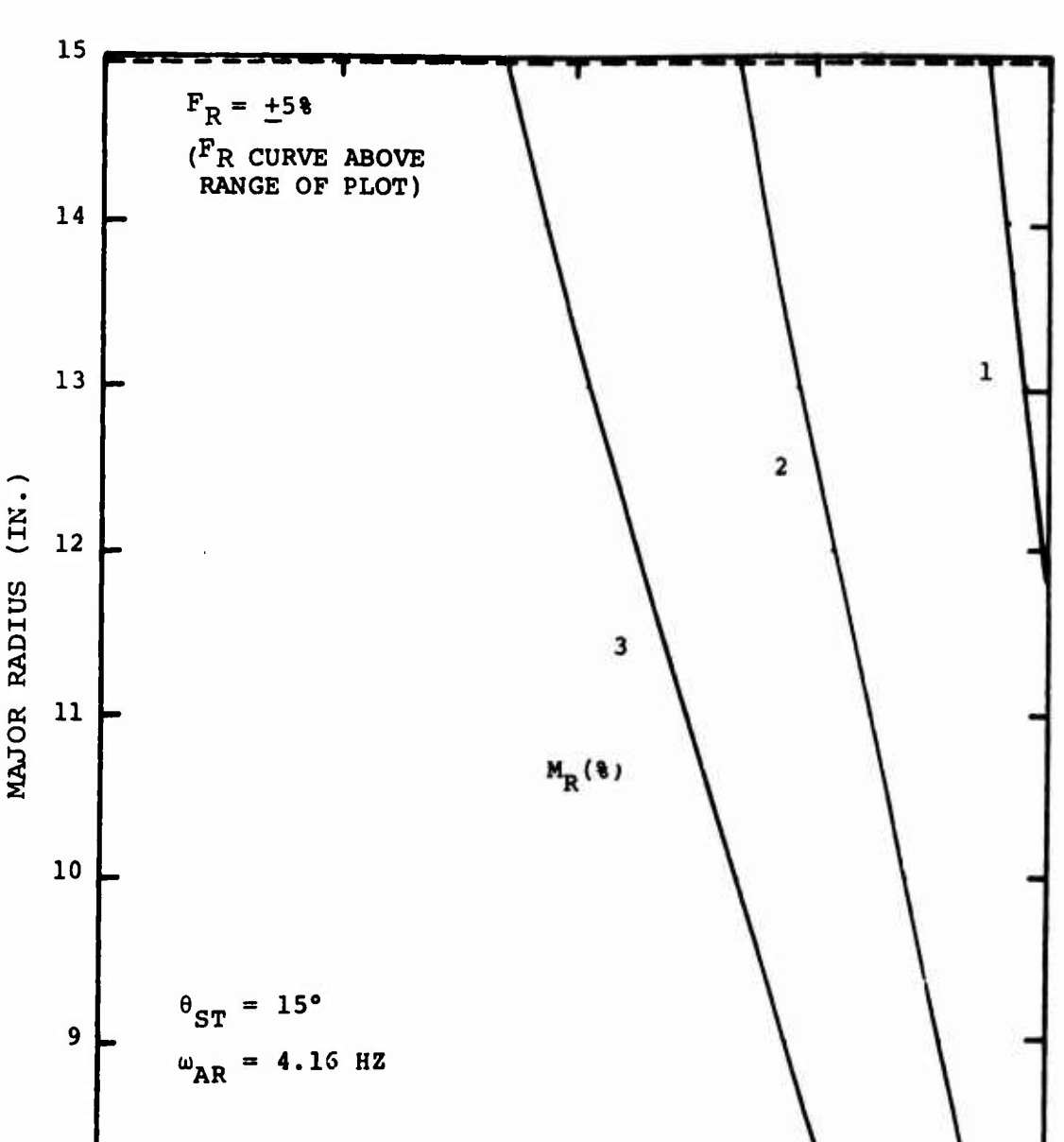

Figure 18. CH-47B/C COZID Parameters.

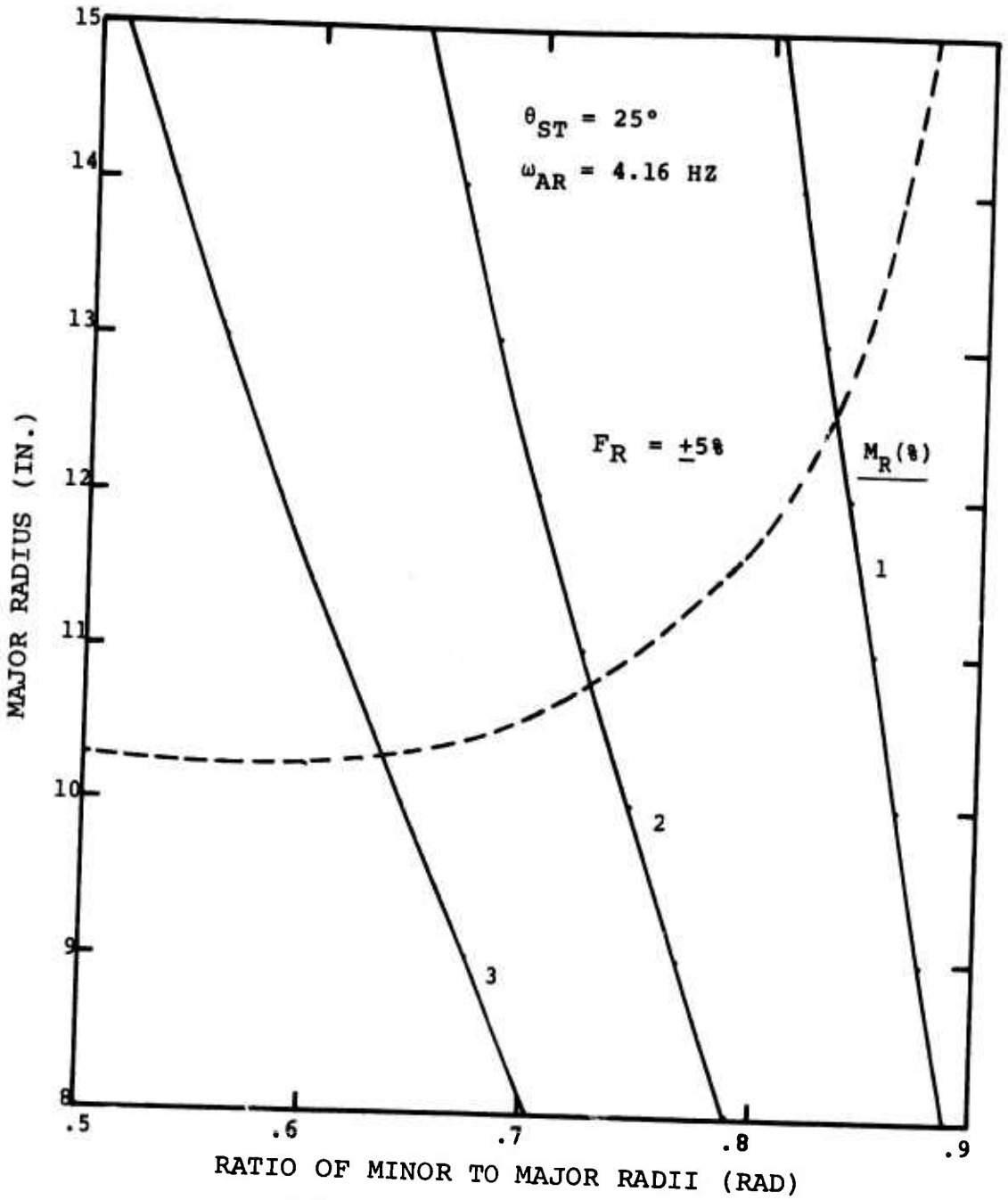

Figure 18 - Continued.

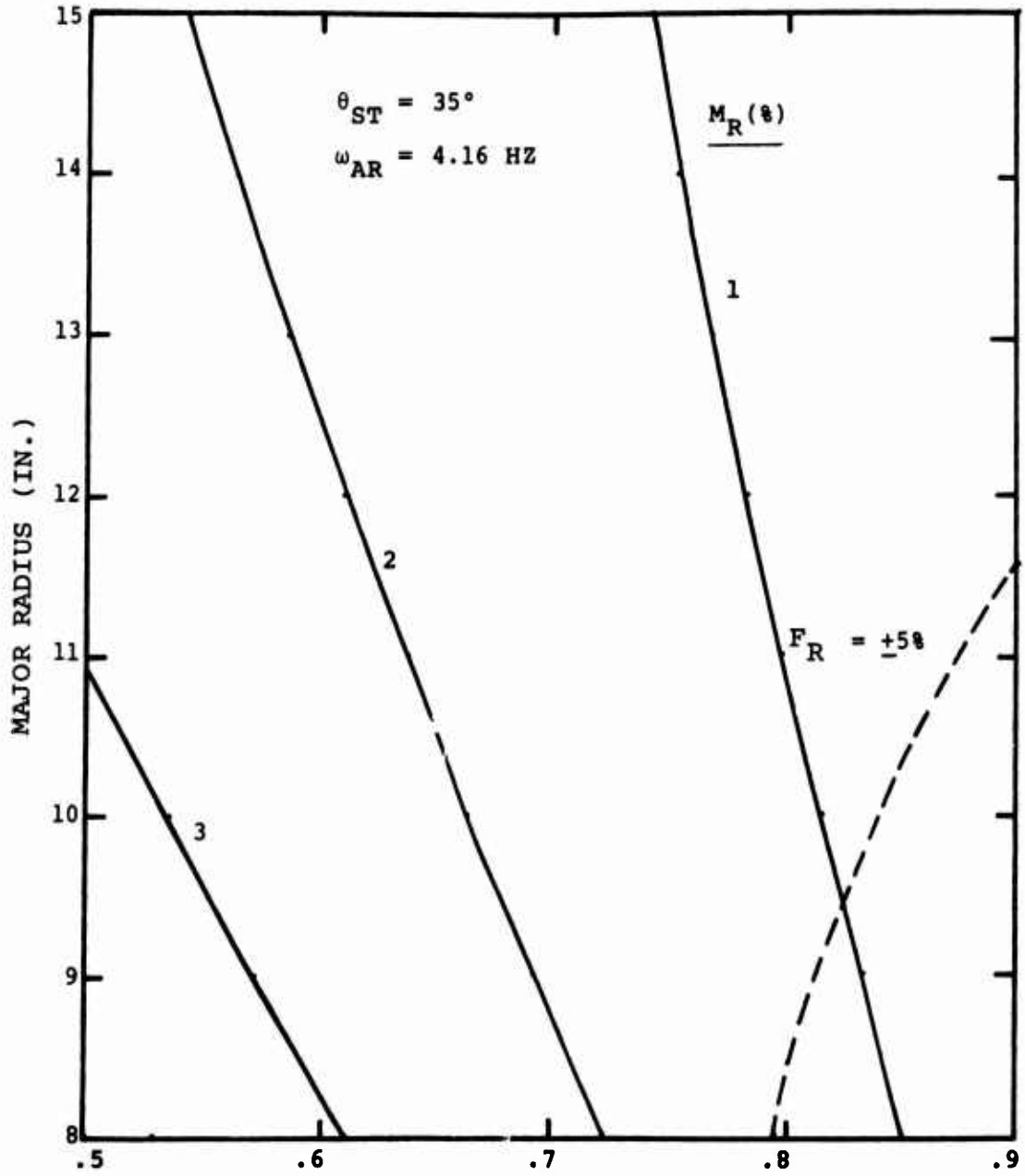

Figure 18 - Concluded.

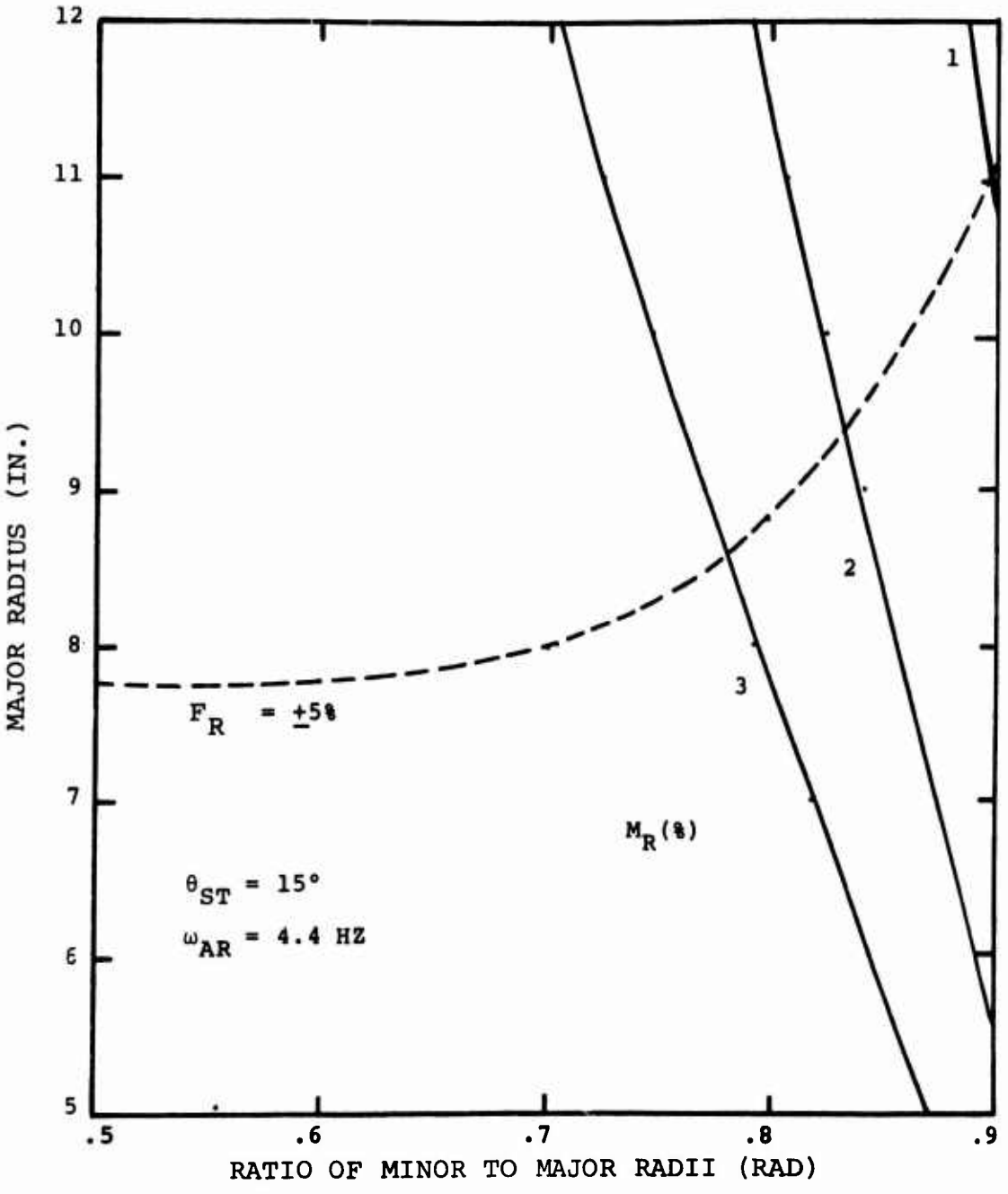

Figure 19. CH-46D COZID Parameters.

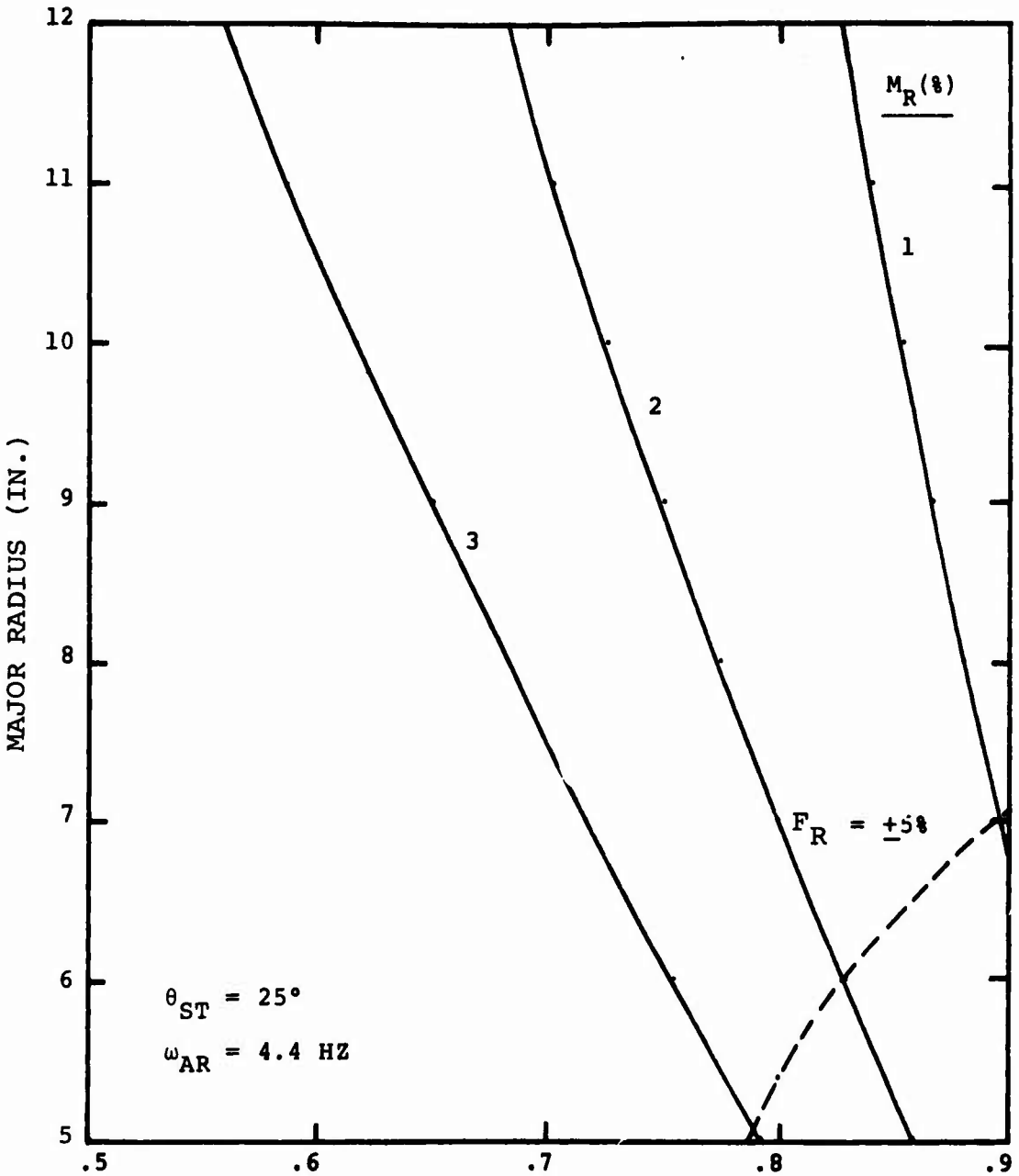

Figure 19 - Continued.

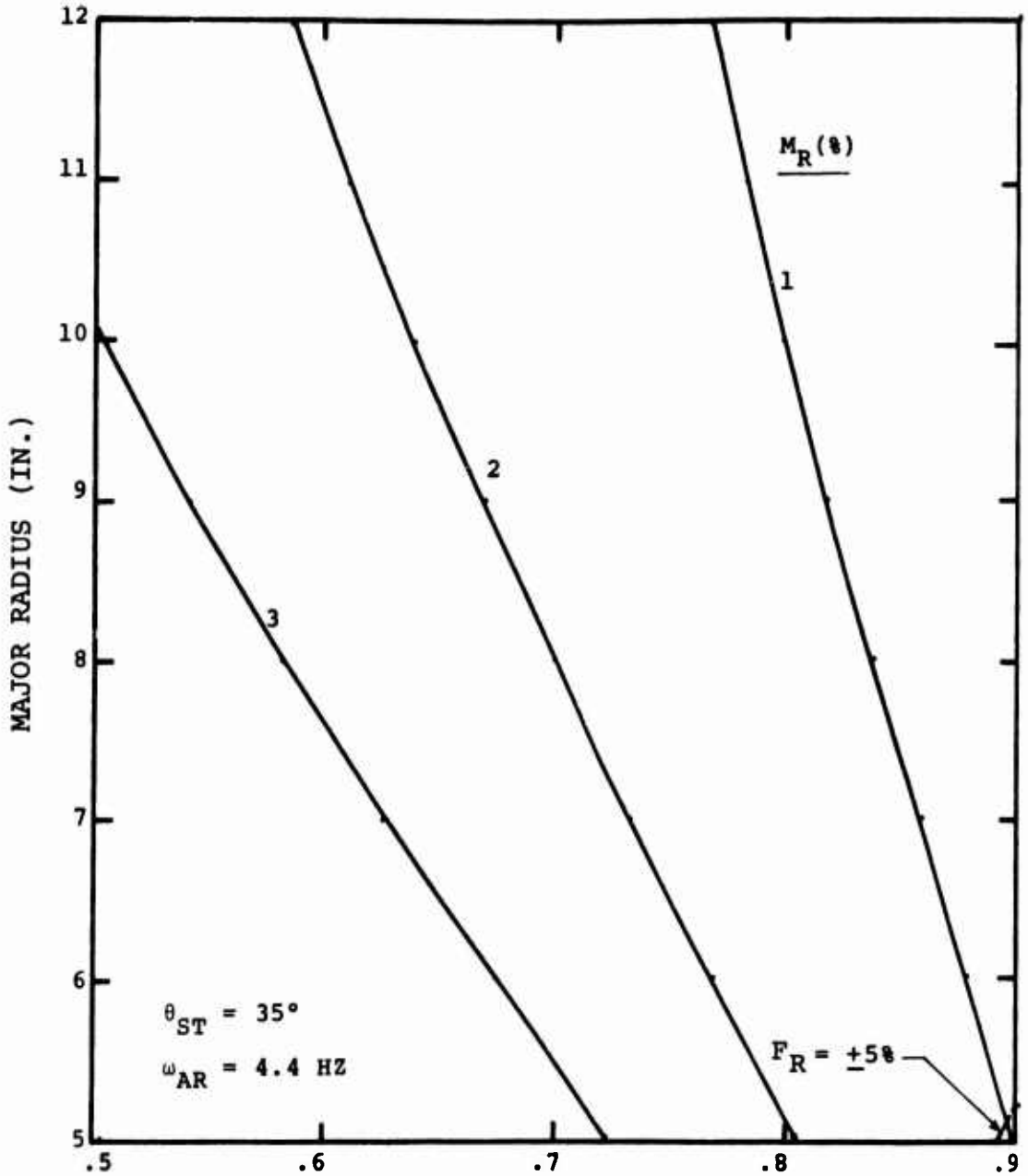

Figure 19 - Concluded.

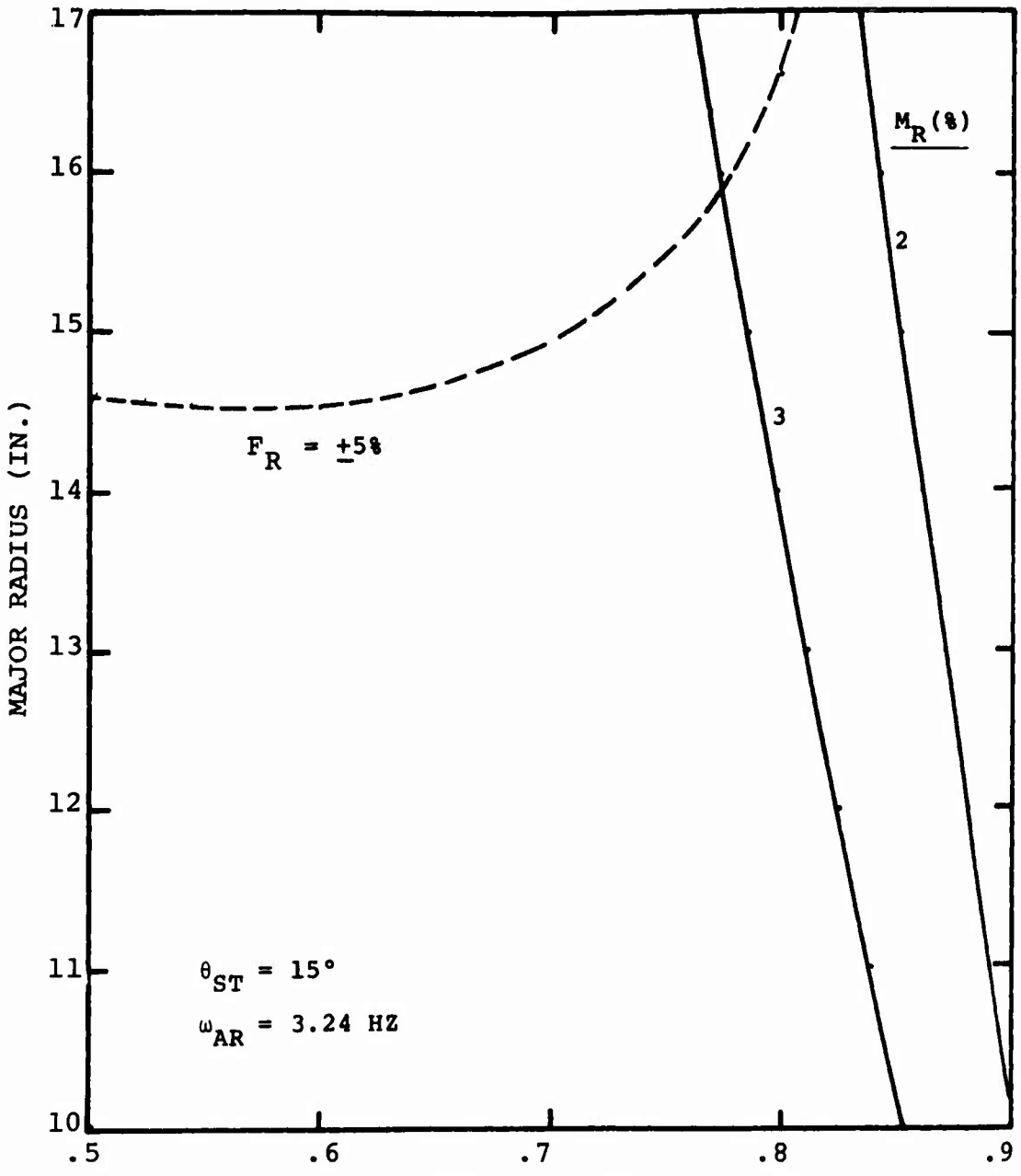

Figure 20. CH-53D COZID Parameters.

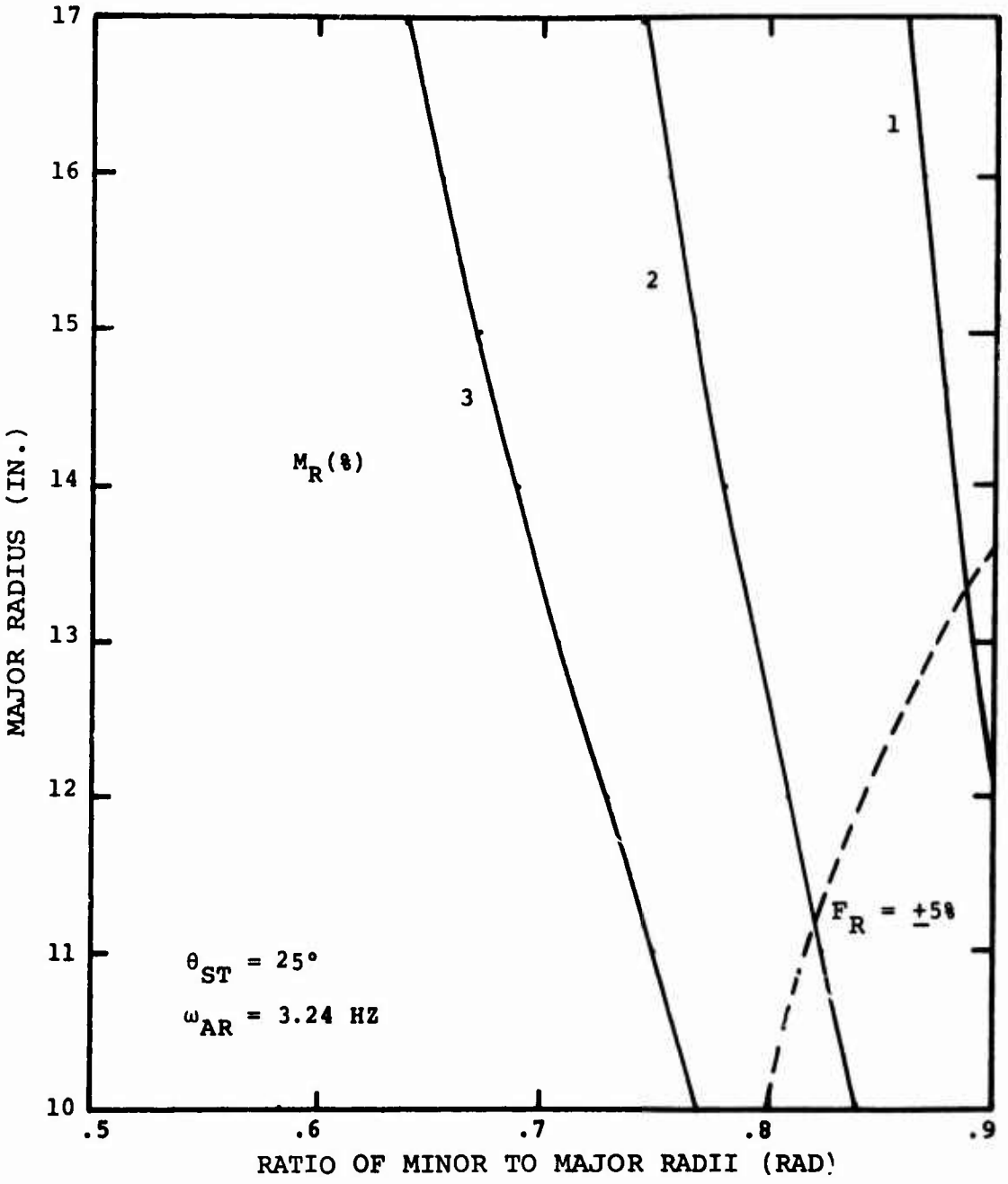

Figure 20 - Continued.

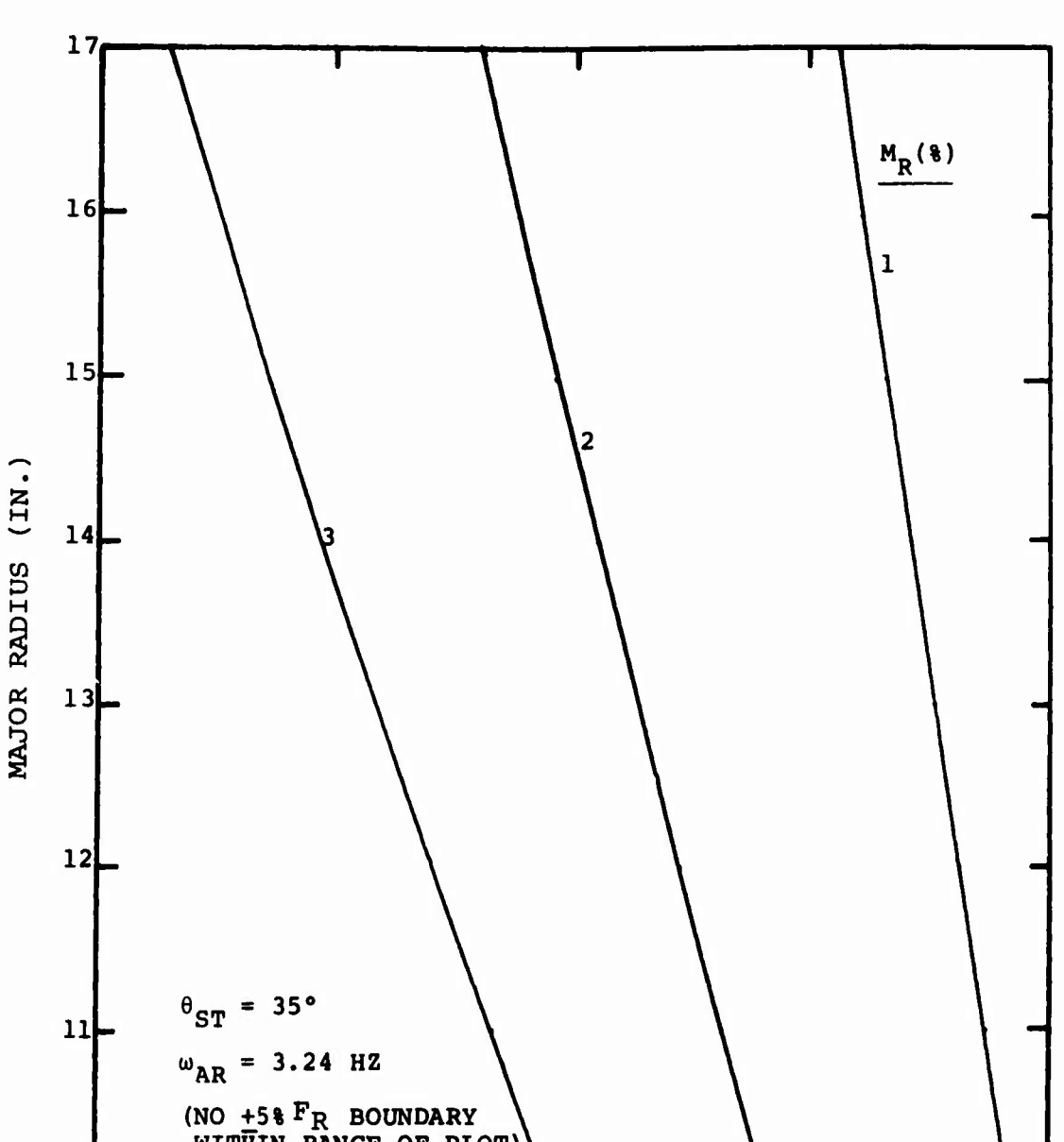

Figure 20 - Concluded.

In addition, these curves demonstrate the interrelationships which exist among the design parameters of stiffness, mass, inertia and geometry. It should be understood, however, that these curves do not encompass the whole range of possible COZID configurations which might be suitable for a given installation. It is possible, for example, to design a stiffer COZID, i.e., with a lower θ_{ST}; but, as shown, this added stiffness must be compensated for by increasing COZID mass, outer radius, or both. The possibility of changing the rotational inertia independent of mass also exists, and it may be used to reduce COZID size, weight, or both.

Selection of the optimum COZID configuration for a given application will depend on a number of factors, many of which may not be considered in a parametric study. Optimization will depend, for example, on such factors as space available, allowable deflection, the existence and location of A/C hardpoints (for attachment), the details of the sling system to be used, available ground clearance, and allowable weight.

These factors may be taken into account only in the preliminary design phase of any application study. In the present effort, these and other factors are discussed and accounted for with respect to CH-47 COZID application. This effort is covered in the Preliminary Design section.

MODEL STUDY

Requirements of the experimental test plan dictated that a COZID model be designed having a variable antiresonant tuning capability. Antiresonance frequency adjustment over a frequency range of 3 Hz to 8 Hz was called for, using a single COZID model with variable internal parameters. The approach taken to achieve this desired characteristic involved the selection of a basic COZID, with fixed internal spring rate and geometry, but having variable mass and inertia. Prior to design of this model, a limited parametric study was undertaken to assure that model parameters would be consistent with the requirements of the test plan.

The geometry of the COZID model was established considering minimum practical inertia wheel size and radius ratio. A minimum inertia wheel outer radius, R, of 2 inches was selected based primarily on ease of handling. Machining considerations dictated a radius ratio, r/R, of .7, with an inner radius of 1.4 inches. Having established these parameters, a derivative of Equation (54) was used to provide the basis for selection of the remaining COZID parameters. The equation used is

$$W_c = \frac{4 \cdot k_c \cdot g}{(2\pi f_{AR})^2 (r/R + \rho_c^2/R^2)} \qquad (61)$$

which relates COZID spring rate, k_c, and antiresonance frequency, f_{AR}, to COZID weight W_c. This equation is plotted in Figure 21 for three values of f_{AR} (3 Hz, 5 Hz, and 8 Hz) covering the range required by the test plan. A practically attainable value of ρ/R, equal to .75, is assumed in this figure, along with values of R and r/R given previously.

Final selection of model parameters was made by arbitrarily selecting a spring rate, k_c, equal to 2.5 lb/in. This resulted in weights of 8.6 pounds, 3.1 pounds and 1.2 pounds for the 3-Hz, 5-Hz and 8-Hz COZID configurations. The COZID model was constructed based on these parameters. Evaluation testing of this model is described in the Experimental Evaluation section.

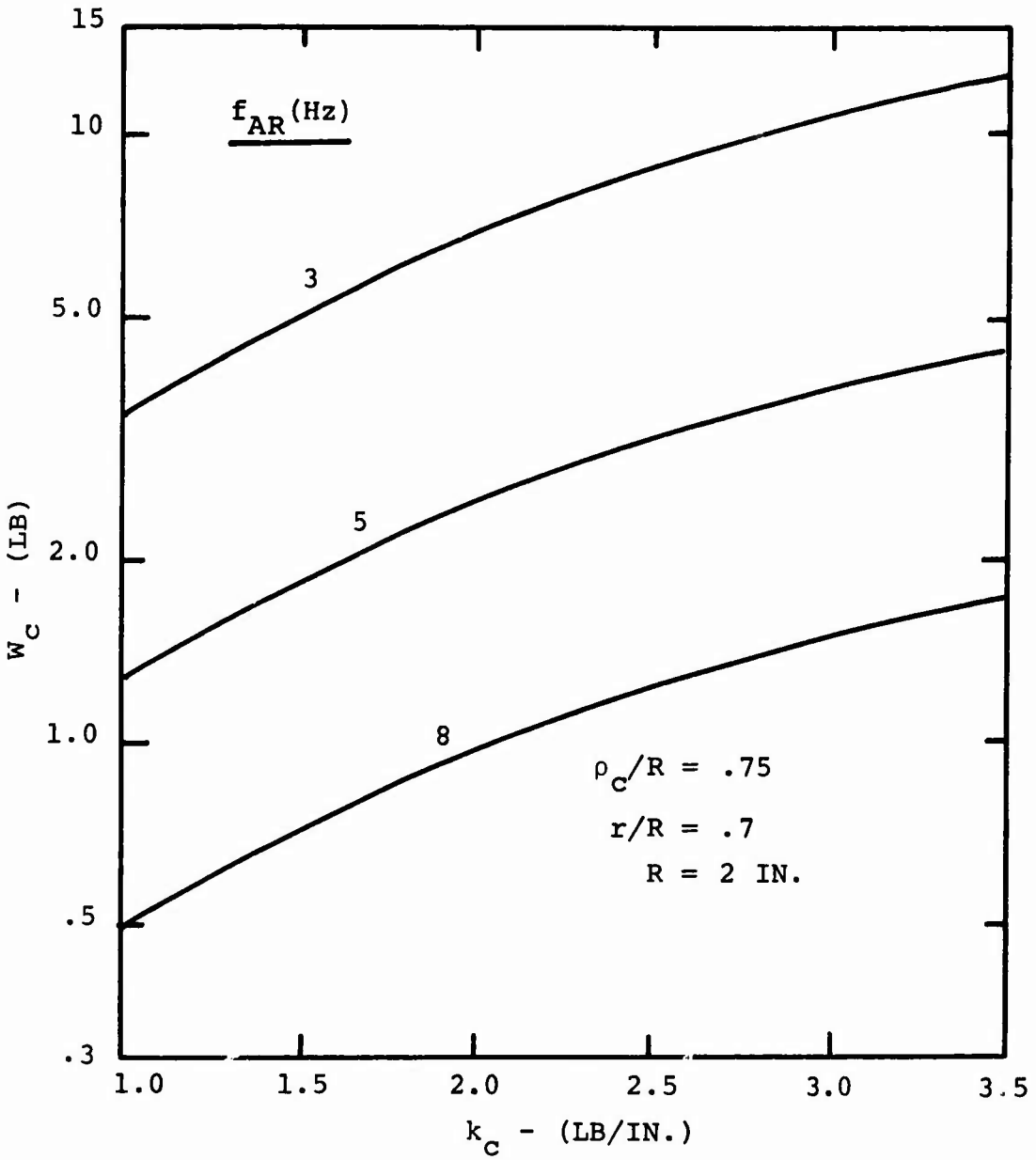

Figure 21. COZID Model Design Chart.

EXPERIMENTAL EVALUATION

A laboratory model of the dual-cylinder COZID was designed, fabricated and tested. The model was based on parameters developed as part of the parametric study, and it incorporated the capability of antiresonant tuning over a range of frequencies from 3 Hz to 8 Hz. Transmissibility testing was performed with the model as part of a dynamic system incorporating simulated helicopter mass, sling spring rate and external load mass. The impact of variable external load mass and sling spring rate on COZID performance was evaluated.

COZID MODEL AND TEST STAND

The test model and stand which were used for the evaluation testing are shown in Figure 22. Details of the model are presented in Figures 23 and 24.

The basic COZID model consists of two inertia wheels, each weighing .46 pound, and two extension springs, with spring rates of 1.25 lb/in. Variable antiresonant tuning is achieved through the addition or subtraction of suitably sized inertia discs to the basic inertia wheels, thereby changing the total COZID mass (M_c) and inertia (I_c). Support/spring cable and load cable attachment radii (R and r) are, respectively, 2 in. and 1.4 in.

TEST OBJECTIVES AND METHODS

The major objective of the test effort was to obtain experimental verification of COZID dynamic performance, including:

- The ability to tune the COZID, i.e., produce zero transmissibility (antiresonance), over a wide range of frequencies, and
- The ability to maintain antiresonant tuning independent of external dynamics.

A secondary objective of this testing was the demonstration of acceptable stress levels in "Stress - Critical" COZID components.

To achieve the desired objectives, an extensive test program was undertaken wherein dynamic response and stress measurements were made on a wide variety of simulated helicopter/external load dynamic systems. An attempt was made to encompass all possible helicopter/external load dynamic

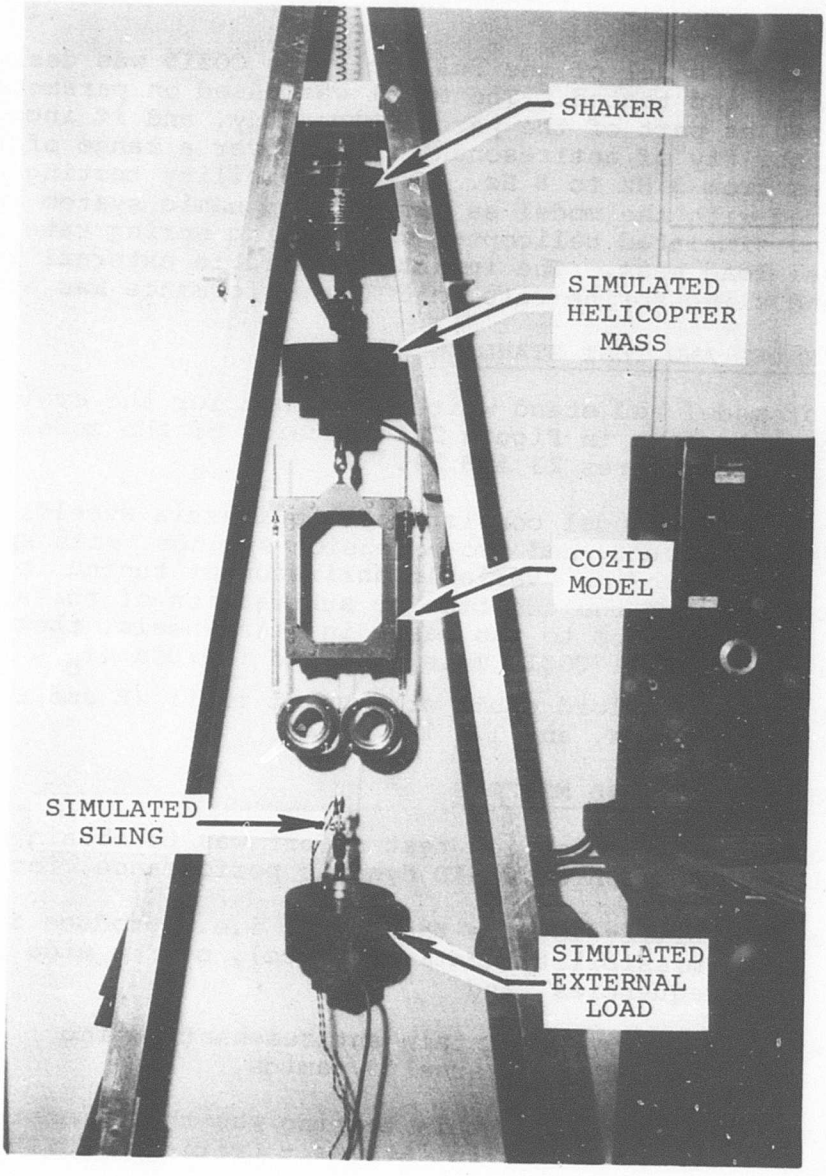

Figure 22. COZID Model and Test Stand.

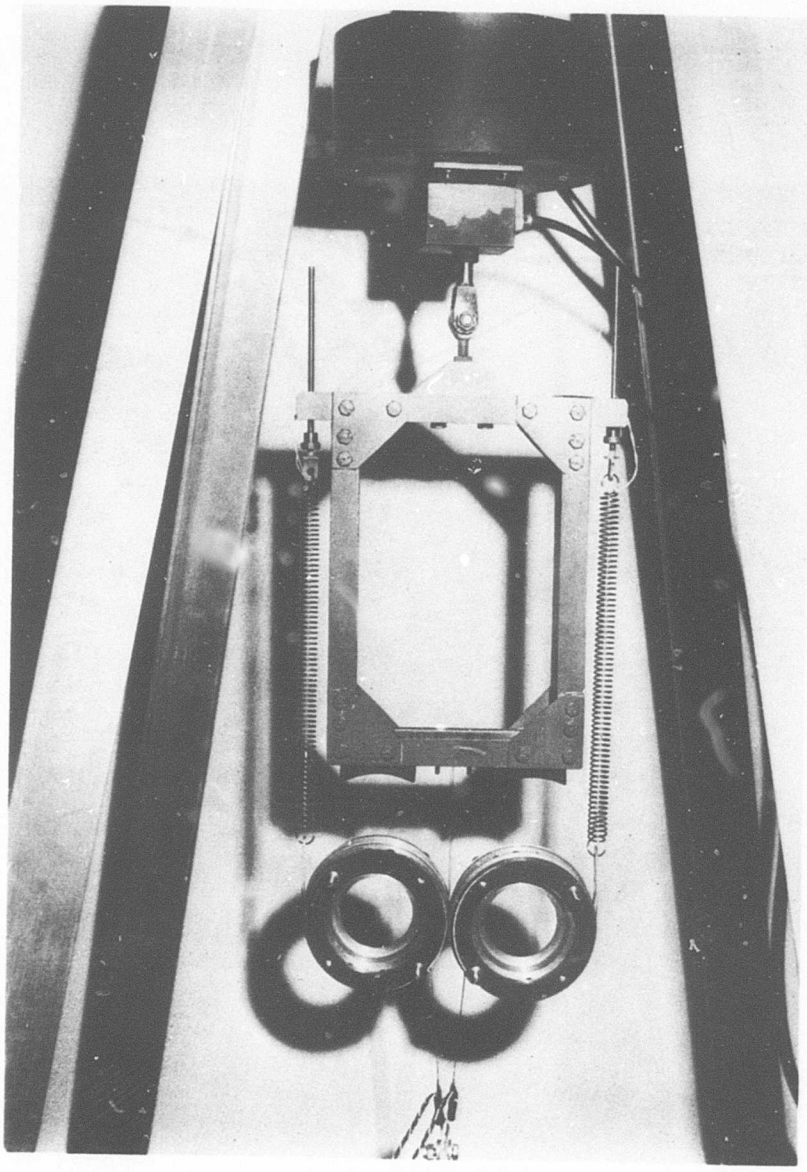

Figure 23. COZID Model.

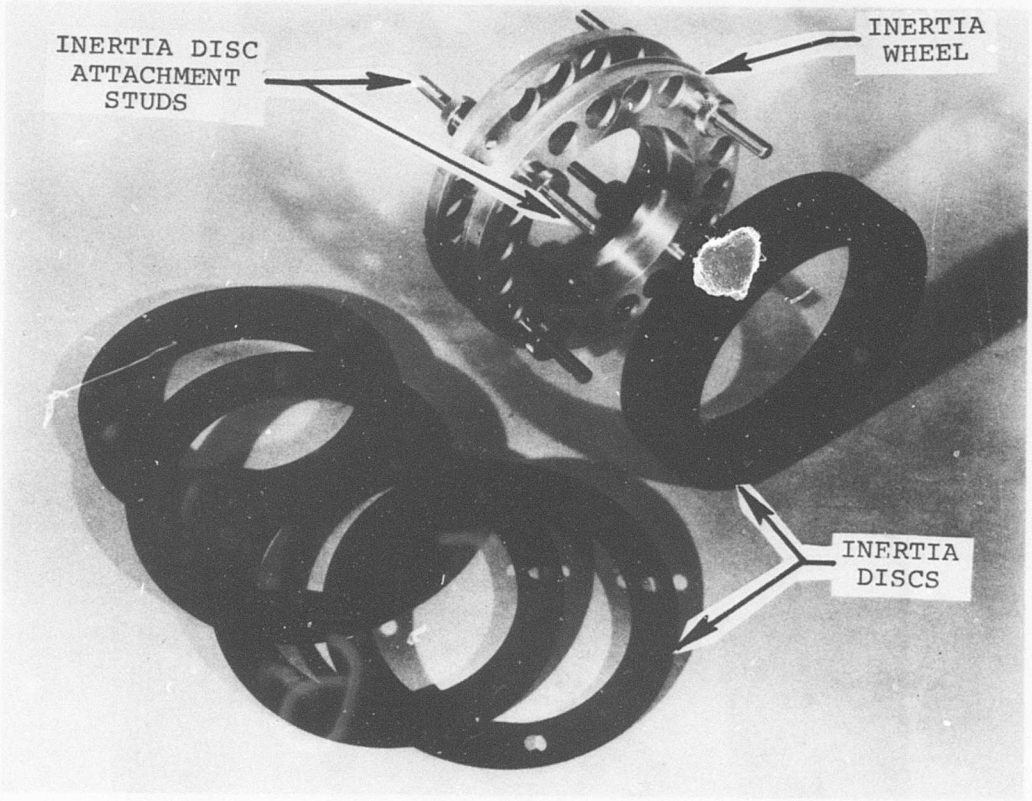

Figure 24. Inertia Wheel and Inertia Discs.

systems, and thereby to evaluate COZID performance over its entire range of application. To this end, three COZID configurations with different antiresonant tuning covering a frequency range of 3 Hz to 8 Hz were tested. Each COZID was tested as part of the complete dynamic system, consisting of simulated helicopter mass, external load mass, and sling spring rate. Variation in the dynamic system was achieved by varying external load mass and sling spring rate.

Eleven dynamic systems were tested for each COZID configuration. Measurements were made for three values of sling spring rate, with separate tests performed for three different sling loads for each sling configuration. Testing of each COZID with no sling ($k_s = \infty$) was also performed, for two values of external load. For each test, dynamic system frequency response was measured over a frequency range of 2.5 Hz to 20 Hz.

Thirty-three dynamic systems incorporating one of the three COZID configurations were tested. In addition to these, nine tests were performed with dynamic systems not incorporating a COZID. These data were taken to provide a baseline for evaluating COZID performance.

In all, forty-three dynamic response/stress measurement tests were performed during the course of the experimental evaluation. Instrumentation and procedures used in the performance of this testing are briefly discussed in the following sections, followed by presentation and discussion of the test results.

Instrumentation

Instrumentation used during COZID model testing is listed in Table III. The equipment arrangement is shown in Figure 25.

The electromagnetic shaker, driven by the oscillator and power amplifier, is utilized to provide dynamic excitation of the simulated helicopter mass, M_H. Velocity pickups, attached to simulated helicopter and external load masses, sense helicopter and load responses to the excitation and generate electrical signals proportional to vibratory velocity. The resultant signals are fed, through the switching box, to the tunable filter, which filters out extraneous signals, passing only that portion of the input signal occurring at the excitation frequency. This signal is then applied to a readout device (meter). Readings taken are manually entered in the computer for storage.

TABLE III. TEST EQUIPMENT

Item	Manufacturer	Model No.
Electromagnetic Shaker	MB Manufacturing Co.	SDA
Oscillator	MB Manufacturing Co.	1122055
Amplifier	MB Manufacturing Co.	1122055
Counter	Hewlett-Packard Co.	523B
Velocity Pickup #1	MB Manufacturing Co.	124
Velocity Pickup #2	MB Manufacturing Co.	124
Computer	Hewlett-Packard Co.	2000-C
Plotter	Hewlett-Packard Co.	7202-A
Oscillograph	Consolidated Electrodynamics Corp.	5-129
Meter	MB Manufacturing Co.	M3
Sound and Vibration Analyzer	General Radio Co.	1564-A

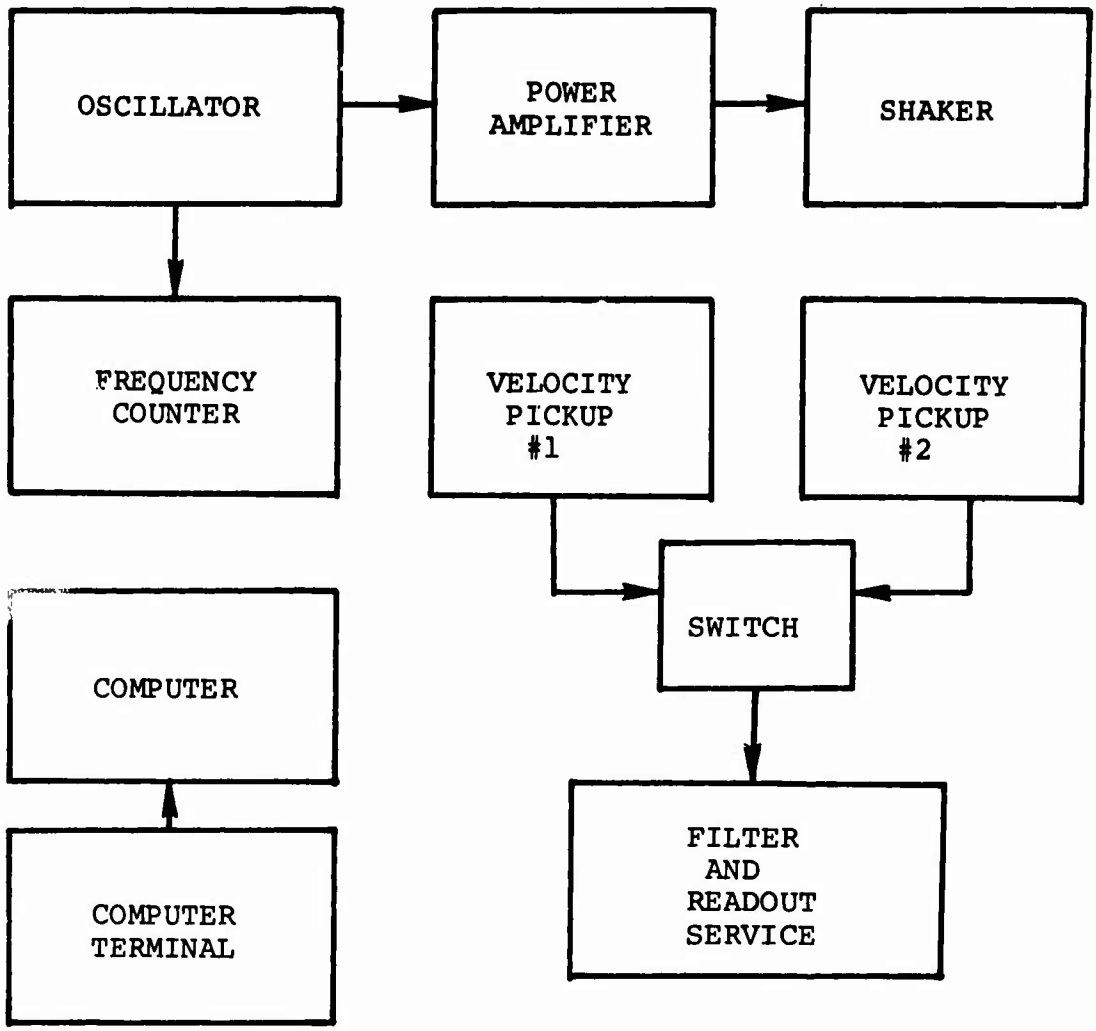

A. Dynamic Response Instrumentation

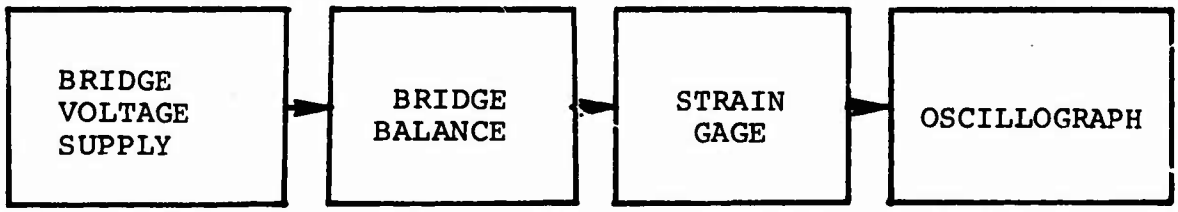

B. Strain Instrumentation

Figure 25. Instrumentation Arrangement.

Stress levels in "stress critical" CCZID components, determined to be the load cables, shown in Figure 23, were monitored using the instrumentation of Figure 25B. Strain gages, applied to the load cables, deliver an electrical signal proportional to load cable stress. This signal is fed into an oscillograph, equipped with a suitable galvanometer, which records a time history of cable stress.

Procedures

Prior to the beginning of evaluating testing, all equipment and transducers were calibrated. Velocity pickups were subjected to simultaneous shake testing, and their respective responses were recorded as a function of frequency. Relative responses of the two transducers were compared and found to be essentially identical over the frequency range of interest, 2 Hz to 20 Hz. The remaining dynamic response instrumentation was subjected to calibration procedures as required by their respective manufacturers.

Strain gage calibration was performed by statically loading the model and measuring output trace displacement for the known input force. The bridge balance and oscillograph were subjected to manufacturer required calibration procedures.

The actual model testing begins with instrumentation setup and checkout. Contact with the computer is established, the test data acquisition program is entered, and preparation for data entry is made. The model and simulated dynamic system are then adjusted to the correct test configuration, i.e., with the appropriate sling spring rate, load mass and COZID antiresonant tuning. Finally, the oscillator excitation frequency and amplitude are set, the filter is tuned to the selected excitation frequency, and the helicopter and load mass responses are read from the meter and input to the computer, along with the excitation frequency, obtained from the counter. Simultaneously, the oscillograph is switched on, and the load cable stress level time history is recorded. Data acquisition proceeds in this manner until response data is obtained covering the frequency range of 2.5 Hz to 20 Hz, at which time the test configuration is changed and the test sequence is repeated. Forty-three configurations were tested in this manner.

TEST RESULTS

Both dynamic response and stress data were obtained during testing of the COZID model. All dynamic response data were reduced to transmissibility curves, relating the ratio of external load response to helicopter response as a function of frequency. These data are discussed, in depth, in the following paragraphs.

Stress data were not reduced, but were scanned in an attempt to detect any unusually high stress conditions. No such high stress conditions were identified. No further use of stress data was made, primarily because of the difficulty of relating measured model stresses to stresses expected in a full-scale application. These data are therefore not discussed further in this report.

Model Sling Dynamics - Without COZID

The full-scale helicopter external load dynamic system consists of a helicopter with mass M_H, a sling (typically made up of a pendant and bridle* and having an effective spring rate k_s), and an external load having mass M_H. In general, all of these parameters are variable. The external load will vary from some small value to a mass (typically) equal to that of the helicopter empty weight**. Helicopter mass will also vary but over a smaller range, reflecting the difference between minimum flying weight and maximum gross weight less external load. Sling spring rate variation may also be great, depending primarily on the type of pendant used and the number of legs and rigging of the bridle***. Variability in these factors results in the possibility of the system resonance (ω_R) occurring below, at, or above the 1-P rotor frequency of the helicopter. Valid evaluation of the COZID model, therefore, requires testing within simulated dynamic systems having no-COZID resonances, i.e., resonances of the dynamic system without the COZID installed, covering a

*Reference 1 presents guidelines for sling design.

**The parametric study section defines sling system parameters for Army helicopters.

***Methods for calculating sling spring rate are given in Appendix I of Reference 1.

frequency range extending above and below the COZID tuned (antiresonant) frequency*.

Nine simulated dynamic systems were utilized. Parameters of each of these systems are given in Table IV. As shown, simulated helicopter weight was held constant at 40 pounds, while sling spring rate and simulated external load weight were varied to achieve the desired variation in system dynamics. Three simulated slings were used: a soft sling with a 15.3-lb/in. spring rate (used in systems 1, 2 and 3), a moderately stiff sling with a spring rate of 59 lb/in. (used in systems 4, 5 and 6), and a stiff sling with a 203-lb/in. spring rate (used in systems 7, 8 and 9). External load weights of 20, 30 and 40 pounds were used with each sling.

Transmissibility data for the Table IV dynamic systems are plotted in Figures 26, 27, and 28. These curves, as expected, show the characteristic response of a linear, undamped single-degree-of-freedom system and are representative of full-scale system responses. Resonances of the systems cover the full required range, i.e., 3 Hz to 8 Hz, and in general agree well with predicted resonance frequencies, as shown in Table V.

COZID Tuning

Antiresonant tuning of the COZID model was achieved using a dynamic system consisting of the simulated helicopter and load masses and the COZID model, but with no simulated sling. This approach was taken in order to simplify the tuning procedure and to permit more accurate tuning. Procedures and results of COZID tuning testing are given below.

The COZID model constructed for the present test is shown in Figures 23 and 24. This model has a fixed geometry (R and r) and internal spring rate (k_s), with variable mass (M_c) and inertia (I_c) used to achieve variation in antiresonant tuning. Geometry, internal spring rate, and basic mass and inertia of the model are such that antiresonant tuning may be achieved at 8 Hz, the upper limit of present test application. Tuning to lower antiresonant frequencies is then achieved by adding inertia discs to the basic inertia wheels, thereby increasing total mass and inertia. For the present test the model was tuned to 7.8 Hz, 4.8 Hz and 3.0 Hz.

*The COZID is assumed to be tuned to 1-P of the simulated helicopter rotor system.

TABLE IV. MODEL HELICOPTER/SLING/LOAD DYNAMIC SYSTEM PARAMETERS

Dynamic System No.	Load Weight (lb)	Sling Spring Rate (lb/in.)	Helicopter Weight (lb)
1	40		
2	30	15.3	
3	20		
4	40		
5	30		
6	20	59.0	40
7	40		
8	30	203.0	
9	20		

TABLE V. MODEL HELICOPTER/SLING/LOAD DYNAMIC SYSTEM MEASURED AND PREDICTED RESONANCE FREQUENCIES

Dynamic System	Measured* Resonance (Hz)	Predicted Resonance (Hz)
1	1.91	1.93
2	2.26	2.23
3	2.76	2.73
4	3.70	3.79
5	4.40	4.38
6	5.20	5.37
7	7.20	7.04
8	8.00	8.13
9	9.80	9.96

*Measured resonance frequencies for the soft sling systems have been extrapolated using the relationship

$$\omega_R = \frac{\omega(T = 1)}{1.414}$$

since these frequencies are below the test range.

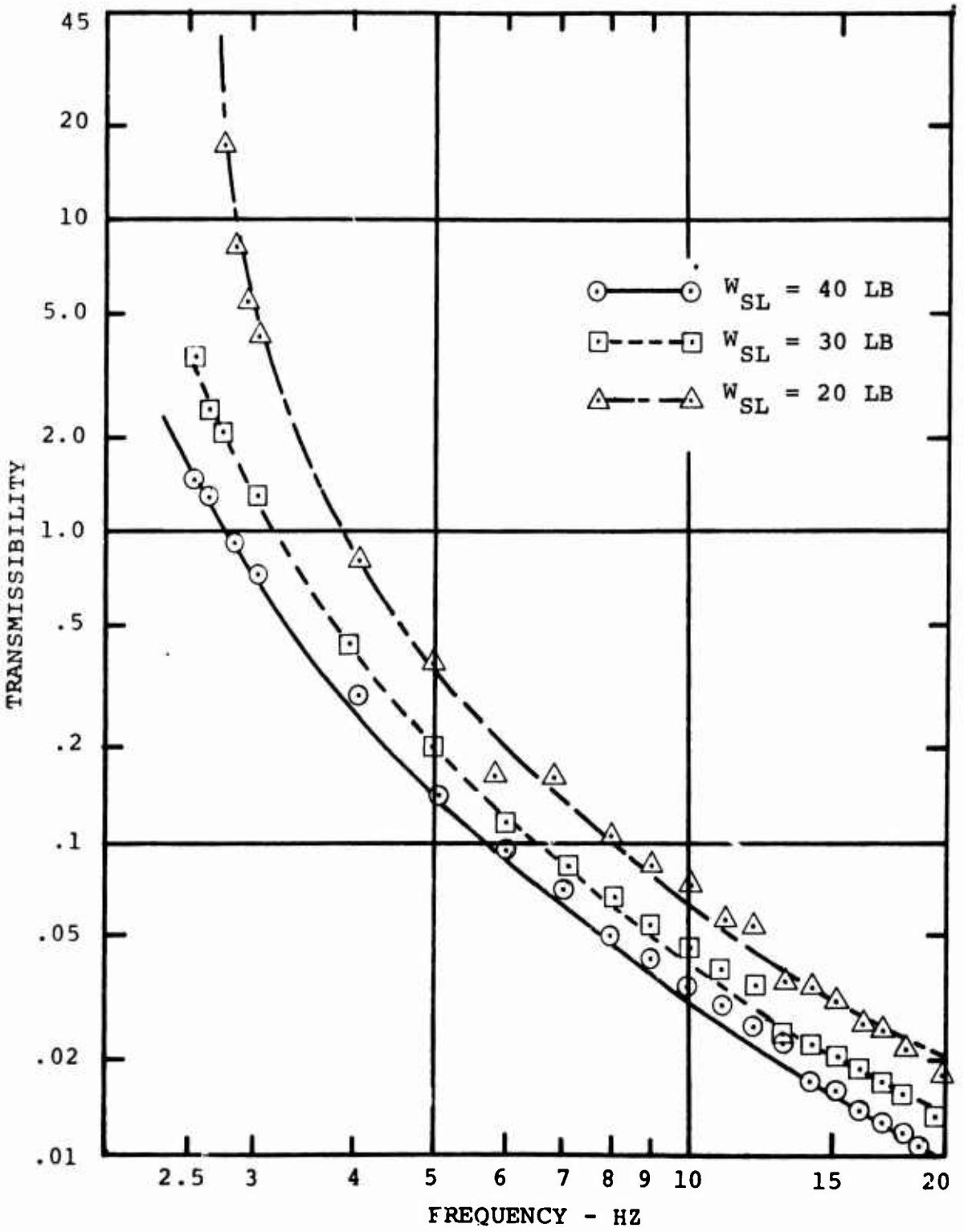

Figure 26. Effect of Isolated Weight on Soft Sling Dynamic System Transmissibility - No COZID.

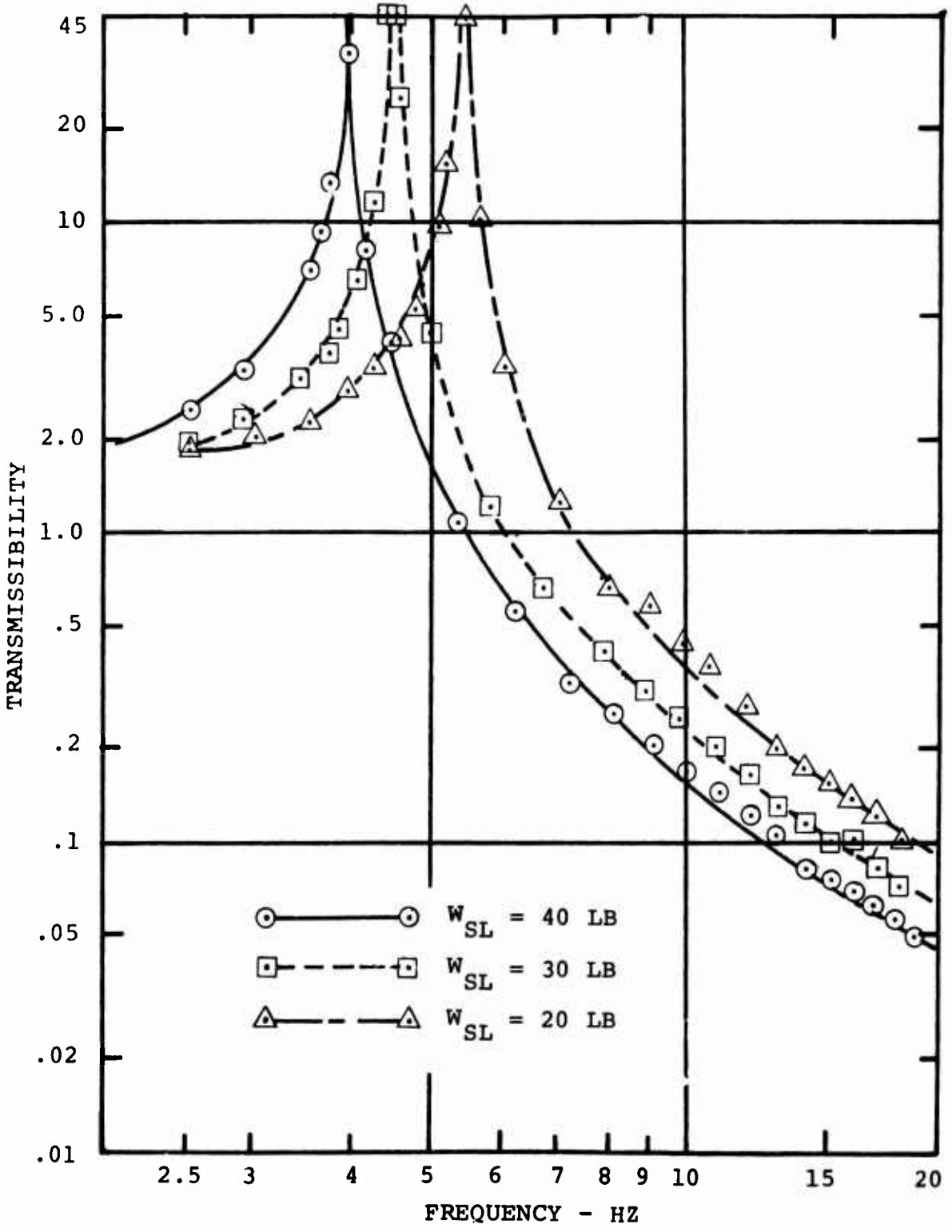

Figure 27. Effect of Isolated Weight on Moderate Stiffness Sling Dynamic System Transmissibility - No COZID.

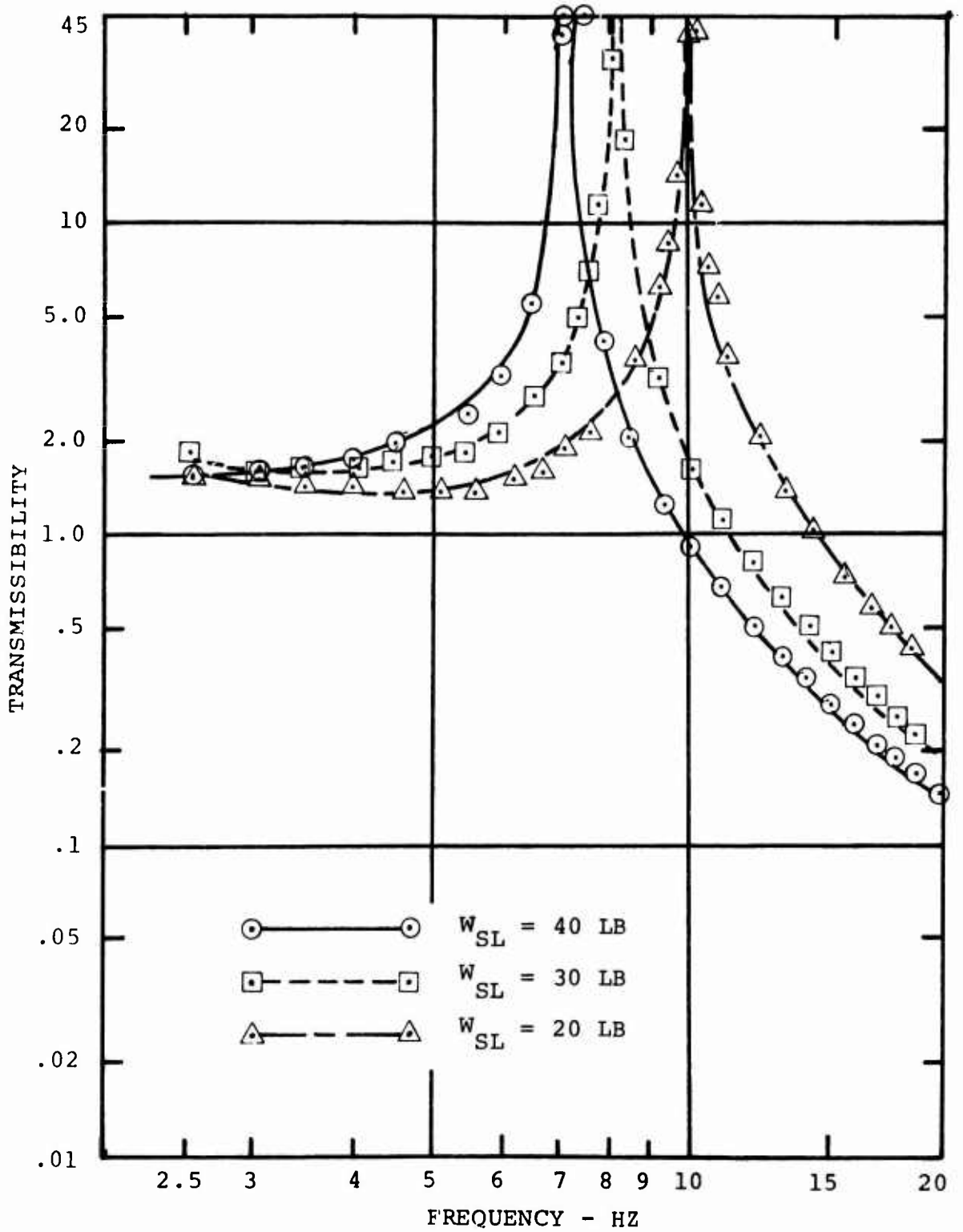

Figure 28. Effect of Isolated Weight on Stiff Sling Dynamic System Transmissibility - No COZID.

COZID model parameters for each of these three configurations are given in Table VI.

TABLE VI. COZID MODEL PARAMETERS

Configuration	f_{AR} (Hz)	R (in.)	r (in.)	k* (lb/in.)	M_C $\left(\frac{\text{lb-sec}^2}{\text{in.}}\right)$	I_C** (in.-lb/sec^2)
1	7.8	2	1.4	2.5	.0032	.0075
2	4.8	2	1.4	2.5	.0090	.0180
3	3.0	2	1.4	2.5	.0220	.0510

* Two springs each with 1.25 lb/in. spring rate.

**Model inertia is based on measured antiresonance frequency.

COZID model transmissibility responses, derived from tuning test data, are shown in Figures 29, 30 and 31. Data are given for two cases of simulated external load mass, having weights of 20 and 40 pounds, for each COZID configuration. In all cases the COZID model worked well, with up to 99 percent isolation measured at the antiresonant frequency. Independence of antiresonance and isolated weight is demonstrated, with no shift in tuned frequency shown for a two-to-one (20-pound to 40-pound) change in simulated external load. Good agreement is shown between measured and predicted model transmissibility responses, as evidenced by the comparison of Figure 31.

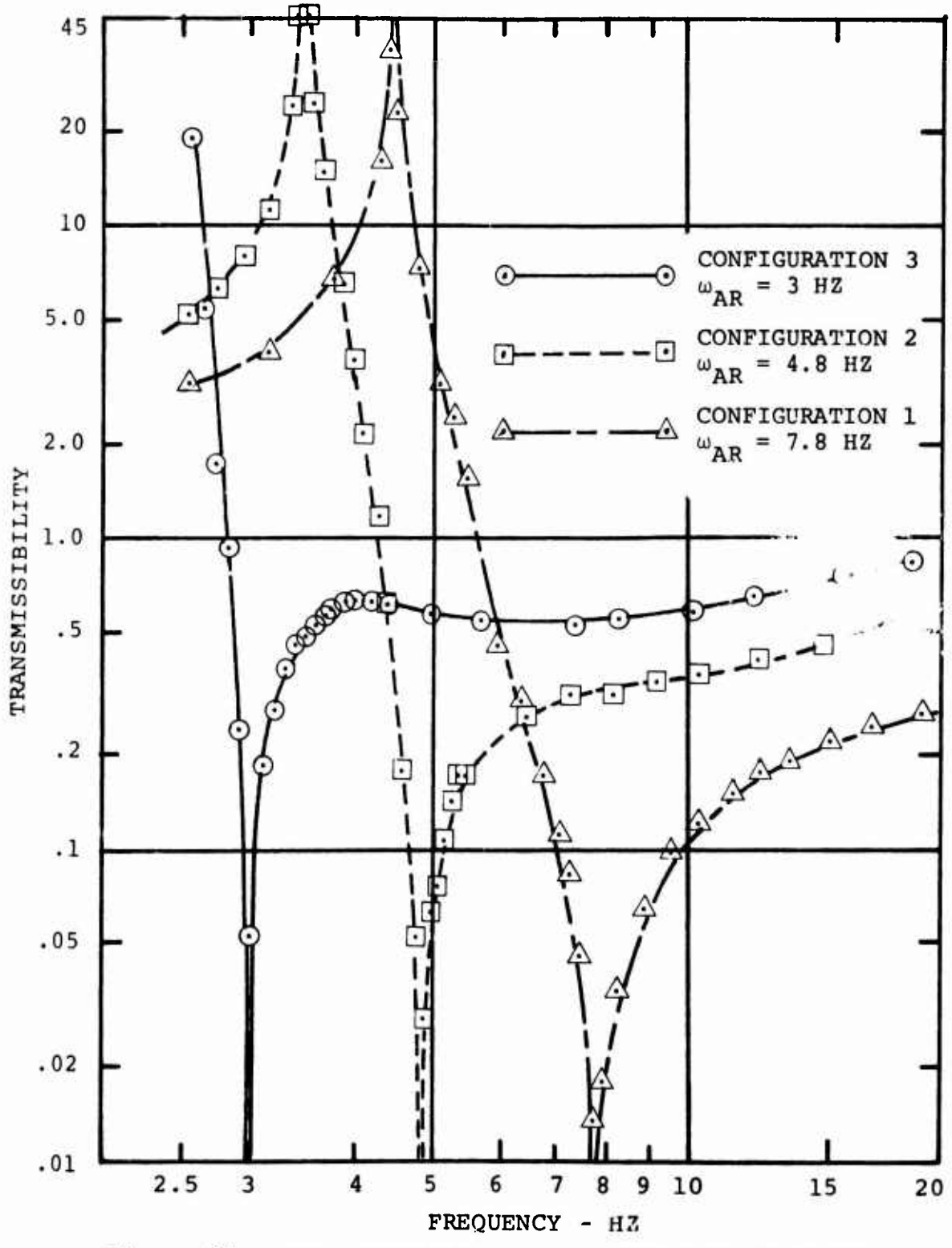

Figure 29. Transmissibilities of COZID Configurations 1, 2 and 3 With No Sling ($k_s \rightarrow \infty$) - 20-Pound Isolated Weight.

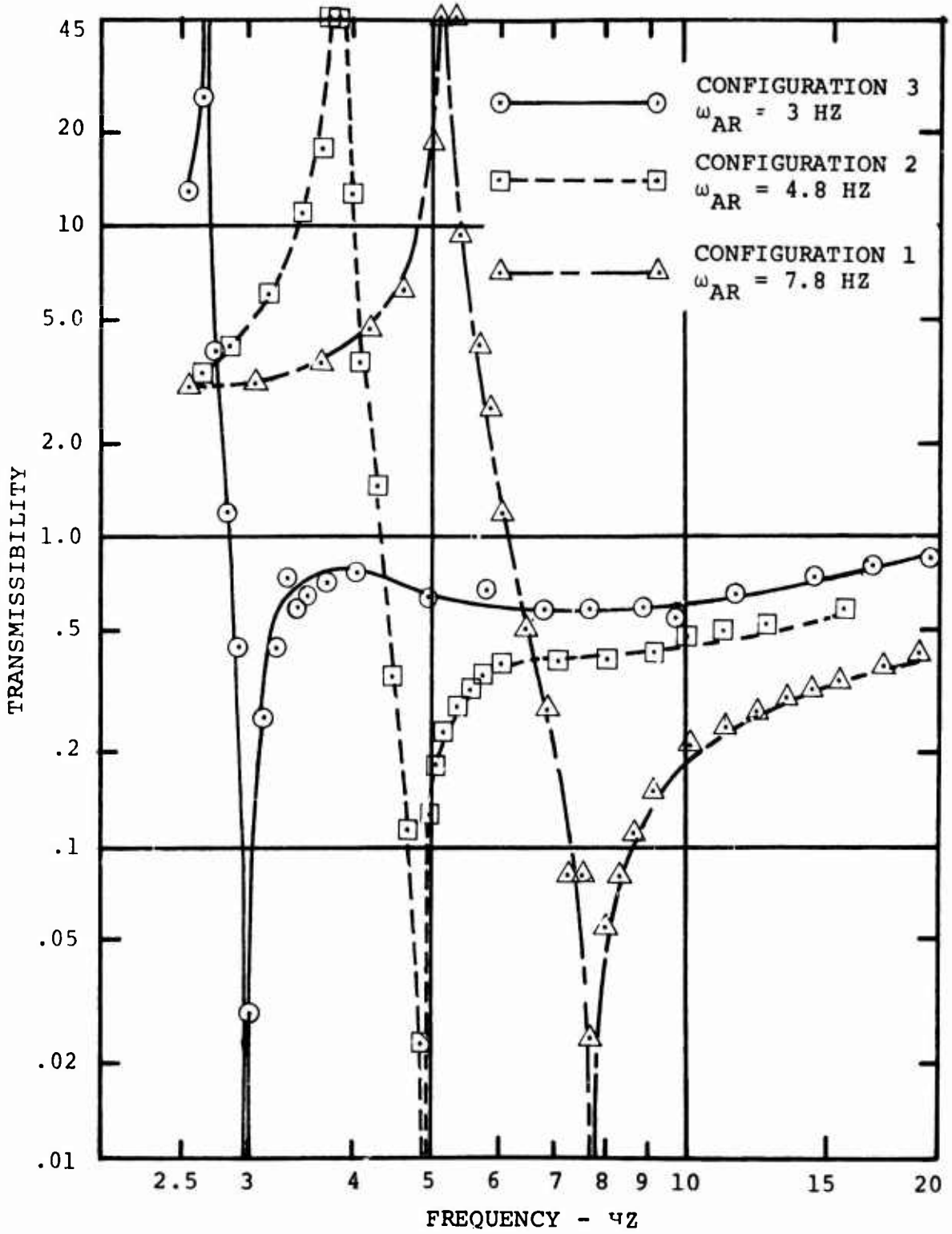

Figure 30. Transmissibilities of COZID Configurations 1, 2 and 3 With No Sling ($k_s \rightarrow \infty$) - 40-Pound Isolated Weight.

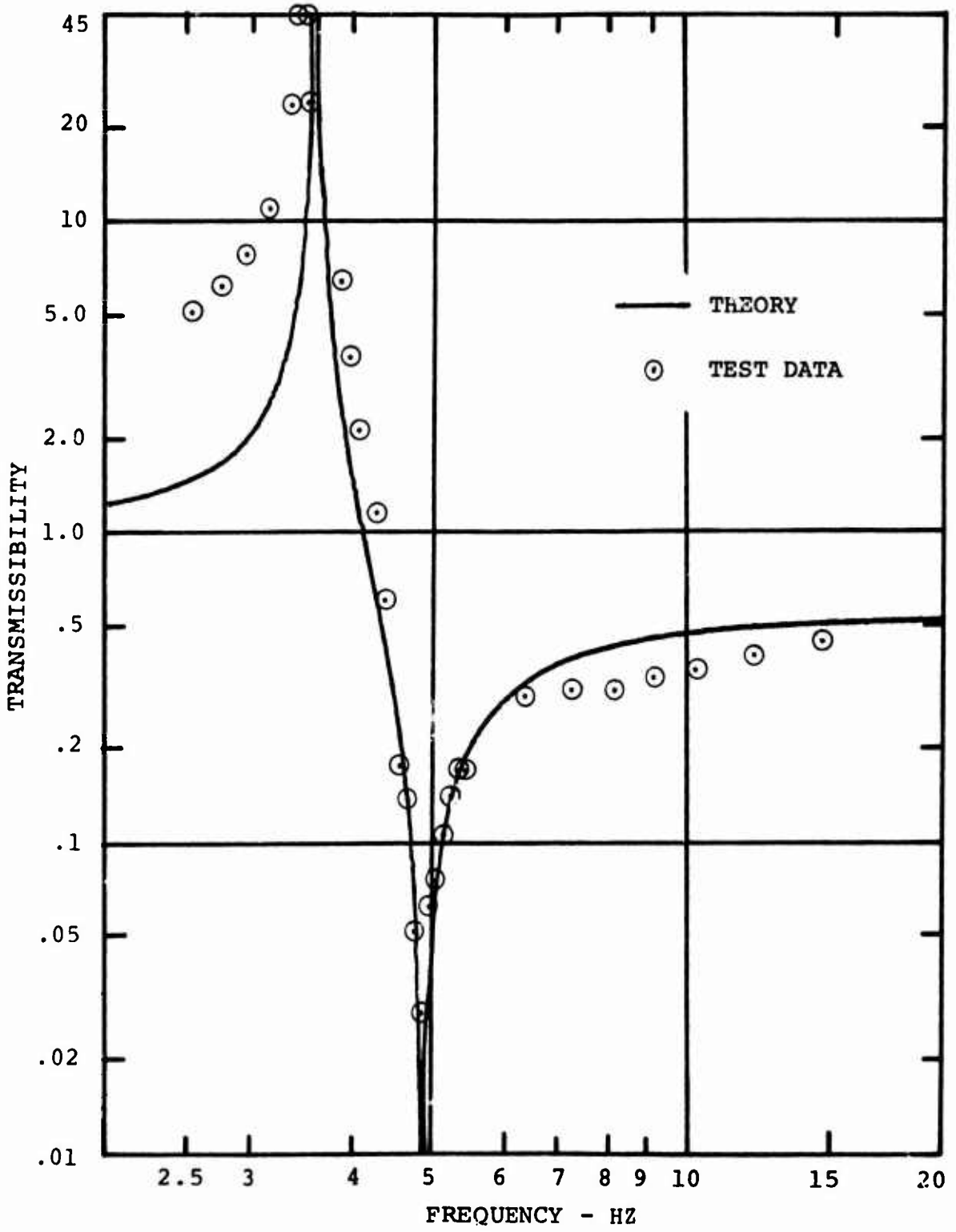

Figure 31. Comparison of Theoretical Transmissibility With Test Data - Configuration 2 COZID With 40-Pound Isolated Weight.

Model COZID Performance

The three model COZID configurations of Table VI were subjected to performance testing within each of the helicopter/sling/load dynamic systems of Table IV. In each case the COZID was installed between the simulated helicopter mass and sling spring, as shown in Figure 22. Transmissibility curves, derived in terms of load to helicopter response ratio from these data, are presented and discussed in the following paragraphs.

7.8-Hz COZID

Transmissibility data for the Configuration 1 model COZID, with a tuned frequency of 7.8 Hz, are given in Figure 32. Data for systems with 15.3-, 59- and 203-lb/in. simulated sling spring rates and 40-pound and 20-pound external loads are given.

In all applications of the Configuration 1 COZID, antiresonance was achieved within 1 percent (approximately .1 Hz) of the nominal 7.8-Hz tuned frequency. Essentially no change in antiresonant frequency occurred corresponding to the wide range of dynamic system parameters tested. Greater than 95 percent isolation was achieved at the tuned frequency with each dynamic system tested.

The data of Figure 32 demonstrate both possible COZID/sling resonance/antiresonance conditions. For all isolated weights, resonances occur both above and below the antiresonant frequency with the 203-lb/in. and 59-lb/in. slings*, while both resonances occur below antiresonance with the 15.3-lb/in. sling.

The impact of COZID installation on sling system dynamics is demonstrated in Figure 33. Shown are transmissibility curves for the stiff sling system (k_s = 203 lb/in.) with an isolated weight of 30 pounds, both with and without the Configuration 1 COZID, which is tuned to a simulated 1-P frequency of 7.8 Hz. Without the COZID the sling system is very nearly in resonance with 1-P, with an amplification of greater than 25. Installation of the COZID

*The lowest transmissibility resonance for the soft sling dynamic system occurs below 2.0 Hz, the lower limit of testing.

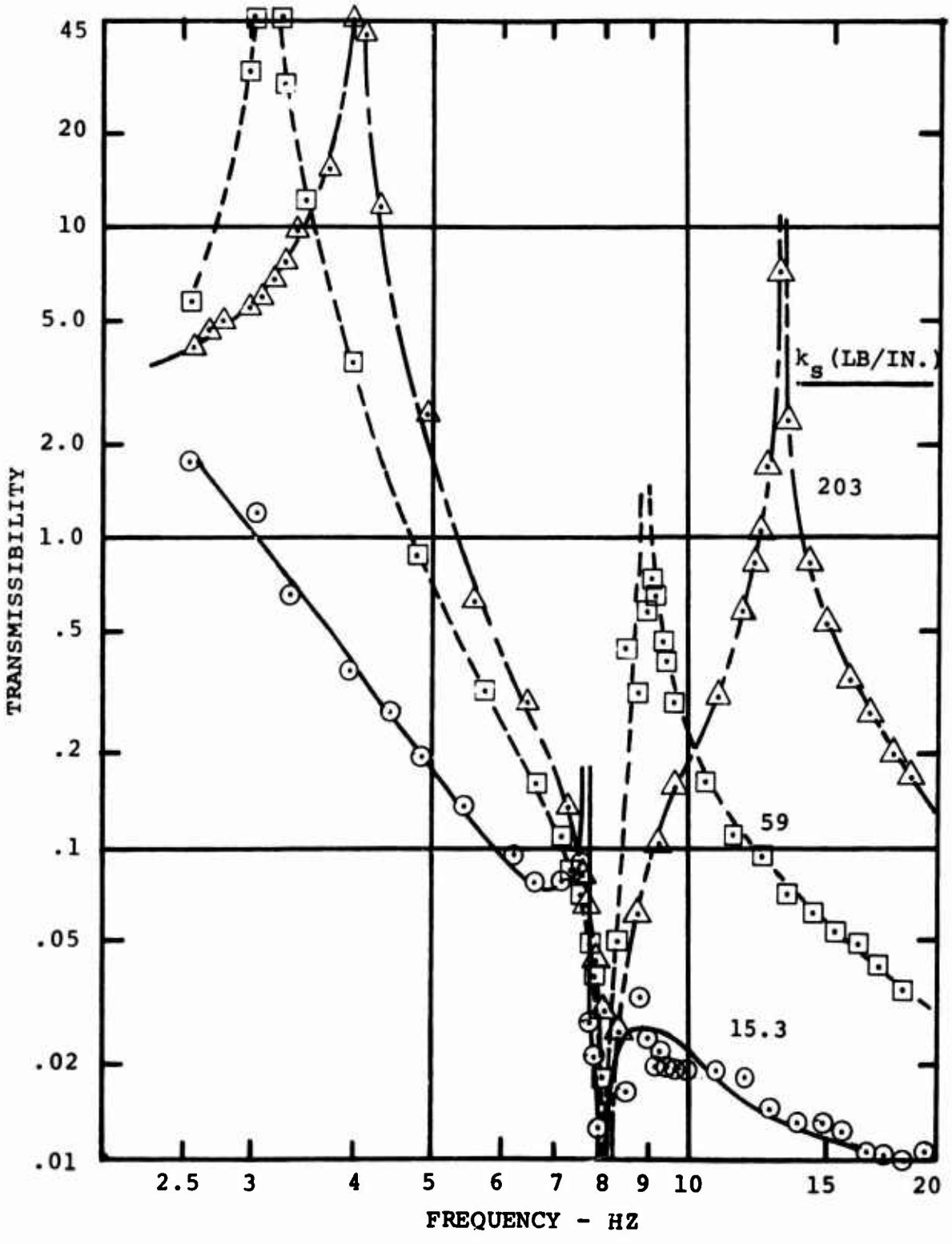

A. 40-Pound Isolated Weight

Figure 32. Effect of Sling Stiffness and Isolated Weight on Configuration 1 COZID Transmissibility.

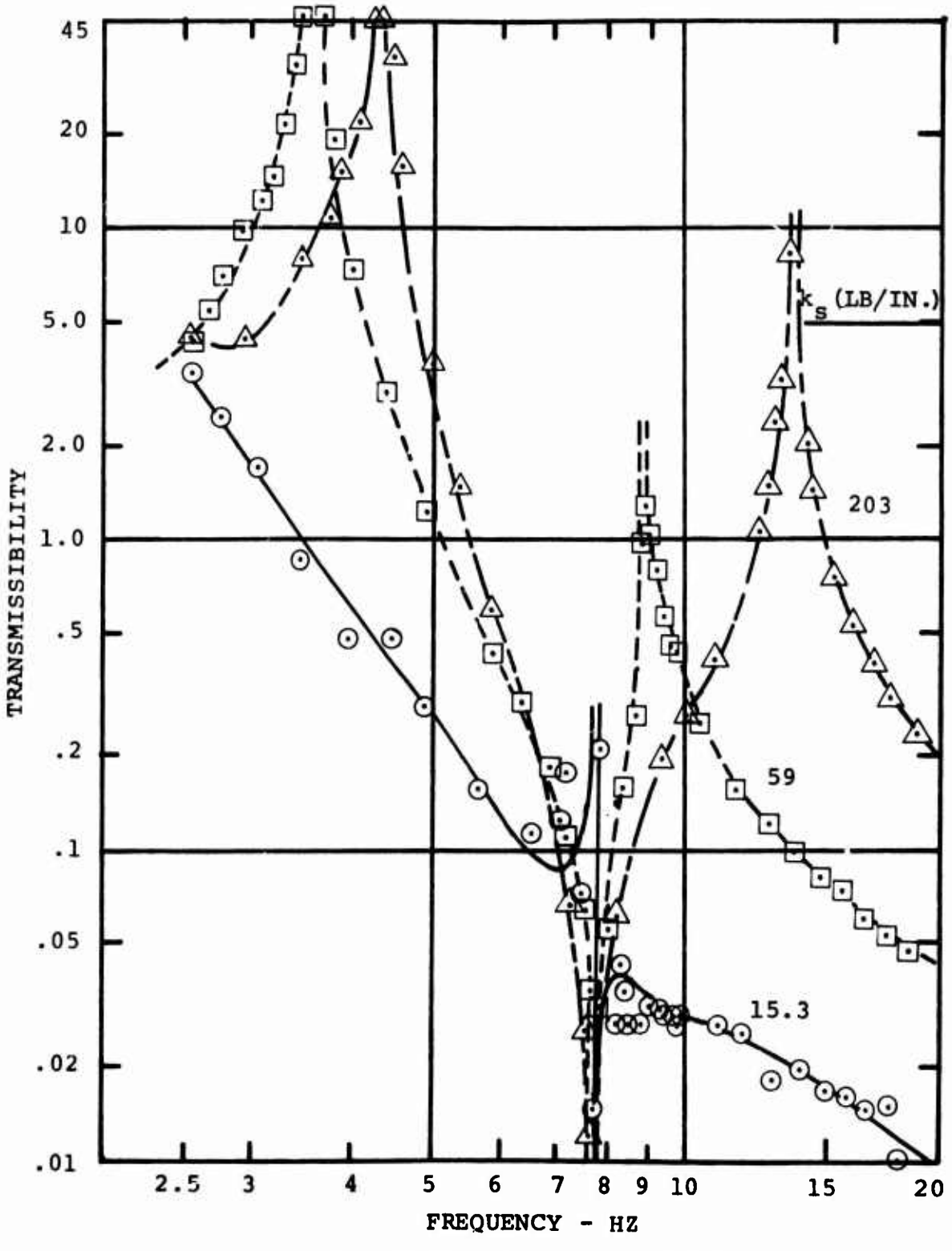

B. 30-Pound Isolated Weight

Figure 32 - Continued.

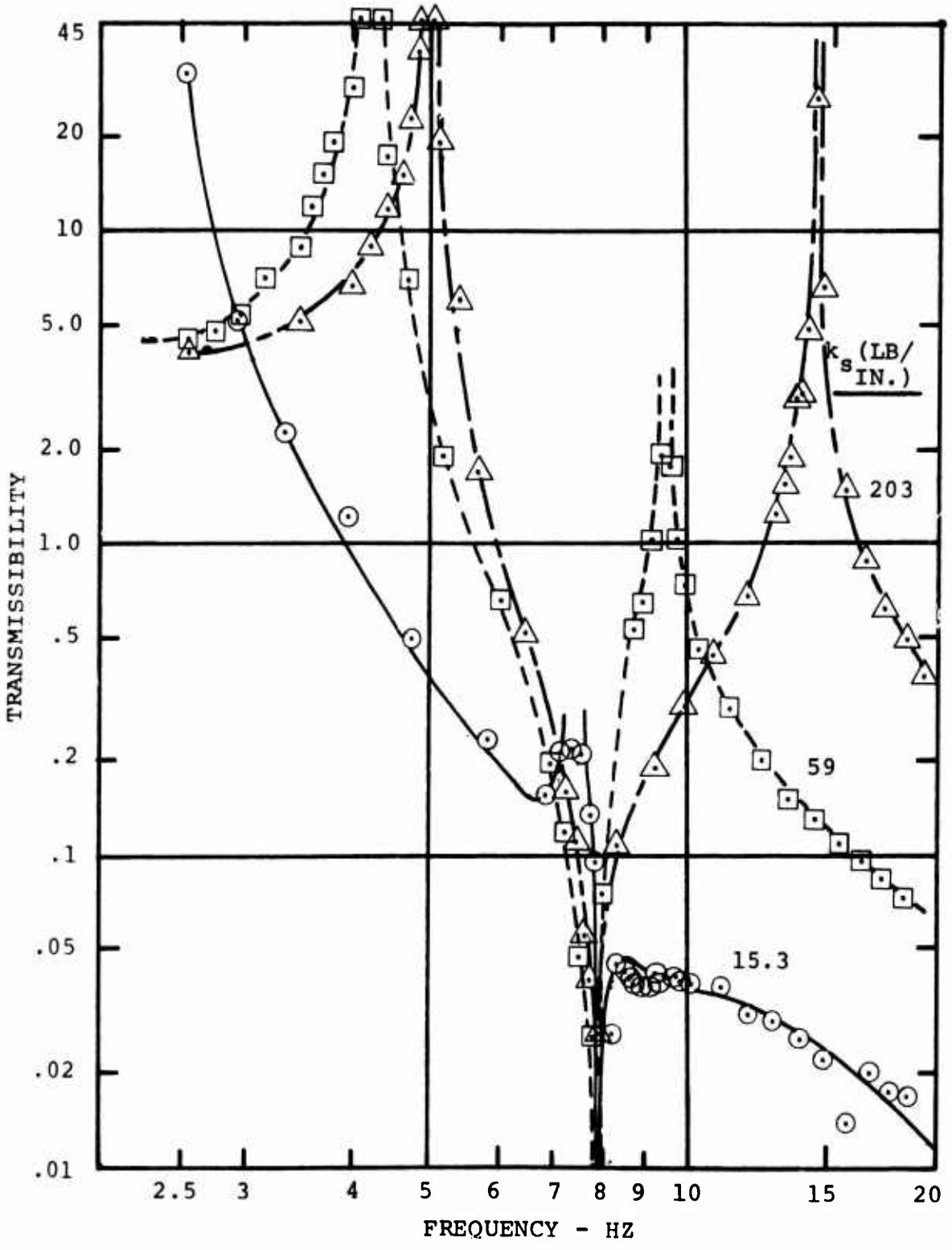

C. 20-Pound Isolated Weight

Figure 32 - Concluded.

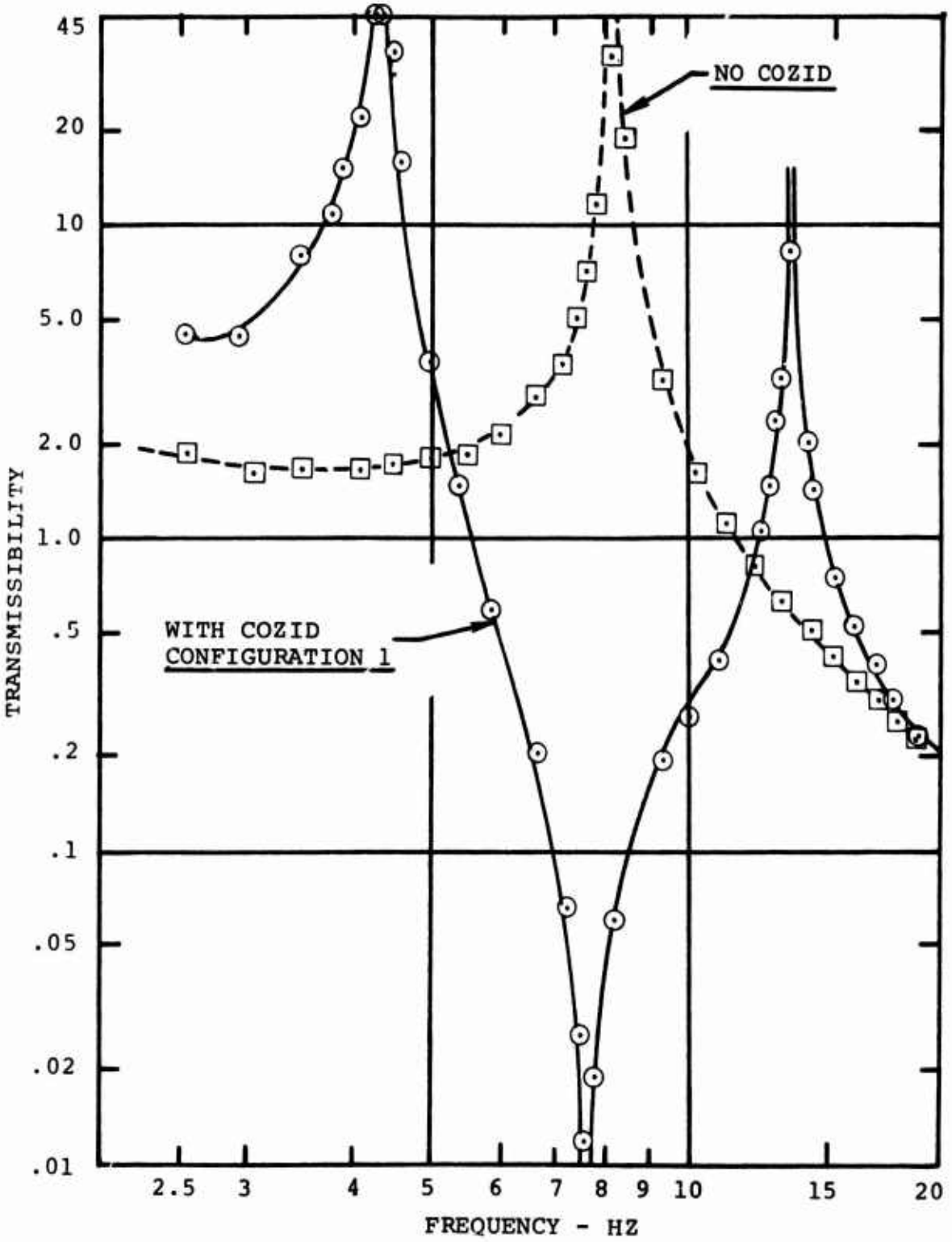

Figure 33. Effect of COZID Use on Dynamic System Transmissibility - k_s = 203 Lb/In., W_{SL} = 30 Pounds.

results in creation of an antiresonance at 1-P, with a reduction in transmissibility to approximately .01 (99 percent isolation). The resonance which previously occurred at 1-P is shifted to a higher frequency, in this case 14 Hz. A similar effect is achieved regardless of the parameters of the sling system, as shown in Figure 32. In all cases, antiresonance is achieved and system resonance at the tuned frequency is precluded.

4.8-Hz COZID

Tuning of the COZID model to a 4.8-Hz antiresonant frequency was achieved by adding inertia discs weighing 2.56 pounds to the basic COZID. The resultant mass and inertia for this configuration (Configuration 2 of Table VI) were, respectively, .009 lb-sec^2/in. and .018 lb.-in-sec^2. Transmissibility data for the sling dynamic systems with this configuration COZID are given in Figure 34. Antiresonances were obtained with each dynamic system, with a negligible (< .05 Hz) spread in antiresonant frequency. Antiresonant isolation ranged from 71.5 percent to 98 percent, with an average of 90 percent isolation. Low values of measured antiresonant isolation are due to the relative placement of resonance and antiresonance frequencies, with near-coincidence resulting in both relatively poor COZID performance and difficulty in accurate response measurement. This situation is illustrated in Figure 34, principally with the soft sling dynamic systems.

Response of the COZID/sling for near-coincidence of antiresonance and resonance frequencies is characterized by suppression of both resonant amplification and antiresonant isolation. In Figure 34, for example, systems incorporating soft slings show antiresonant/resonant frequency separation of only 4 percent (.2 Hz). As a result, the highest measured resonant amplification is less than 20 percent, while the highest measured antiresonant isolation is 83 percent. This response-limiting effect is attributable to damping in the dynamic system.

A second COZID characteristic evident in the Figure 34 data is the ability of the COZID to restrict the shift of resonance frequency in response to changing external dynamics. Essentially no change in the second transmissibility resonance, at 4.6 Hz, of the soft sling systems is shown, while the isolated weight decreases from 40 pounds to 20 pounds. In the absence of the COZID, this resonance would be expected to shift 40 percent in frequency.

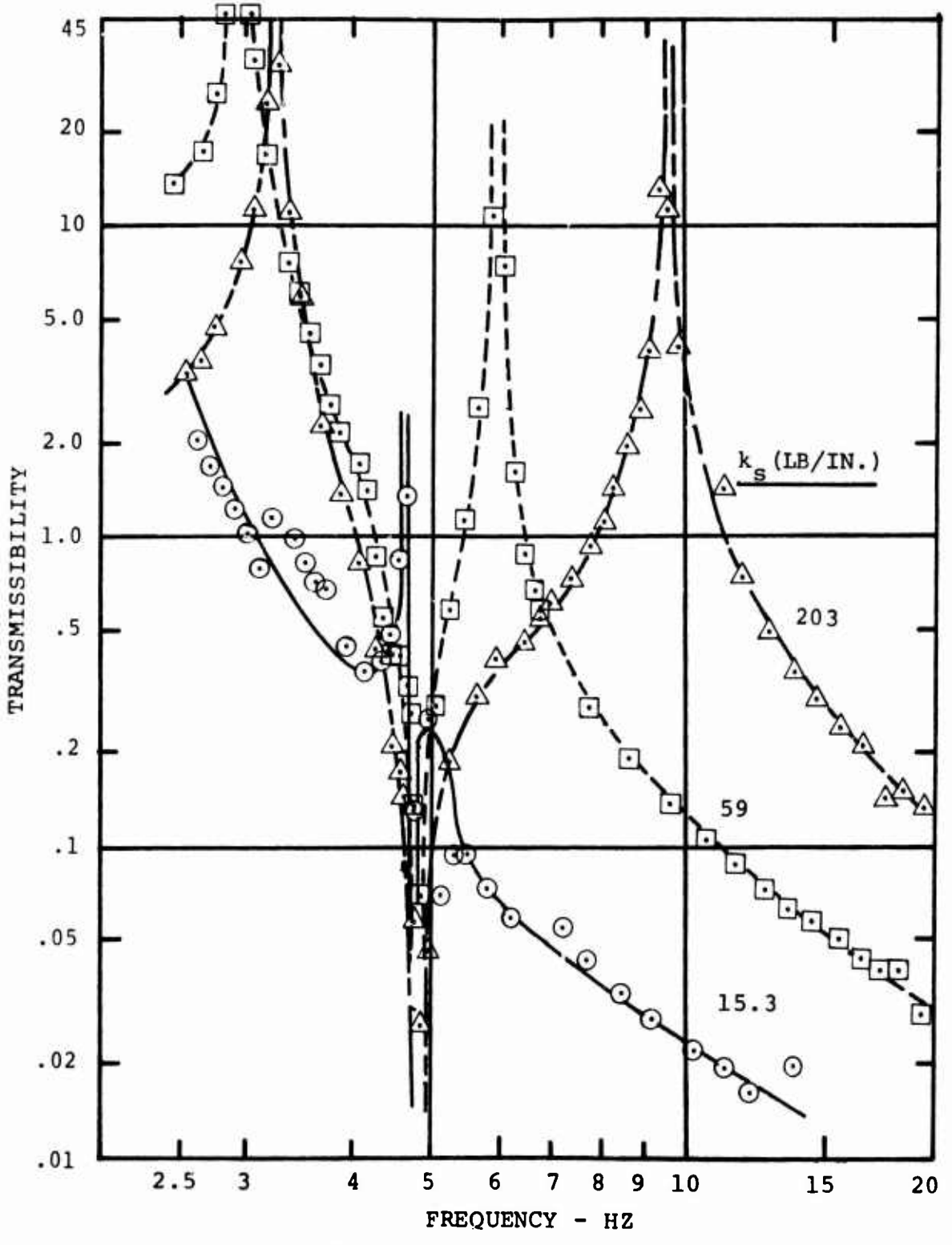

A. 40-Pound Isolated Weight

Figure 34. Effect of Sling Stiffness and Isolated Weight on Configuration 2 COZID Transmissibility.

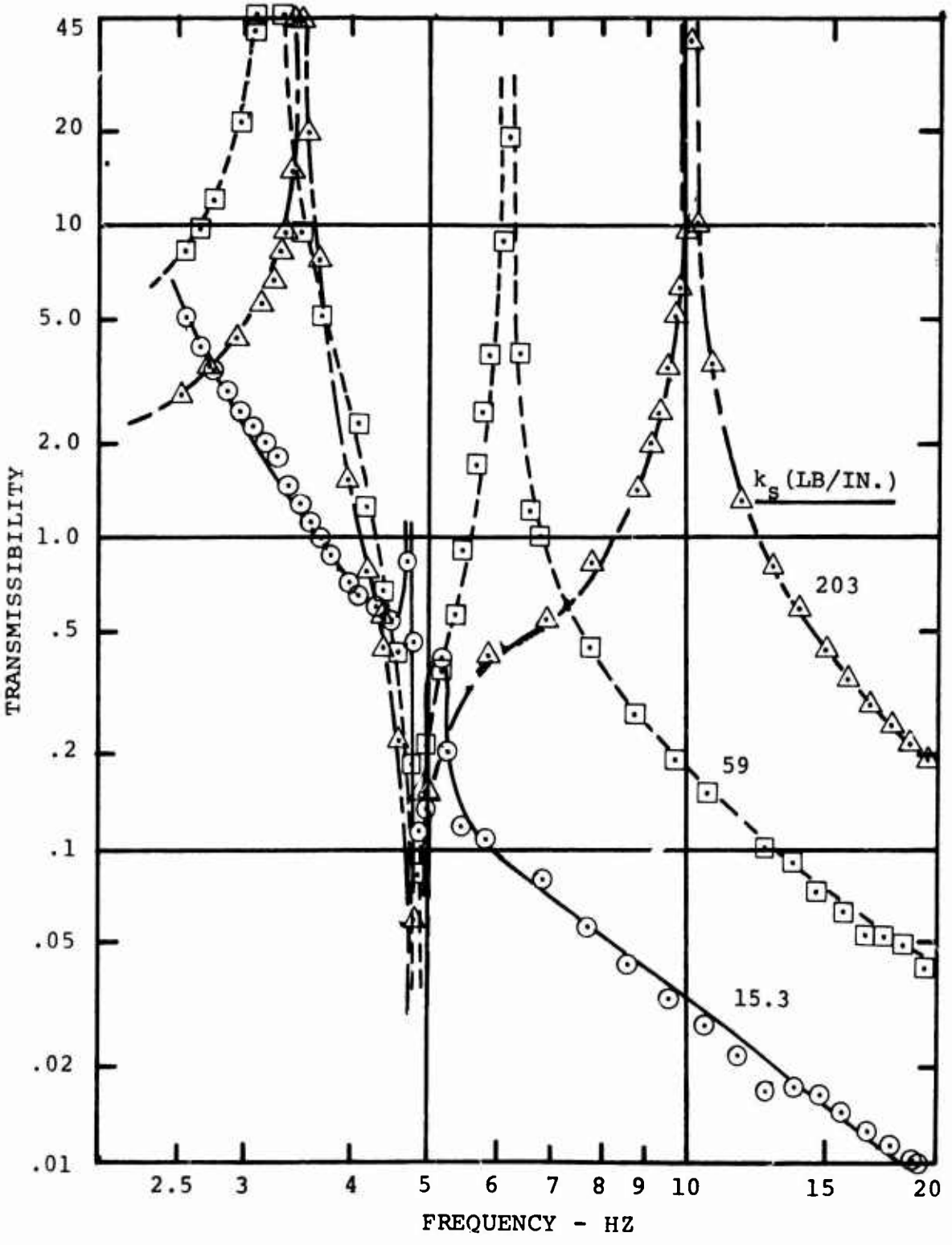

B. 30-Pound Isolated Weight

Figure 34 - Continued.

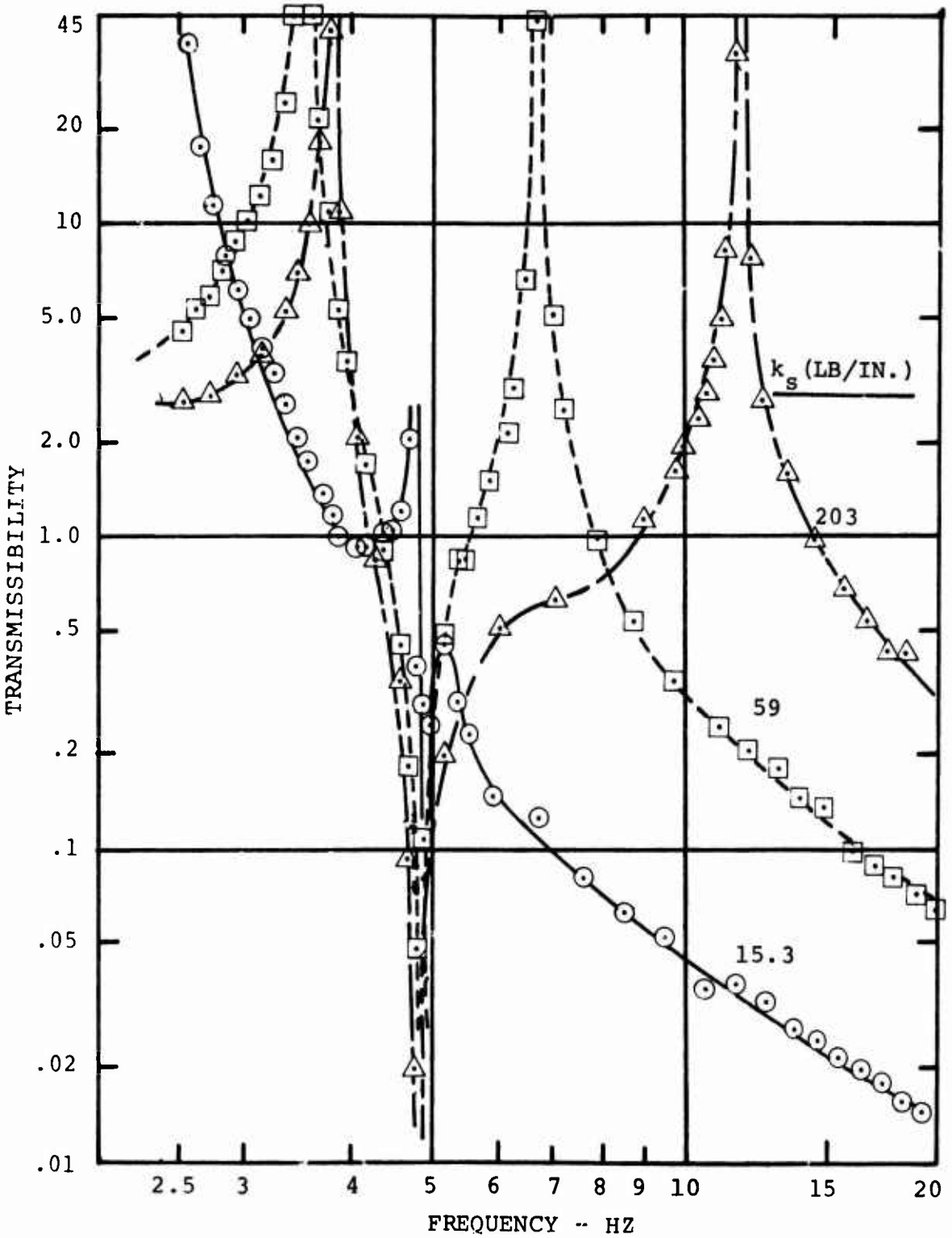

C. 20-Pound Isolated Weight

Figure 34 - Concluded.

While the resonance frequency is shown to approach the antiresonance frequency (near-coincidence), at no time do resonance and antiresonance coincide. As pointed out in the Analysis section, resonance/antiresonance separation may be controlled by adjusting COZID geometrical parameters R and r. With the test model, however, geometry was fixed and no attempt was made to control resonance frequency placement, as would be done in the case of a COZID designed for a specific helicopter application having a fixed 1-P frequency (and range), load capability requirement, and range of sling spring rates. The test data do serve to demonstrate the primary COZID capability, namely, the ability of a COZID, with fixed paramaters, to achieve and maintain low 1-P (antiresonant frequency) response and thereby prevent 1-P resonance, regardless of the parameters of the helicopter/sling/external load system within which it is used.

3.0-Hz COZID

The COZID model was tuned to a 3.0-Hz antiresonant frequency by the addition of inertia discs having a total weight of 7.44 pounds. Inertia and mass of this Configuration 3 model are given in Table VI. Transmissibility data are plotted in Figure 35.

As shown in Figure 26, antiresonance was achieved for all applications of the 3.0-Hz COZID. No shift in antiresonance frequency with changing external load mass and sling spring rate is shown, and in general, good antiresonant isolation was obtained. Transmissibilities measured at the 3.0-Hz tuned frequency range from .757 (25 percent isolation) to .03 (97 percent isolation), with the worst COZID performance obtained for dynamic systems using the soft sling (k_s = 15.3 lb/in.).

The impact of resonant/antiresonant frequency separation on COZID performance is evident in Figure 35, particularly for the case of the soft sling with the maximum 40-pound load. In this case, the second system resonance* occurs at approximately 3.1 Hz, giving a resonance/antiresonance separation of only .1 Hz. As discussed previously, this condition results in suppression of both antiresonant isolation

*The first resonance occurs below the test range.

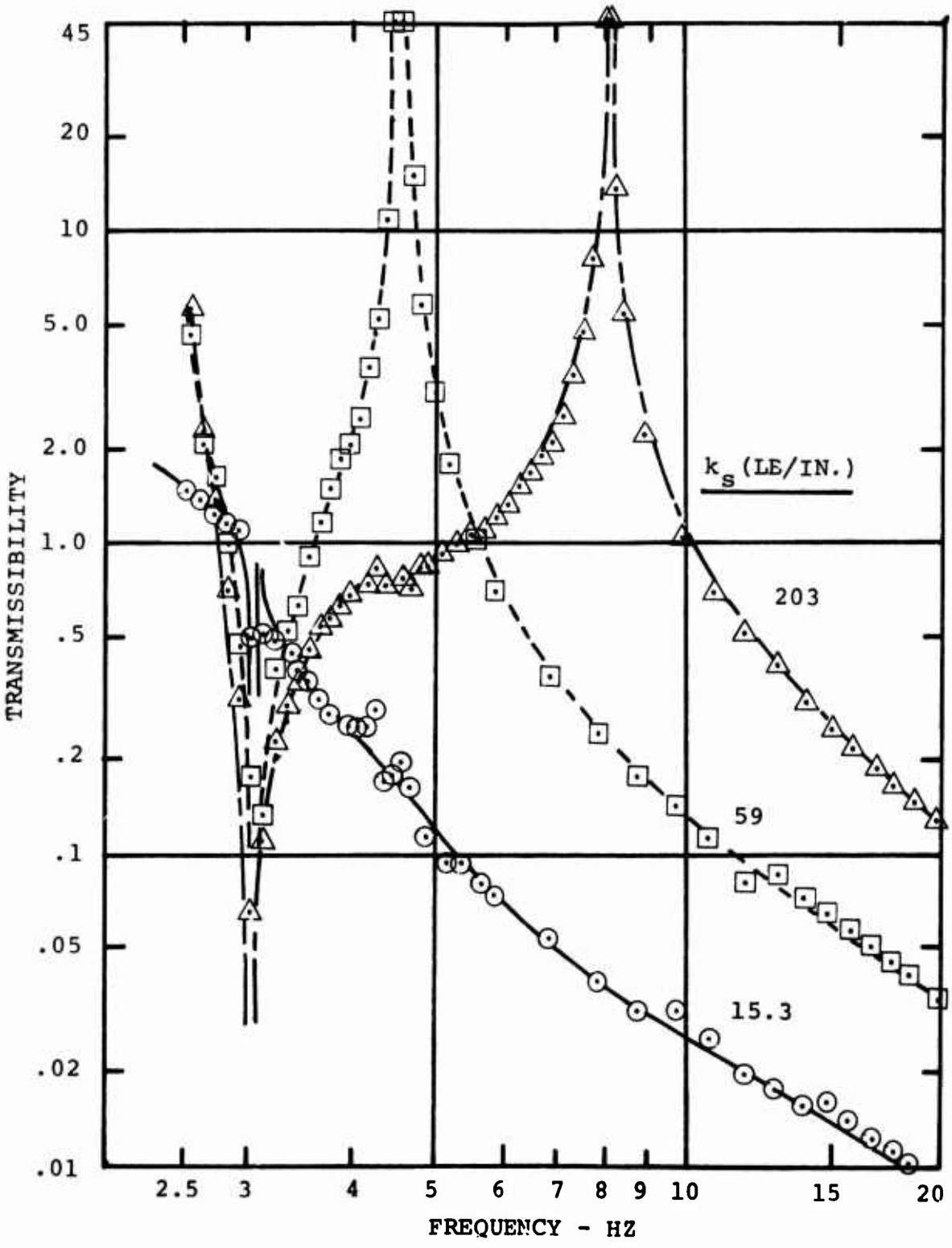

A. 40-Pound Isolated Weight

Figure 35. Effect of Sling Stiffness and Isolated Weight on Configuration 3 COZID Transmissibility.

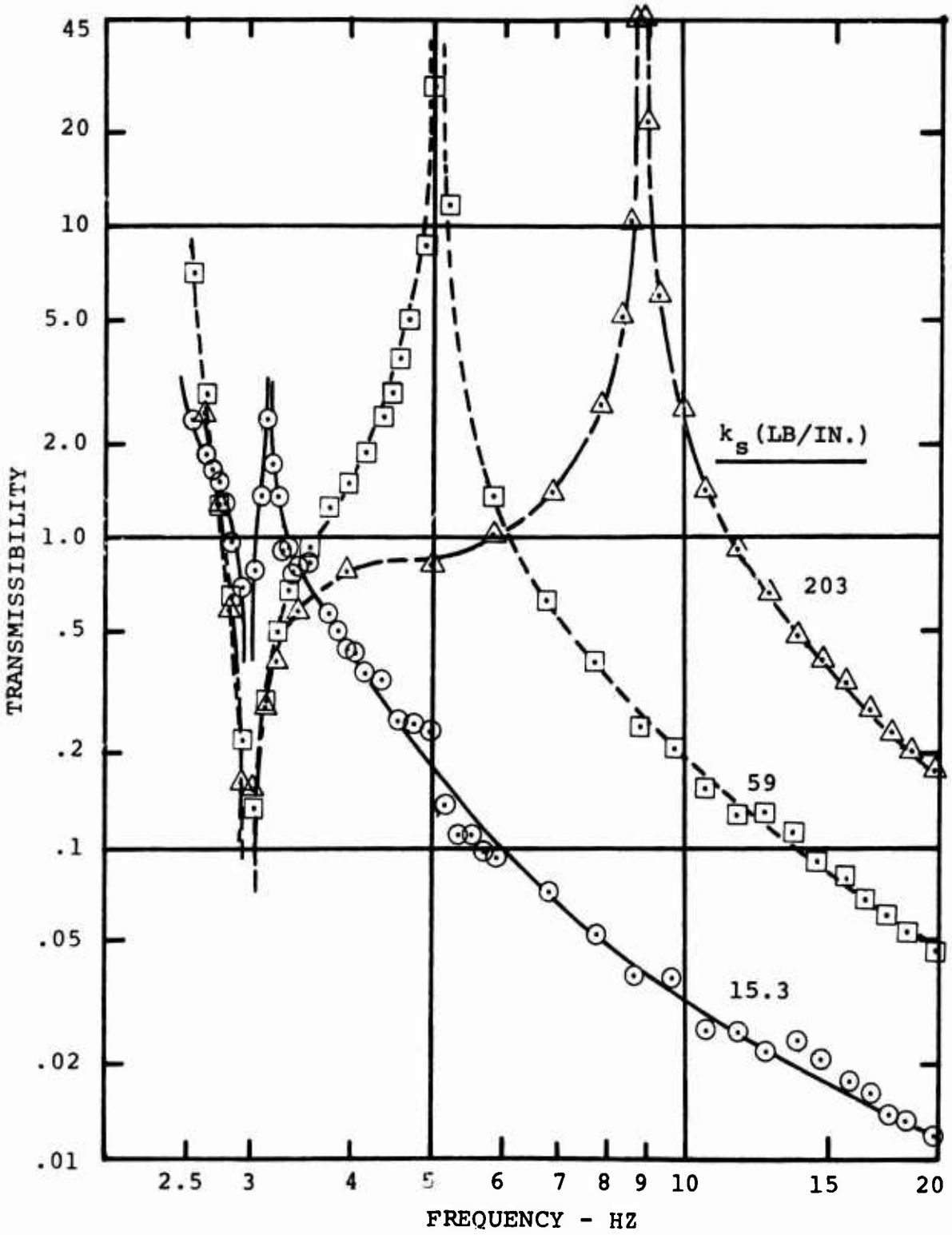

B. 30-Pound Isolated Weight

Figure 35 - Continued.

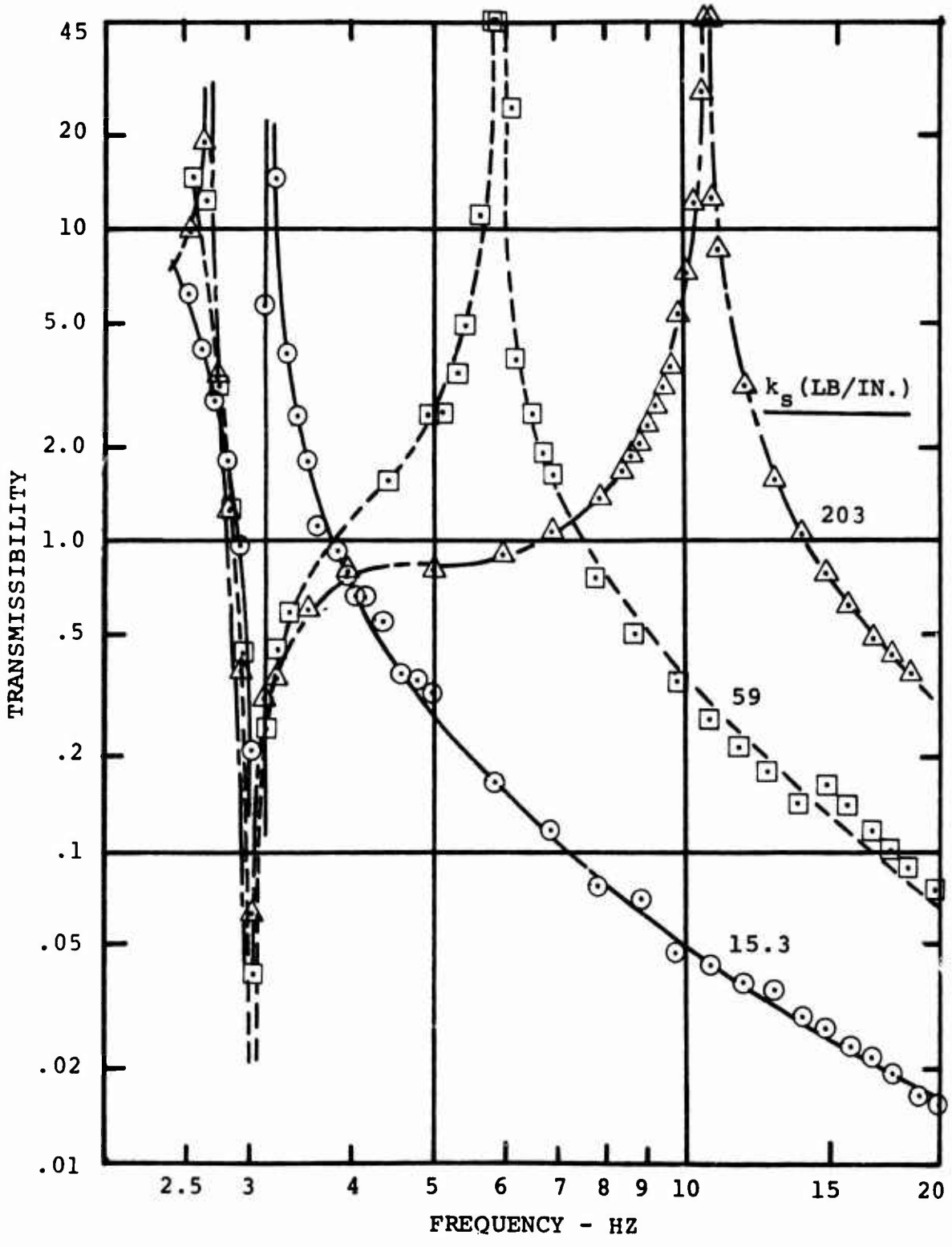

C. 20-Pound Isolated Weight

Figure 35 - Concluded.

and resonant amplification. For the application under discussion, measured transmissibilities at the resonant and antiresonant frequencies are nearly equal, with a value of approximately .5.

CH-47B/C COZID PRELIMINARY DESIGN

A preliminary design for a full-scale COZID has been prepared. This design is based on a CH-47B/C helicopter application, and it has a design load capacity of 20,000 pounds. The COZID is designed to requirements of infinite life, low maintenance, high reliability and fail-safe operation. As designed, the system may be installed with no modification of the CH-47B/C, and it will function without interfering with any aircraft system or operation. Compatibility with the proposed universal sling system has been maintained, both with regard to total system dynamic performance and hardware use. Provisions have been made for storage of the COZID during missions not requiring its use. Producibility of the design has been assessed. Details of the preliminary design are presented in the following paragraphs.

DESIGN CRITERIA

The CH-47B/C helicopter is a medium-gross-weight cargo- and troop-carrying aircraft, capable of performing both internal and external cargo missions. The maximum cargo which may be carried externally is 20,000 pounds, and the maximum gross vehicle weight is on the order of 40,000 pounds. The normal rotor rpm range of the CH-47B/C is 240 to 250 rpm, with resulting 1-P frequency limits of 4.00 to 4.16 Hz. The aircraft is required to operate at the upper limit of rotor rpm while at or near maximum gross weight.

The external cargo system of the CH-47B/C consists of a cargo hook which is attached to the aircraft structure through a curved support rail. This is shown in Figure 36. This arrangement permits fore-aft aircraft cg travel, due to fore-aft pendular motion of the load, while preventing load pitching moments from being introduced into the ship. Pitching moments are eliminated by pivoting of the hook support rail. Lateral cg travel is minimized by allowing the cargo hook to roll on the curvature of the hook support rail, which has its center of curvature just below the aircraft cg.

Figure 36 shows the cargo hook in its extended, or working, position. For nonexternal cargo-carrying missions, the hook is stowed as shown in Figure 37. In this condition, the cargo hook and support rail are contained entirely below the cargo compartment floor line, permitting use of the aircraft for internal cargo- or troop-carrying missions.

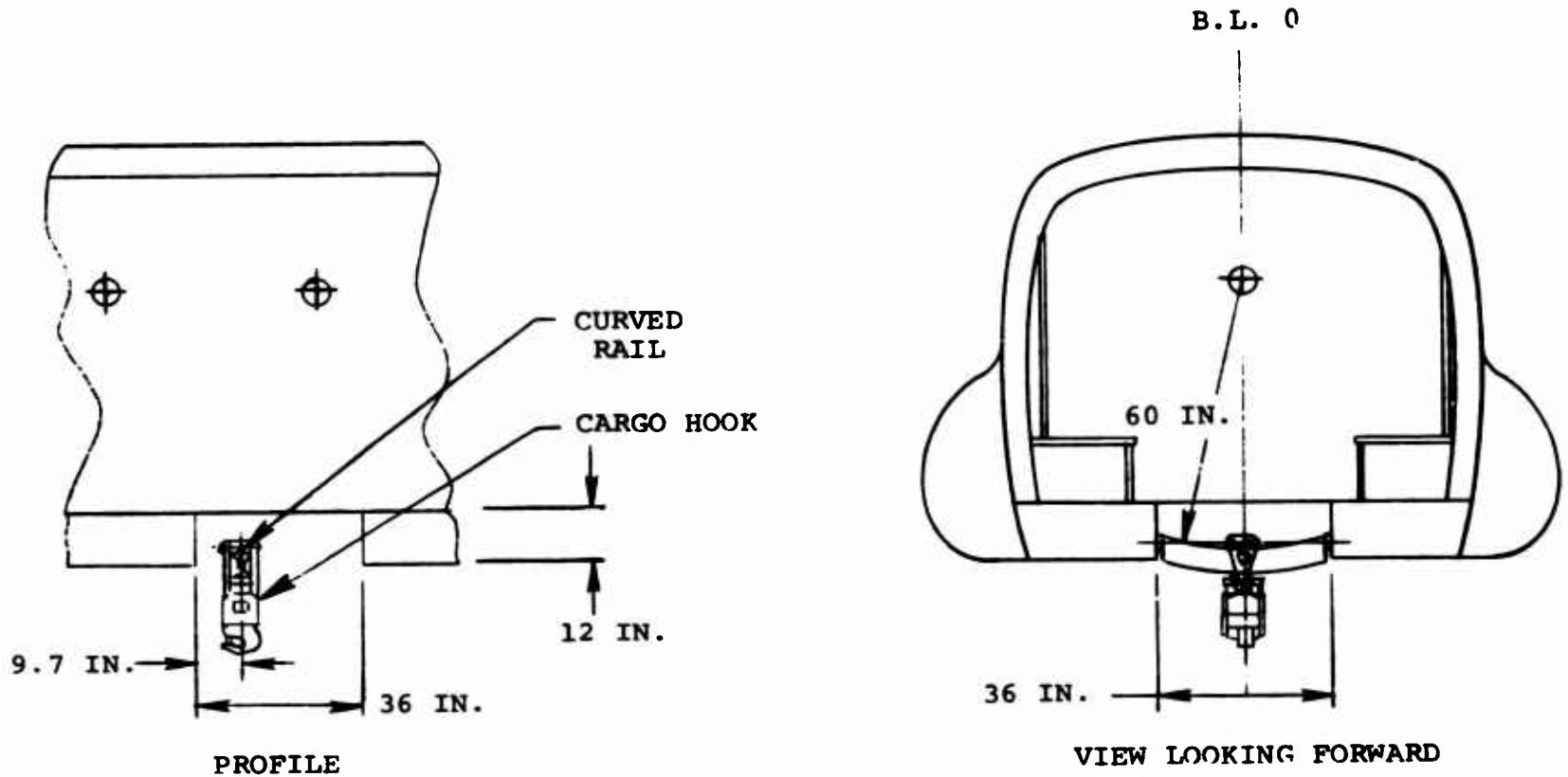

Figure 36. CH-47B/C External Cargo System Arrangement.

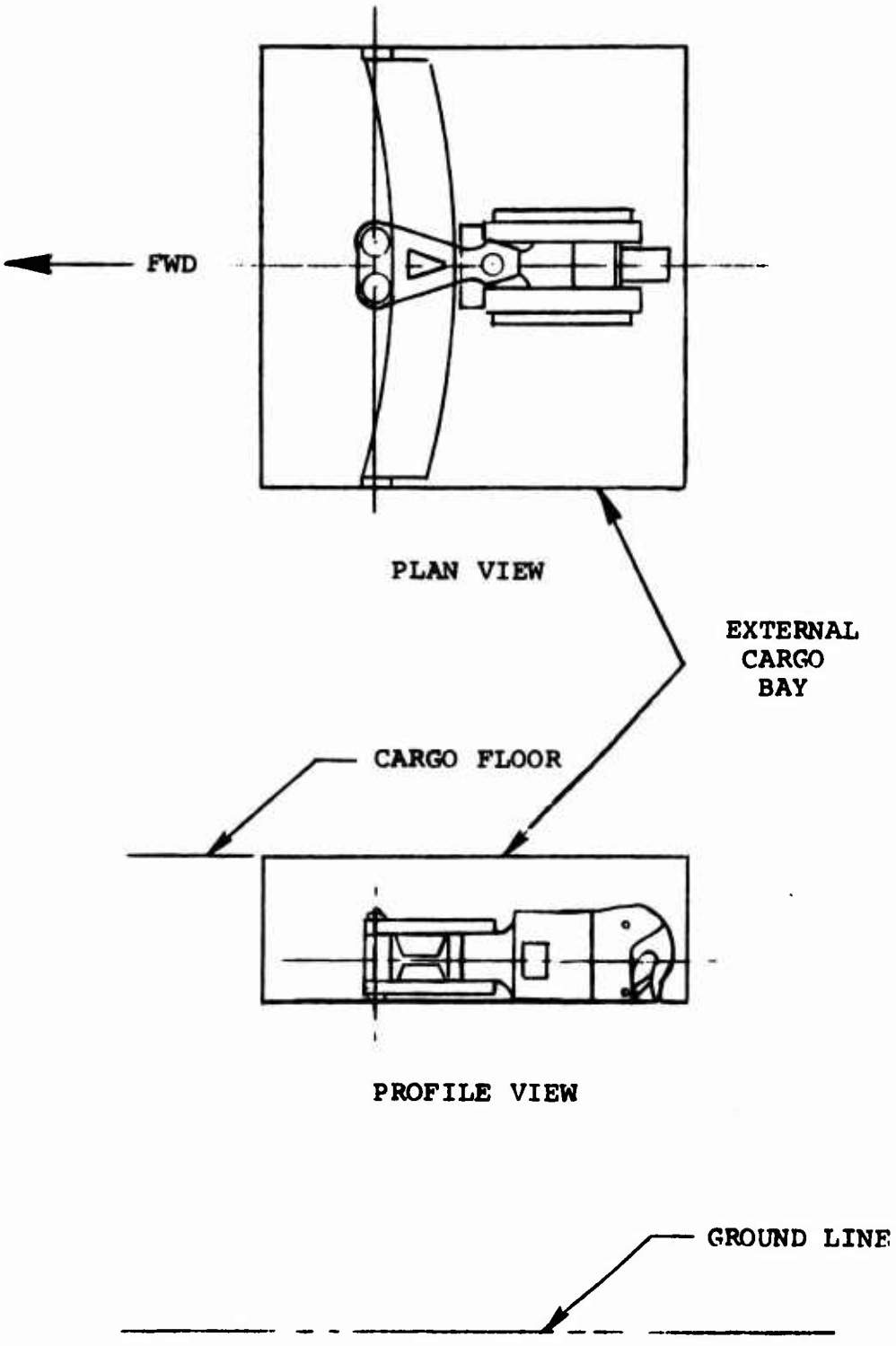

Figure 37. Standard CH-47B/C External Cargo Hook in Stowed Position.

The cargo hook used in the existing CH-47B/C external cargo system is a relatively large, complex device, owing to the number of functions which it serves. When used with the proposed universal sling system, however, the cargo hook attached to the aircraft will be used only as an attachment point for the sling system pendant, shown in Figure 38. The aircraft hook will not be required to swivel (to eliminate load-induced yawing moments), since this feature is incorporated into the pendant swivel hook. Requirements for the cargo hook are therefore reduced to those of adequate strength, physical compatibility with the pendant apex fitting, and incorporation of normal and emergency mechanical release mechanisms.

COZID design criteria are based on physical and dynamic compatibility with the CH-47B/C external cargo system and the universal sling system, as well as projected modifications of the universal sling system which would result from production incorporation of the COZID. Physically, the COZID is required to be attached to the existing hook support rail and to make use of the moment minimization features (pitch and roll freedom of movement) incorporated in the support rail. The device must incorporate a pendant attachment hook (cargo hook), which permits attachment of the pendant apex fitting, shown in Figure 38. Size of the COZID and hook must be such that, with the device in its normal working position, ready to accept the apex fitting, clearance with the ground line is obtained. Lateral and longitudinal dimensions are limited by the requirement to store the device within the external cargo bay in such a manner that it does not protrude into the cargo compartment.

With regard to dynamic performance, the COZID is required to prevent resonance of the helicopter/external load dynamic system with f_{lp} of the helicopter rotor Dynamic system transmissibility must be kept below 1.5 over a frequency range of 4.0 Hz to 4.16 Hz (240 to 250 rotor rpm), with all possible dynamic system configurations. Use of both a soft sling system (k_s = 4000 lb/in., universal sling system) and a stiff sling system (k_s = 50,000 lb/in.) must be considered, with external loads ranging from 25 percent to 100 percent of maximum (5000 pounds to 20,000 pounds).

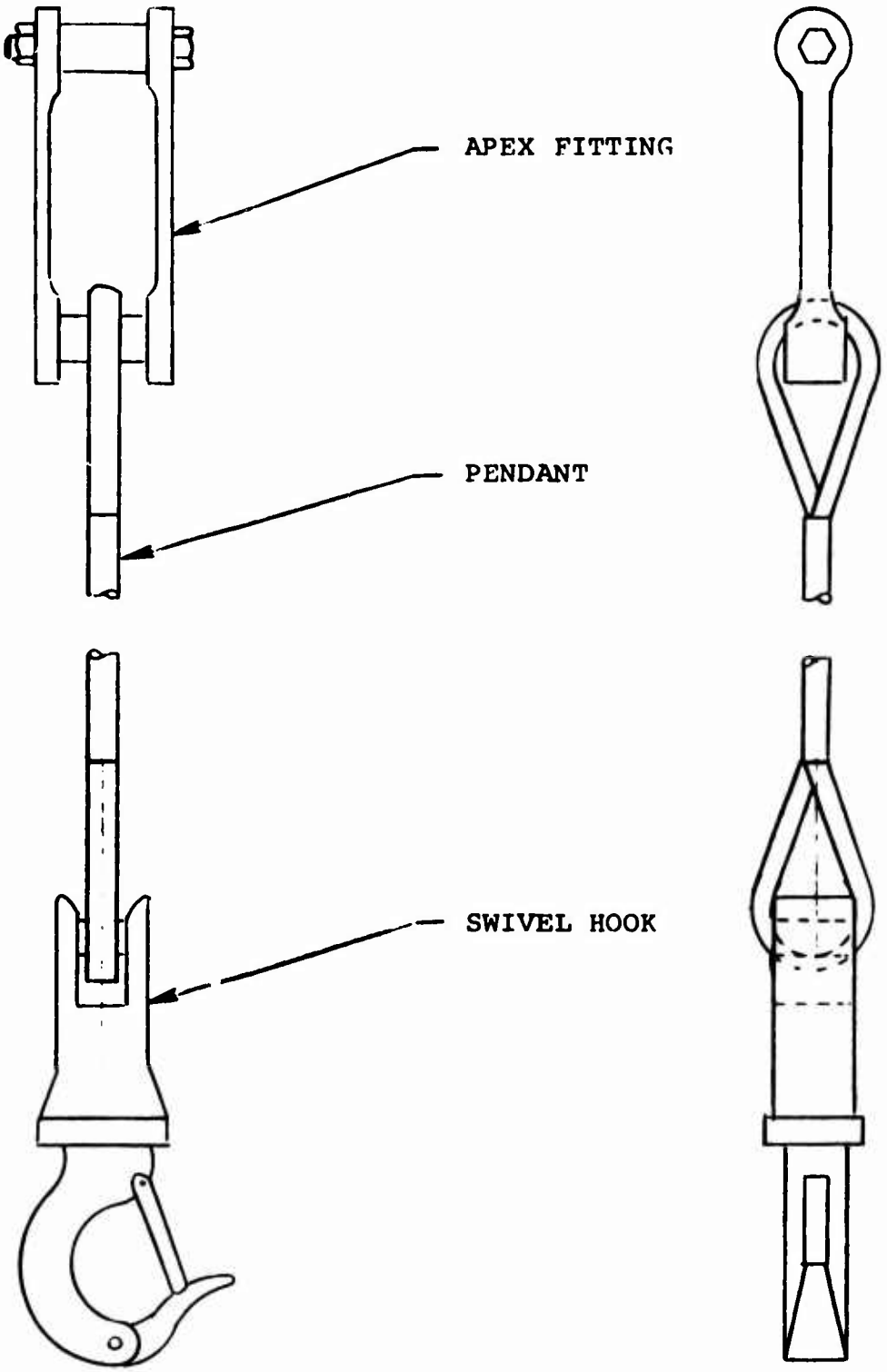

Figure 38. Universal Sling System Pendant - 20,000-Pound Capacity.

COZID DESIGN

Interpretation of the design criteria of the previous section results in the generation of a maximum size envelope for the CH-47B/C COZID. In the vertical dimension, COZID size is dictated by the spacing between the hook support rail and the ground, a distance of approximately 21 inches. The remaining COZID dimensions are dictated by storage requirements, with the device required to fit within the external cargo bay, and below the cargo compartment floor, during storage. Maximum stored configuration lateral and longitudinal dimensions are thus 36 inches and 15 inches, respectively.

The stringent space requirements dictate the use of one of the alternate COZID configurations illustrated in Figure 13. Specifically, the folded dual cylinder COZID was found to be most appropriate to the CH-47B/C application. This configuration, which is described in detail in Appendix II, was selected because its space envelope conforms most closely to the space available within the CH-47B/C external cargo bay. Drawings relating the primary features of the CH-47B/C COZID are shown in Figures 39, 40 and 41.

The CH-47B/C COZID is designed around a maximum angular deflection including static and dynamic deflection of less than 20 degrees. A small angular deflection is necessitated by a maximum strain restraint of 50 percent across the torsional elastomeric spring. Maintaining a small angular deflection also permits reduction of the COZID vertical dimension, since nonworking segments of the inertia wheels may be left out, leaving the truncated inertia wheels of Figure 39. Removal of these inertia wheel segments, and their contributions to total COZID mass and inertia, is compensated for by the addition of concentrated inertia mass elements.

In the CH-47B/C COZID design, the mass/inertia and compound pulley functions of the inertia wheels are, in fact, separated. The inertia wheels are made as light as possible, with size and strength sufficient only to provide rolling surfaces for the load and support cables. Concentrated mass elements are used to provide the required mass and inertial properties, thereby allowing independent adjustment of COZID inertia/mass and cable radii. Design refinement permits independent specification of COZID cable radii (R and r) and radius of gyration (ρ_c), enabling COZID design parameters to

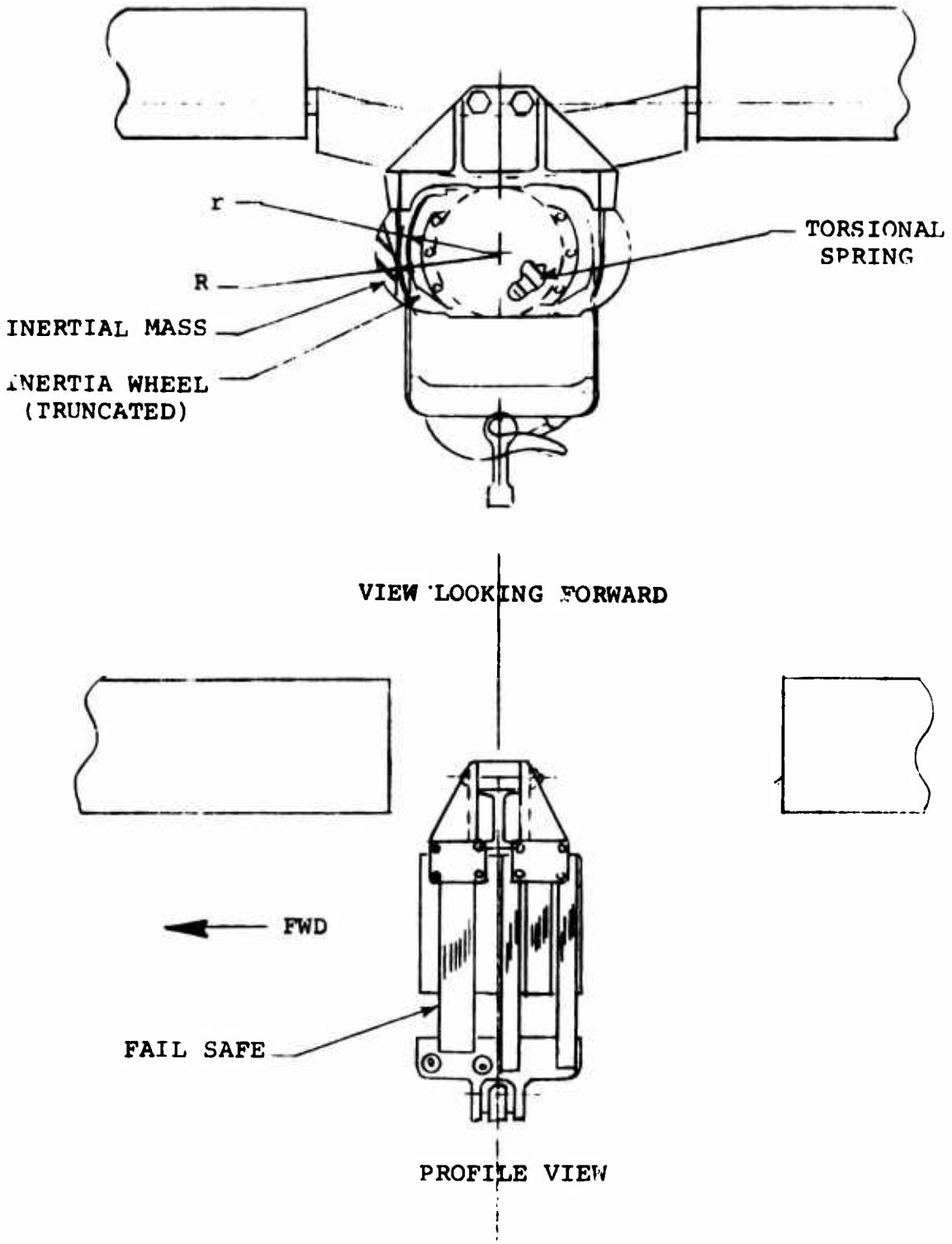

Figure 39. CH-47B/C COZID Installation.

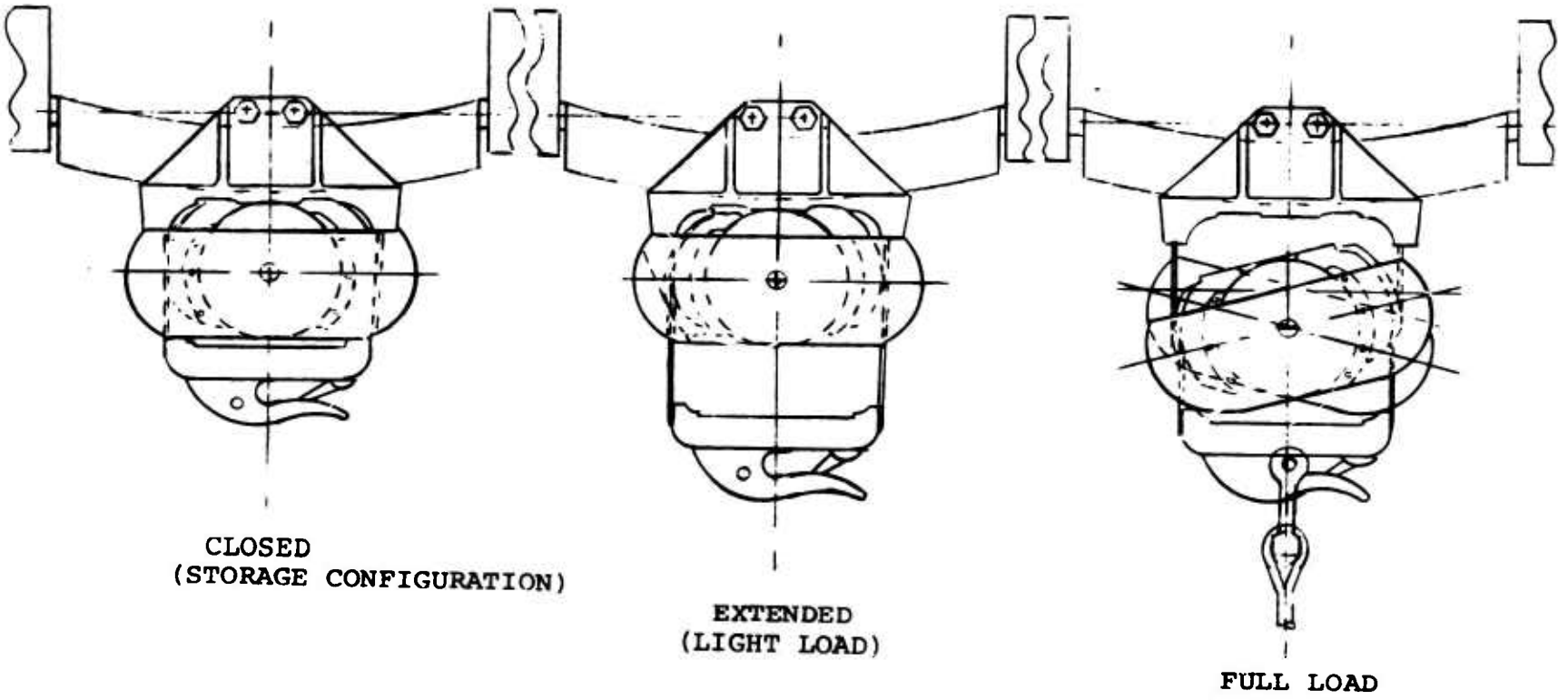

Figure 40. CH-47B/C COZID in Closed, Extended and Full-Load Conditions.

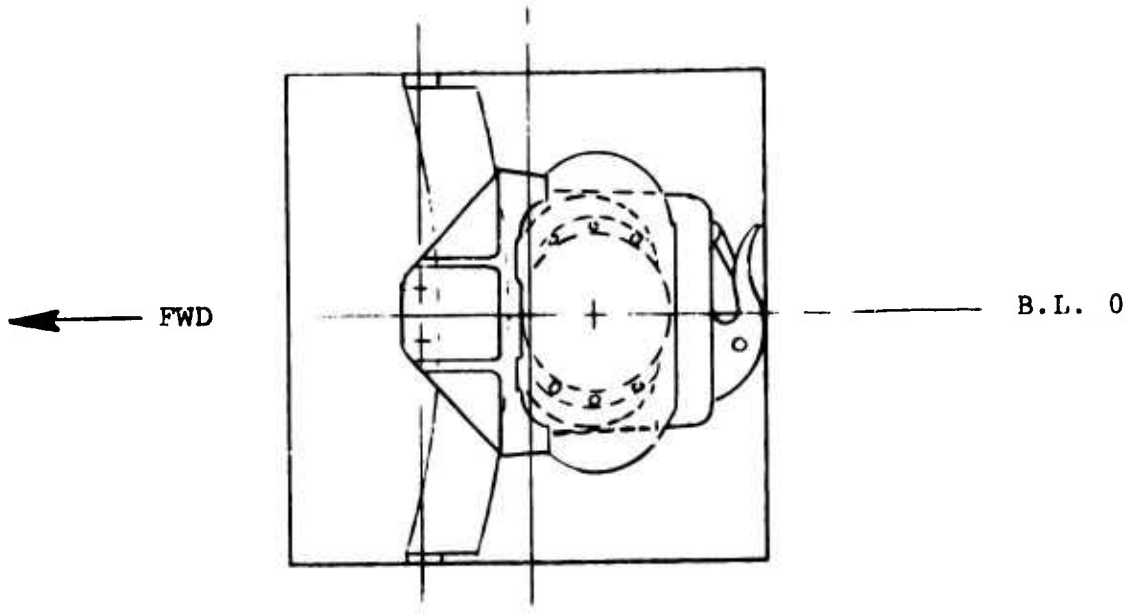

PLAN VIEW

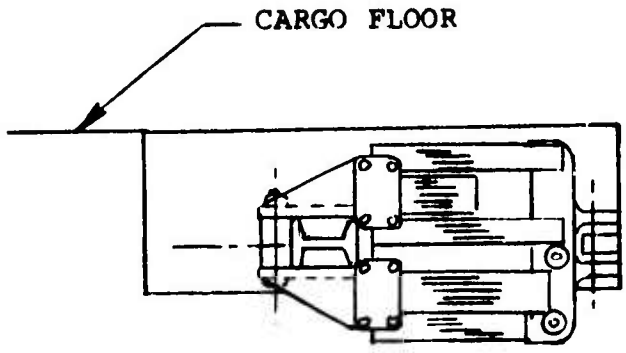

PROFILE VIEW

Figure 41. CH-47B/C COZID Storage.

be selected which are not within the allowable limits as defined in the parametric study section*. Design parameters of the CH-47B/C COZID are given in Table VII.

TABLE VII. DESIGN PARAMETERS FOR CH-47B/C COZID

Parameter	Value
R	9.3 in.
r	8.5 in.
ρ_c	10.3 in.
M_c	.479 (lb-sec^2)/in.
k_θ	262.0 (in.-lb)/deg

Hook Retraction and Releasing Mechanisms

Ground clearance and storage considerations dictate a very small COZID vertical dimension in the unloaded condition The vertical dimension of the device is determined by two factors: the physical size of the inertia wheel and the relative deflection which takes place between the inertia wheels and the cargo hook support in response to static and dynamic loading**. The maximum relative deflection, illustrated in Figure 40, is 5.5 inches, and therefore a spacing of 5.5 inches is required between the COZID inertia wheel and the hook support structure when the device is in its working configuration.

*The parametric study results are predicated on a fixed relationship between COZID cable radii and radius of gyration, with the radius of gyration always less than the support cable radius. The CH-47B/C design utilizes a radius of gyration greater than the support cable radius.

**Loading of the cargo hook results in rotation and translation of the COZID inertia wheels as well as translation of the hook. Inertia wheel translation exceeds hook translation by an order of magnitude; therefore, space must be provided between the hook support and the inertia wheels to accommodate this relative deflection.

The vertical dimension of the COZID is reduced appreciably by truncation of the inertia wheels discussed previously. Further size reduction is obtained by retraction of the hook support structure in the no-load condition. This retraction, which reduces COZID vertical size by 5.5 inches, is accomplished automatically through the use of a spring mechanism located in the hook support structure. With no load on the COZID, this mechanism draws the load cable into the support, thereby raising the support structure until interference with the bottom of the COZID inertia wheel takes place. This stored configuration is maintained by a residual tensile force generated by preloading the spring in the retraction mechanism. Attachment of a minimum load of 100 pounds to the hook causes complete extraction of the hook support with transfer of cable loading directly to the support structure. The retraction mechanism functions only up to a load of 100 pounds, at which time it is effectively removed from the system. This mechanism is not part of the dynamic system for loads in excess of 100 pounds.

Because of the limited nature of the preliminary design effort, no attempt was made to include detail designs of required normal (electrical or hydraulic) and emergency mechanical pendant release mechanisms. Sufficient space exists, however, to include these features within the hook support structure.

Storage

In the stored configuration, the overall dimensions of the COZID (including the hook support structure and hook) are such that the device may be stored within the external cargo bay, as shown in Figure 41. Storage is accomplished by tilting the COZID on its side, with pivoting of the curved support rail about its pitching axis. In this configuration, the COZID is contained entirely below the cargo compartment floor line and extends below the aircraft fuselage approximately 3 inches.

Stress Considerations

Stress-critical COZID components are the support and load cables and the torsional spring. Details of these components have been selected to provide infinite life, based on the stress analyses of Appendix III.

Support and load cables are subjected to combined bending and tensile stresses resulting from wrapping and unwrapping from the inertia wheels in response to static and dynamic loading.

This type of loading is best handled* with a wire-rope belt made up of a number of small-diameter wire ropes constrained to equal load sharing. For the present application, stress analyses indicate the need for belts made up of 1/4-inch-diameter, 6 x 37 IWRC wire rope utilizing extra improved plow steel, having a breaking strength of 325,000 psi.

Twenty cables are required for the severe loading expected. Two 10-cable wire rope belts are used as support cables, with two pairs of 5-cable belts used in the load cables. In all cases, swage end fittings are used to terminate the individual cables which make up each belt.

The torsional elastomeric element is subjected to static and dynamic torque loading due to the moments produced by offset of the support and cable radii. The element has been designed around a maximum strain of 50 percent, in keeping with standard design practice**. Stress analyses (Appendix III) indicate a maximum shear stress of less than 30 psi, which is well within accepted limits defined by infinite life considerations. While natural rubber is used in the element itself, environmental compatibility is obtained through the use of a synthetic, environmentally stable neoprene covering.

Producibility, Reliability and Maintainability

The CH-47B/C COZID design may be fabricated using standard aircraft materials and manufacturing methods. All structural parts, including the upper and lower (hook) support structures, and the truncated inertia wheels will be forged and finish machined using 2014-T6 or 7079-T6 aluminum alloy forging stock. The inertia mass elements will be machined from high-density tungsten alloy, and the wire rope belts will be built up using existing aircraft-quality wire rope and construction details defined in Reference 8. The torsional elastomeric spring will be vulcanized as a unit and bolted to the inertia wheels.

Based on the preliminary design, the weight of a CH-47B/C COZID unit is estimated to be 367 pounds. Of this weight, 59 pounds and 63 pounds are estimated for the upper and lower (hook) support structures, respectively; the inertia wheels are estimated to weigh 185 pounds; and the elastomeric spring has an estimated weight of 36 pounds. The remaining 24 pounds is accounted for by the wire rope belts and miscellaneous hardware.

* Using existing tension member technology as determined in the study of Reference 8.

**As defined in Reference 6.

The CH-47B/C COZID weight represents approximately 1.8 percent of the external load capacity of the helicopter. While this is not a restrictive weight, it should be understood that the weight penalty associated with COZID use is not equal to the total COZID weight, since the COZID replaces the existing cargo hook assembly. The actual weight penalty, taking into account the weight of the existing hook, is estimated to be on the order of 1.5 percent of the maximum external load.

The CH-47B/C COZID design includes no rubbing or sliding parts requiring lubrication. The inertia wheels roll without sliding on the wire rope belts, which are permanently lubricated during manufacture. A case will be provided, enclosing the COZID and preventing damage due to improper handling. It is anticipated that maintenance will be limited to periodic disassembly and inspection.

Reliability of the COZID is expected to be satisfactory. The device contains few moving parts and is a closed unit requiring no field adjustment. A fail-safe system is provided consisting of wire rope belts connecting the upper support structure and hook support. These belts are long enough to allow COZID operation under normal circumstances, but in the event of system failure (or overload), the belts assume the load of the external cargo.

CONCLUSIONS AND RECOMMENDATIONS

The problem of vertical bounce has been and continues to be a serious hindrance to the performance of helicopter external cargo-carrying missions. Vertical bounce has occurred on a number of aircraft, including the CH-47, CH-54 and UH-1, and as yet there exists no completely satisfactory solution for this problem.

Development and use of a COZID suitable for the helicopter external cargo system application will result in the elimination of vertical bounce. Use of the COZID will have no undesirable impact on aircraft performance or safety other than a relatively minor increase in aircraft weight.

An extensive experimental effort has been conducted, evaluating the performance of a small-scale COZID model. Satisfactory performance has been demonstrated for COZID tuned frequencies of from 8 Hz to 3 Hz, simulating COZID use on helicopters having 7.8-Hz, 4.8-Hz and 3-Hz main rotor 1-P frequencies. Actual model performance has been shown to agree well with theoretically predicted performance, and the impact of simulated sling system dynamics on COZID anti-resonant tuning has been found to be negligible, as expected.

Parametric studies have indicated the COZID to be applicable to all Army cargo helicopters, including the UH-1, CH-47, CH-46, CH-53, YUH-60 and YUH-61. In all cases it has been found that COZIDs may be designed with parametric weights not exceeding 2 percent of the maximum external load, and with reasonable size. In most cases the increase in helicopter basic empty weight does not exceed 2 percent.

A preliminary COZID design for CH-47B/C application demonstrates the practicability of the device. Size of this COZID has been kept small enough to permit installation in the CH-47B/C with no modification of the aircraft. Provisions have been made for storage of the COZID during periods of nonuse, with the storage within the external cargo bay, entirely below the cargo compartment floor. During operation, the device functions entirely outside of the aircraft and does not interfere with any aircraft system or operation. Use is made of the roll moment relief capability of the existing curved hook support rail, and freedom of the rail to pivot in the pitch plane is retained.

The present program has shown the COZID to be a viable concept having practical application to an existing, significant problem. Further development is required, however, before the COZID reaches the production phase. It is recommended that development be continued through an experimental program involving flight testing of full-scale hardware.

REFERENCES

1. Briczinski, S. J., and Karas, G. R., CRITERIA FOR EXTERNALLY SUSPENDED HELICOPTER LOADS, United Aircraft Corporation, Sikorsky Aircraft Division; USAAMRDL Technical Report 71-61, Eustis Directorate, U. S. Army Air Mobility Research and Development Laboratory, Fort Eustis, Virginia, November 1971.

2. Gabel, R., and Wilson, G. J., TEST APPROACHES TO EXTERNAL SLING LOAD INSTABILITIES, Journal of the American Helicopter Society, Vol. 13, No. 3, July 1968, pp. 44-55.

3. Veca, A. C., VIBRATION EFFECTS ON HELICOPTER RELIABILITY AND MAINTAINABILITY, United Aircraft Corporation, Sikorsky Aircraft Division; USAAMRDL Technical Report 73-11, Eustis Directorate, U. S. Army Air Mobility Research and Development Laboratory, Fort Eustis, Virginia, April 1973.

4. HUMAN ENGINEERING DESIGN CRITERIA FOR MILITARY SYSTEMS, EQUIPMENT AND FACILITIES; Section 5.8, Environment, Para. 5.8.4, Vibration; Military Standard 1472A, 15 May 1970.

5. Flannelly, W. G., and Bowes, M. A., CABLE OPERATED ZERO IMPEDANCE DECOUPLER (COZID) - ANALYTICAL DEVELOPMENT AND PRELIMINARY PARAMETRIC DESIGN INVESTIGATION, Kaman Aerospace Corporation Research Note 71-10, Kaman Aerospace Corporation, Bloomfield, Connecticut, 8 October 1971.

6. Bowes, M. A., CABLE OPERATED ZERO IMPEDANCE DECOUPLER (COZID) - PRELIMINARY VIBRATION TEST REPORT, Kaman Aerospace Corporation Research Note 71-12, Kaman Aerospace Corporation, Bloomfield, Connecticut, 29 December 1971.

7. Uthgenannt, E. B., CABLE OPERATED ZERO IMPEDANCE DECOUPLER (COZID) - VIBRATION TEST #2, Kaman Aerospace Corporation Research Note 72-1, Kaman Aerospace Corporation, Bloomfield, Connecticut, 21 January 1972.

8. Minor, J. C., Gibson, P. T., and Cress, H. A., HELICOPTER-LOAD TENSION-MEMBER STUDY, Battelle Columbus Laboratories; USAAMRDL Technical Report 72-20, Eustis Directorate, U. S. Army Air Mobility Research and Development Laboratory, Fort Eustis, Virginia, November 1972.

9. Frye, W. A., RUBBER SPRINGS, CH. 35, Vol. 2, Shock and Vibration Handbook, McGraw-Hill Book Co., 1961, C. M. Harris and C. E. Crede, ed.

10. Spotts, M. F., DESIGN OF MACHINE ELEMENTS, New York, Prentice-Hall, Inc., 1953, p. 392.

APPENDIX I
TORSIONAL SPRING (FOLDED) COZID ANALYSES

A schematic diagram of the folded dual-cylinder COZID, incorporating a torsional elastic element, is shown in Figure 42. The device consists of two inertia wheels connected at their centers with a torsionally elastic element having spring rate k_θ (in.-lb/degree). The inertia wheels are identical, with total mass M_c and inertia I_c, and with support and load cable radii R and r. The cables are attached in a manner similar to that discussed in the Analysis section, allowing rotation of the inertia wheels, with alternating cable wind-up and release. Static and dynamic equations for this COZID configuration are derived in the following paragraphs.

STATIC RESPONSE

Application of a static force, of magnitude L (corresponding to the weight of mass M_L), to the Figure 42 COZID results in rotation of the inertia wheels in opposite directions, accompanied by translation of both wheels in the direction of the applied load. Considering forces and moments acting on one inertia wheel only, as shown in Figure 43, results in the following equation:

$$L/2(R - r) = \tau_s \tag{62}$$

Since the torsional elastic element is subjected to a relative rotation equal to twice the inertia wheel rotation*, the torque generated in the element (τ_s) is

$$\tau_s = 2k_\theta\theta \tag{63}$$

Then, combining Equations (62) and (63),

$$\theta = \frac{L(R - r)}{4k_\theta} \tag{64}$$

*The inertia wheels rotate in opposite directions, with the relative rotation equal to twice inertia wheel rotation.

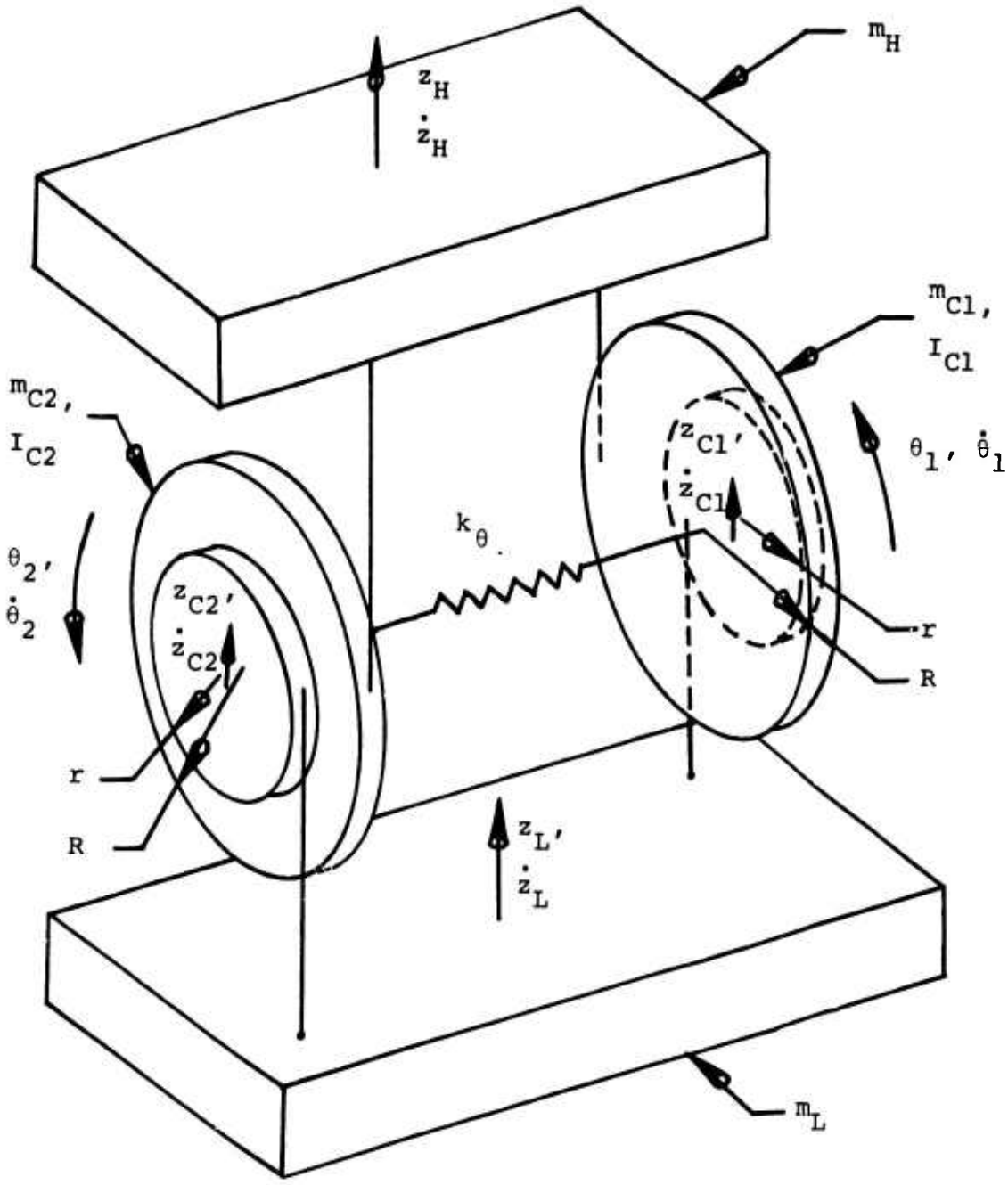

Figure 42. Folded Dual-Cylinder COZID.

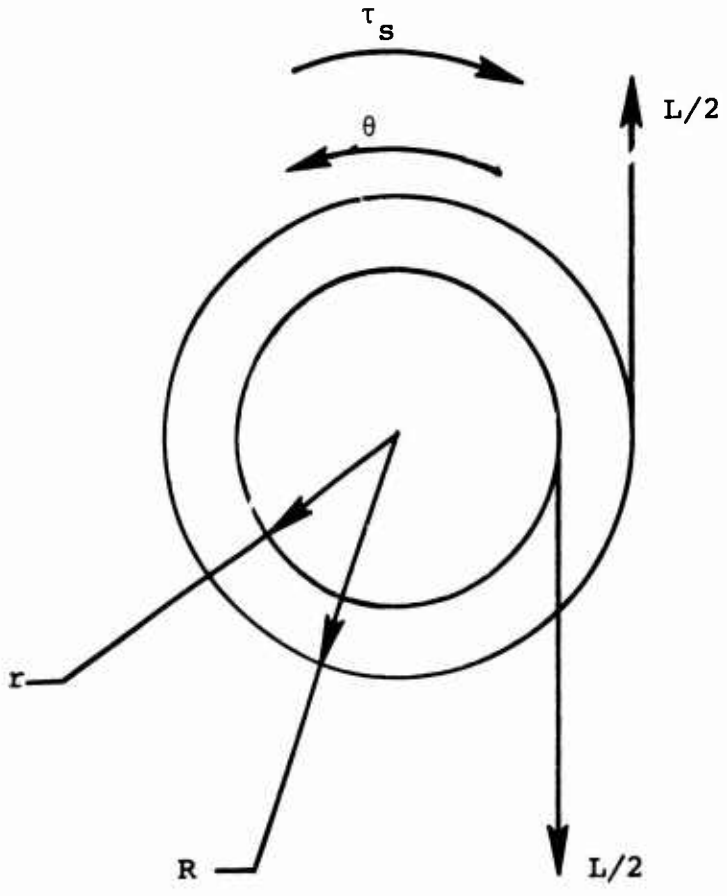

Figure 43. Static Forces and Moments Acting on One Inertia Wheel of Folded, Dual-Cylinder COZID.

The relative rotation across the elastic element is then

$$\Delta\theta = 2\theta = \frac{L(R - r)}{2k_\theta} \tag{65}$$

Deflection of the load, z_L, is equal to the vector sum of the translation of the inertia wheel center and translation of the load cable point of tangency due to rotation. Load deflection is then

$$z_L = \frac{L(R - r)^2}{4k_\theta} \tag{66}$$

and the effective stiffness of the COZID is

$$K_c = \frac{4k_\theta}{(R - r)^2} \tag{67}$$

Comparison of this equation with Equations (11) and (42) reveals the folded COZID to be statically identical to the other configurations discussed in the Analysis section if a substitution for the equivalent torsional spring rate is made. Equivalent torsional spring rate is then

$$k_\theta \equiv k_c \cdot R^2 \tag{68}$$

DYNAMIC RESPONSE

Referring to the dynamic system of Figure 42, potential and kinetic energy equations are

$$V = 1/2\ k_\theta(\theta_{C1} - \theta_{C2})^2 \tag{69}$$

$$T = 1/2\ M_L\dot{z}_L^2 + 1/2\ M_{C1}\dot{z}_{C1}^2 + 1/2\ M_{C2}\dot{z}_{C2}^2 + 1/2\ I_{C1}\dot{\theta}_{C1}^2 + 1/2\ I_{C2}\dot{\theta}_{C2}^2 \tag{70}$$

Consideration of geometry yields

$$\theta_{C1} = -\theta_{C2} = \frac{1/R(z_L - z_H)}{(1 - r/R)} \tag{71}$$

$$\dot{\theta}_{C1} = -\dot{\theta}_{C2} = \frac{1/R(\dot{z}_L - \dot{z}_H)}{(1 - r/R)} \tag{72}$$

$$\dot{z}_{C1} = \dot{z}_{C2} = \frac{\dot{z}_L - (r/R)\dot{z}_H}{(1 - r/R)} \tag{73}$$

Substitution of Equations (71), (72) and (73) into Equations (69) and (70) results in energy equations involving helicopter and load motions (z_H and z_L) only, with

$$V = 1/2 \frac{k_\theta(4)}{R^2(1 - r/R)^2} (z_L - z_H)^2 \tag{74}$$

$$T = 1/2\ M_L \dot{z}_L^2 + \frac{1/2 M_C}{(1 - r/R)^2} [(\dot{z}_L - (r/R)\dot{z}_H]^2$$

$$+ 1/2 \frac{I_C}{R^2(1 - r/R)^2} (\dot{z}_L - \dot{z}_H)^2 \tag{75}$$

Assuming that the mass and inertial properties of the two COZID inertia wheels are equal,

$$M_{C1} = M_{C2} = 1/2\ M_C$$

$$I_{C1} = I_{C2} = 1/2\ I_C \tag{76}$$

Application of Lagrange's equation, Equation (23), for load motions (z_L) leads to the equation of motion:

$$\left\{ 4k_\theta/R^2 - \omega^2[M_L(1 - r/R)^2 + M_C + I_C/R^2] \right\} z_L$$

$$- \left\{ 4k_\theta/R^2 - \omega^2[M_C(r/R) + I_C/R^2] \right\} z_H = 0 \qquad (77)$$

Resonance and antiresonance frequencies are then

$$\omega_R = \sqrt{\frac{4k_\theta/R^2}{M_L(1 - r/R)^2 + M_C + I_C/R^2}} \qquad (78)$$

$$\omega_{AR} = \sqrt{\frac{4k_\theta/R^2}{M_C(r/R) + I_C/R^2}} \qquad (79)$$

Equations (78) and (79) reduce to Equations (28) and (29) of the Analysis section with substitution of the effective torsional spring rate of the conventional COZID, given by

$$k_\theta = R^2 k_c \quad \text{(Equation (68)}$$

The folded dual-cylinder COZID is thus shown to be both statically and dynamically identical to the conventional COZID.

APPENDIX II
TORSIONAL ELASTOMERIC SPRING DESIGN*

Figure 44 defines the geometry of a torsional elastomeric element. This element, when loaded in rotational shear in the direction θ, generates a restoring torque, τ_s, which is proportional to the applied angular deflection. This torque vs deflection relationship is given by

$$\tau_s = .0365 \frac{GR_2\theta}{t} (R_2^3 - R_1^3) \tag{80}$$

where

G = shear modulus of elasticity of the elastomer used - psi

R_2 = outer radius of the element - in.

R_1 = inner radius of the element - in.

t = thickness of the element - in.

θ = relative angular deflection across the element - deg

The stress in the elastomer (τ) is approximately uniform, given by

$$\tau = \frac{GR_2\theta}{(57.3)t} \tag{81}$$

The spring rate, k_θ, and strain, σ, are then

$$k_\theta = .0365 \frac{GR_2}{t} (R_2^3 - R_1^3) \tag{82}$$

$$\sigma = \frac{R_2(\theta/57.3)}{t} \tag{83}$$

*The analysis contained in this appendix is taken from Reference 9.

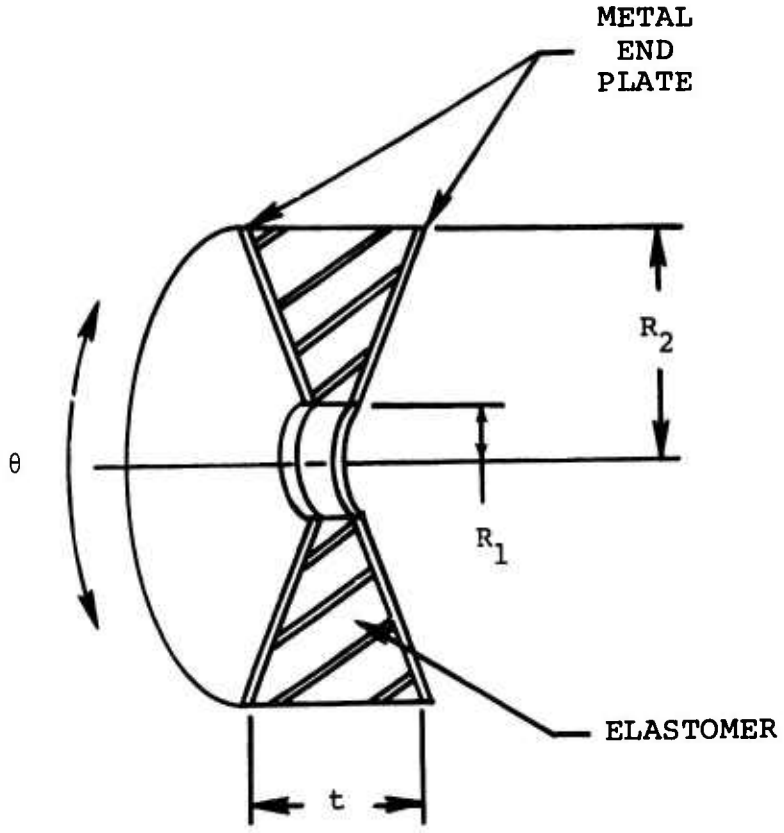

Figure 44. Torsional Elastomeric Spring.

Equations (82) and (83) are used to design the element, based on considerations of maximum strain allowable, size of envelope, and spring rate and deflection required. Equation (83) is plotted in Figure 45 for various values of the parameters, and Equation (82) is plotted in Figure 46 for ranges of R_2, k_θ, and R_1/R_2 and for a strain (σ) of 50 percent and a modulus of 50 psi.

These figures may be used to design an elastomeric element meeting specific spring rate, deflection, strain and size requirements. Their use is illustrated in the following example.

EXAMPLE

An element is required having a torsional spring rate of 262 in.-lb/degree. This element must be no more than 12 inches in diameter and must be capable of tolerating up to 40 degrees of relative rotation with no more than 50 percent strain. 30 durometer rubber, with a shear modulus of 50 psi, is to be used. The input parameters are then:

k_θ = 262 in.-lb/degree

θ = 38 degrees

σ = 50 percent

G = 50 psi

R_2 = 6 in. (max)

Figure 45 is first entered with the given θ and σ, and a value of R_2/t is found. In this case,

$$R_2/t = .75$$

Figure 46 is then used, with the given k_θ and R_2max, and a value of R_1/R_2 is selected. The maximum value of R_1/R_2 possible is used, to preclude bending in the element. The parameters of the element are then:

R_2 = 5.9 in.

R_1 = .59 in.

t = 7.9 in.

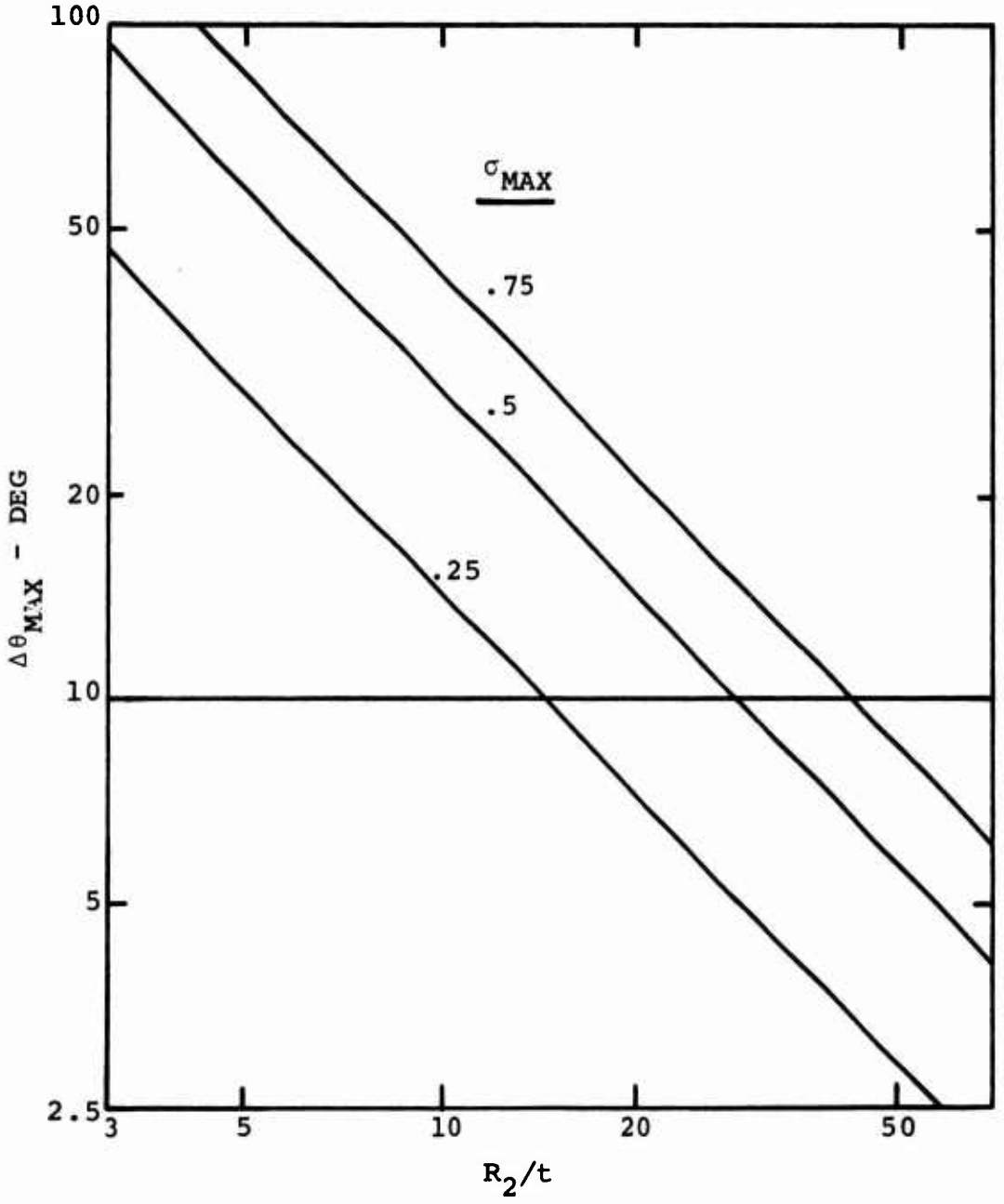

Figure 45. Strain Relationship for Torsional Elastomeric Spring.

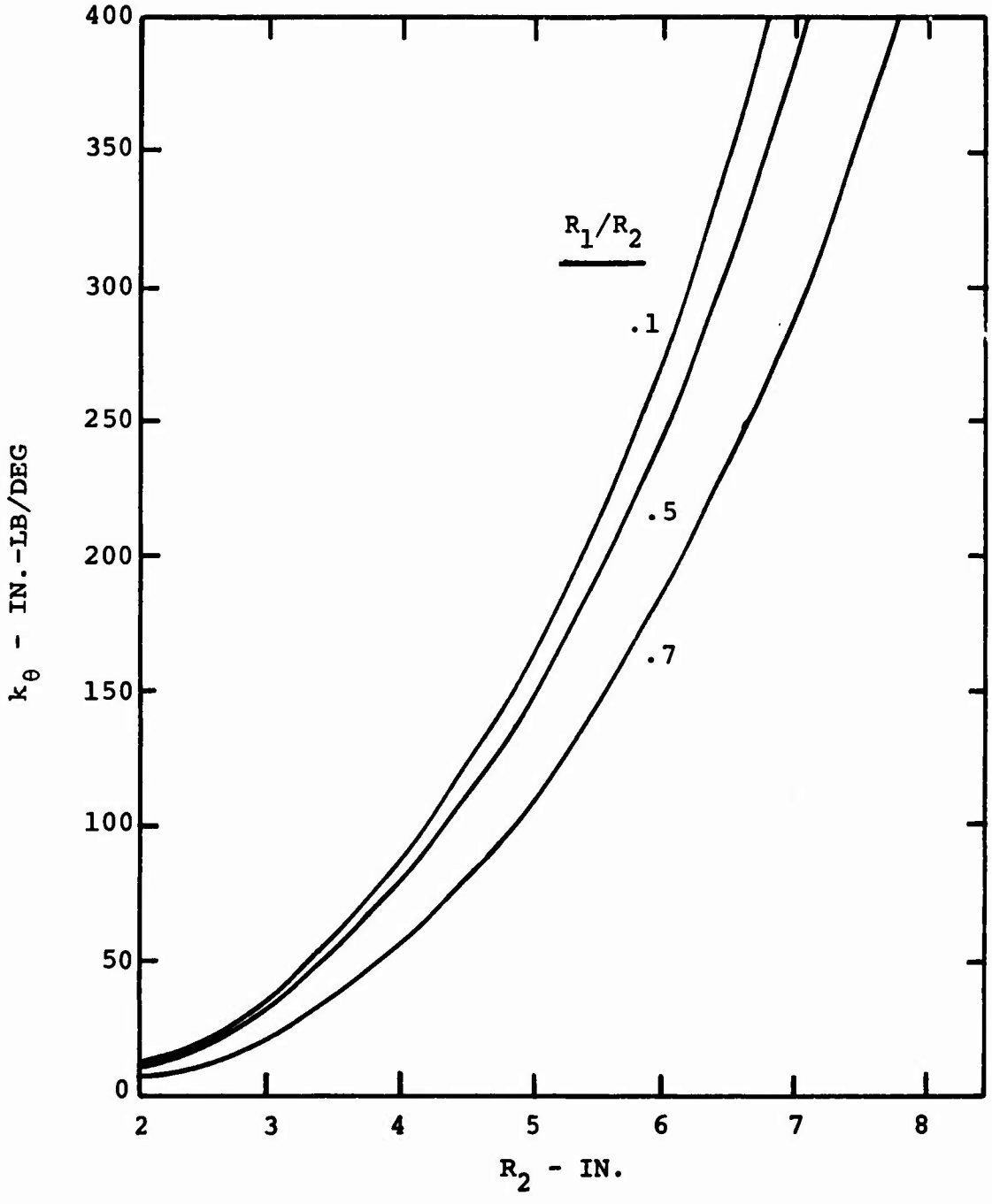

Figure 46. Spring Rate Relationship for Torsional Elastomeric Spring With σ_{max} = 50%, G = 50 psi.

APPENDIX III
STRESS ANALYSES

Stress-critical components of the CH-47B/C COZID are the wire rope belts and the torsional elastomeric spring. Stress analyses for these components are given in the following paragraphs.

WIRE ROPE BELTS

The wire rope belts used in the COZID are constructed using a number of single wire ropes (cables) bonded together using the techniques of Reference 8. Each cable is independently terminated, using swaged ball fittings, in such a way that equal load sharing is obtained and full cable strength is developed. The number and diameter of the wire ropes and their internal construction are dictated by tensile and bending stress considerations.

Maximum bending stress, σ_B, developed in the wire ropes is given by

$$\sigma_B = \frac{d_w E}{d_s} \tag{84}$$

where

d_w = diameter of outermost wire in wire rope - in.

σ_B = maximum bending stress - psi

d_r = wire rope diameter - in.

E = material modulus of elasticity - psi

d_s = sheave (inertia wheel) diameter - in.

For 6 x 37 IWRC steel wire rope,

$$d_w = 1/22\ d_r \tag{85}$$

$$E = 30 \times 10^6 \text{ psi} \tag{86}$$

*All equations are given in Reference 10, Chapter 12.

Maximum bending stress as a function of wire rope diameter is given in Table VIII. Based on a maximum working stress allowable of 20,000 psi, the largest usable cable diameter is 1/4 inch.

TABLE VIII. MAXIMUM BENDING STRESS VS CABLE DIAMETER

dr (in.)	σ_B (psi)
1/8	10,000
3/16	15,000
1/4	20,000

The maximum tensile stress which each individual cable may be subjected to is determined by considering the fatigue factor (P/S_{ult}), given by

$$(P/S_{ult}) = \frac{2T}{S_{ult}\, d_r d_s} \tag{87}$$

where

T = cable tension - lb

S_{ult} = ultimate (breaking) stress - psi

d_s, d_r = defined previously

The number of cables required (N_C) for a given load is calculated using

$$N_C = \frac{2T}{S_{ult}(P/S_{ult})\, d_s d_r} \tag{88}$$

For 6 x 37 IWRC wire rope, infinite fatigue life is obtained if the fatigue factor is less than .0019*. With 1/4-in.-diameter (d_r = .25 in.) cables, a 17-in.-diameter inertia wheel (d_s = 17 in.), and a 20,000-pound tensile load (T = 20,000 lb), the required ultimate strength vs number of cables is given in Table IX.

TABLE IX. ULTIMATE STRENGTH REQUIRED VS NUMBER OF CABLES USED*

N_C	S_{ult} (psi)
25	200,000
20	250,000
17	300,000
16	325,000

*Using 1/4-in.-diameter, 6 x 37 IWRC cables.

The use of plow steel wire rope material, with an ultimate stress of 325,000 psi**, permits a minimum of 16 cables. For the present design, 20 cables are used, with a safety factor of 1.3.

ELASTOMERIC SPRING

The elastomeric spring is loaded in torsion, which results in pure shear within the material. Shear stress is given by***

$$\tau = \frac{GR_2\Delta\theta}{(57.3)t} \tag{89}$$

* Figures 12-20 of Reference 10.

** Based on Reference 8 data.

*** All equations are given in Reference 9.

where

τ = shear stress - psi

G = shear modulus - psi

$\Delta\theta$ = relative angular deflection across the spring - deg

t = spring thickness - in.

R_2 = spring outer radius - in.

For the present design,

t = 8 in.

R_2 = 6 in.

α = 40 deg

G = 50 psi

and the maximum shear stress is 26 psi, which equals the bond stress.

LIST OF SYMBOLS

d_r	wire rope diameter - in.
d_s	sheave (inertia wheel) diameter - in.
d_w	diameter of outermost wire in wire rope - in.
E	modulus of elasticity - psi
E_p	potential energy - in.-lb
E_s	stored energy - in.-lb
f_{AR}	antiresonant frequency - Hz
F_k	force acting on COZID due to spring cable tension - lb
F_R	resonant/antiresonant frequency separation - %
F_s	force acting on COZID due to support cable tension - lb
f_{1-P}	main rotor once-per-revolution frequency - Hz
G	shear modulus of elasticity for elastomer - psi
g	acceleration of gravity - ft/sec^2
I_C	COZID polar moment of inertia - $in.-lb-sec^2$
I_{C1}, I_{C2}	rotational inertia of inertia wheels - $in.-lb-sec^2$
K_c	effective spring rate of the COZID - lb/in.
k_c	COZID spring rate - lb/in.
k_{DHR}	minimum pendant spring rate which will prevent DHR - lb/in.
K_E	effective COZID/sling spring rate - lb/in.
k_{max}	upper limit of soft sling spring rate - lb/in.
k_{min}	lower limit of stiff sling spring rate - lb/in.
k_p	pendant spring rate - lb/in.

LIST OF SYMBOLS (Continued)

k_s	sling spring rate - lb/in.
k_θ	torsional spring rate - in.-lb/deg
L	force acting on COZID due to load cable tension - lb
ℓ	pendant length - in.
m_C	COZID mass - lb/sec^2/in.
m_{C1}, m_{C2}	mass of inertia wheels - lb-sec^2/in.
m_L	external load mass - lb-sec^2/in.
M_R	ratio of COZID inertia mass to maximum external cargo mass - %
N_C	number of cables - rad
(P/S_{ult})	fatigue factor - rad
R	radius from center of COZID to support cable point of tangency - in.
r	radius from center of COZID to load cable point of tangency - in.
R_2, t	geometrical parameters - in.
S_{ult}	ultimate cable stress - psi
T	kinetic energy - in.-lb
T_c	cable tension - lb
V	potential energy - in.-lb
$W_{a/c}$	aircraft weight - lb
W_C	COZID weight - lb
W_H	cargo hook weight - lb
W_{SL}	external cargo weight - lb
z_c	translation of COZID cg - in.

LIST OF SYMBOLS (Continued)

$\dot{z}_C$	vibratory velocity of COZID cg - in./sec
z_H	vibratory displacement of helicopter - in.
$\dot{z}_H$	vibratory velocity of helicopter - in./sec
z_k	translation of the point of tangency of the COZID spring cable with the inertia wheel - in.
$\dot{z}_k$	vibratory velocity of COZID at point of tangency of spring cable - in./sec
z_L	translation of load supported by COZID - in.
$\dot{z}_L$	vibratory velocity of external load - in./sec
z_o	translation of the point of tangency of the COZID load cable with the inertia wheel, due to rotation of the COZID - in.
z_s	translation of COZID/sling attachment point - in.
$\dot{z}_s$	vibratory velocity of COZID/sling attachment point - in./sec
Δf_{1-p}	range of once-per-revolution/main rotor frequencies - Hz
$\Delta\theta$	relative rotation across torsional elastic element - deg
δ_{ST}	static deflection - in.
θ	angular rotation - deg
θ_C	rotation of COZID - rad
$\dot{\theta}_C$	vibratory rotational velocity of COZID - rad/sec
θ_{C1}, θ_{C2}	angular rotation of inertia wheels - rad
$\dot{\theta}_{C1}$, $\dot{\theta}_{C2}$	angular rotation rates of inertia wheels - rad/sec
θ_{ST}	static rotation of COZID inertia wheel - deg
ρ_C	radius of gyration of COZID inertia wheel - in.

LIST OF SYMBOLS (Continued)

σ	strain - in./in.
σ_B	bending stress - psi
τ	rotational shear stress - psi
τ_s	torque due to relative rotation across torsional spring - in.-lb
T	transmissibility, ratio of output to input
ω_{AR}	antiresonant frequency - rad/sec
ω_R	resonant frequency - rad/sec
$\omega_{(T=1)}$	frequency at which the transmissibility is equal to unity - rad/sec